EVALUATION OF CORROSION-RESISTANT STEEL REINFORCING BARS

By

Matthew R. Senecal

David Darwin

Carl E. Locke, Jr.

A Report on Research Sponsored by

THE NATIONAL COOPERATIVE HIGHWAY RESEARCH PROGRAM
TRANSPORTATION RESEARCH BOARD
NATIONAL RESEARCH COUNCIL
Innovations Deserving Exploratory Analysis Program
Contract No. NCHRP-93-ID009

FLORIDA STEEL CORPORATION

Structural Engineering and Engineering Materials
SM Report No. 40

UNIVERSITY OF KANSAS CENTER FOR RESEARCH, INC.
LAWRENCE, KANSAS
JULY 1995

EVALUATION OF CORROSION-RESISTANT STEEL REINFORCING BARS

ABSTRACT

The corrosion performance of a new reinforcing steel is compared with that of conventional steel. The effects of both microalloying and a special heat treatment are evaluated. The microalloying includes small increases in the percentages of copper, phosphorus, and chromium compared to conventional reinforcing steel (less than 1.5 percent total), and the heat treatment involves quenching and tempering after hot rolling. The increase in the phosphorus content exceeds the amount allowed in the ASTM specifications for reinforcing steel. The steels are evaluated using the Southern Exposure and Cracked Beam tests, which are generally accepted in United States practice, plus rapid corrosion potential and macrocell tests developed at the University of Kansas. Corrosion potential, macrocell corrosion rate, and macrocell mat-to-mat resistance are measured. Mechanical properties are compared with the requirements of ASTM A 615 to measure the affects of microalloying and heat treatment on the ductility and strength of the steel.

The results indicate that the corrosion resistant steel has a macrocell corrosion rate equal to half that of conventional steel. The corrosion resisting mechanisms exhibited by the microalloying appear to involve the deposition of protective corrosion products at both the anode and the cathode. The epoxy-coated corrosion resistant steel had a greater time-to-corrosion than epoxy-coated conventional steel. The microalloyed steel met the mechanical requirements of ASTM A 615 for reinforcement.

Key words: chlorides; concrete; corrosion; corrosion testing; heat treatment; microalloys; reinforcing bars.

ACKNOWLEDGMENTS

This report is based on a thesis prepared by Matthew R. Senecal in partial fulfillment of the requirements of the MSCE degree. The research was supported by the National Cooperative Highway Research Program – Innovations Deserving Exploratory Analysis Program under Contract Number NCHRP-93-ID009. Major monetary and material support were provided for the project by Florida Steel Corporation. In addition, corrosion inhibiting admixtures were provided by Master Builders, Inc. and W. R. Grace & Co. Calcium magnesium acetate for use in this study was provided by Cryotech Deicing Technology.

TABLE OF CONTENTS

LIST OF TABLES

LIST OF FIGURES

CHAPTER 1

INTRODUCTION

1.1 General

The use of deicing salts to keep our nation's roadways clear has resulted in the steady deterioration of roadway bridge decks. The deicers penetrate the bridge deck and attack the reinforcing steel, causing corrosion. Due to this problem, the cost of maintaining our nation's highway structures has continued to increase. In 1979, the cost to repair bridges in the Federal-Aid system due to corrosion damage was estimated to be $6.3 billion (Locke 1986). By 1986, the estimated cost was $20 billion and was forecast to increase at the rate of $500 million per year (Cady and Gannon 1992). Therefore, methods that can significantly reduce or halt corrosion caused by deicers are aggressively being pursued.

Current methods that are used to reduce corrosion of reinforcing steel in bridge decks may be divided into two categories. The first category includes methods that slow the initiation of corrosion. The initiation of corrosion is the time it takes the roadway deicer to reach the reinforcing steel in the concrete. The second category includes methods that lengthen the corrosion period, the time after the initiation of corrosion to the end of the service life.

The methods most often used to slow the initiation of corrosion involve the use of corrosion-inhibiting concrete admixtures, low permeability concrete, greater concrete cover over the reinforcing steel, or waterproof sealers. Corrosion-inhibiting concrete admixtures have been demonstrated to reduce or halt corrosion (Berke, Shen, and Sundberg 1990, W. R. Grace 1993, and Nmai, Bury, and Farzam 1994). Admixtures represent a relatively new method of deterring corrosion and their effectiveness has yet to be demonstrated over long periods of time. Low permeability concrete reduces the access of oxygen and moisture to the steel and increases the chloride ion transport time through the concrete. Concrete with a low water/cement ratio or made with materials such as silica fume will decrease the permeability of concrete (Pfeifer, Landgren, and Zoob 1987). Greater concrete cover over the reinforcing

steel significantly increases the amount of time it takes deicers to reach the reinforcement (Schiessl 1988). Waterproof sealers work most of the time, if applied early, evenly, and often.

Methods used to lengthen the service life of reinforced concrete are cathodic protection, epoxy coated reinforcing bars, and patching. Cathodic protection has been used with limited success, but it is costly, and it is difficult to ensure that the entire structure is protected. Epoxy coating prevents the deicer from reaching the bar surface. However, if any bare spots or "holidays" exist in the epoxy, that area may become a hot spot for accelerated corrosion. Patching allows for continued short-term use of a bridge deck that has already deteriorated. Patching should only be done once complete deck replacement is necessary, due to the fact that patching may accelerate the corrosion of adjacent sections of reinforced concrete. Overall, the cost, effectiveness, and reliability of today's corrosion-reducing methods vary widely, and a final solution has yet to be derived on how to protect bridge decks from corrosion due to deicing salts.

The research presented in this report addresses another solution: development of new iron-alloys that are corrosion resistant. This research expands upon work done by the Tata Iron and Steel Company of India. Tata tested a number of alloying combinations that are both corrosion resistant and feasible to manufacture (Jha, Singh, and Chatterjee 1992). They found that the most effective iron-alloy contains increased amounts of chromium, copper, and phosphorus. Tata also evaluated the effects of heat treatment of the steel on corrosion. They found that quenching and tempering the steel improved its corrosion resistance. Tata Steel tested the new steel in five atmospheric tests and one concrete test. The test in concrete entailed cycling a reinforced concrete block through salt water and air and recording the total metal loss after one year. The test results showed that quenched and tempered, microalloyed bars had half the metal loss of conventional steel. The technique does not measure macrocell corrosion nor does it allow for the corrosion rate of the specimen to be measured over time, which would provide information on how the metal loss occurred.

Florida Steel Corporation is interested in using this new alloy, along with a quenching and tempering heat treatment, to produce a corrosion resistant reinforcing steel. However, they need more quantitative data to determine if the new reinforcing bars will provide a significant improvement in corrosion resistance compared to conventional reinforcing steel. To aid in determination, they have provided the University of Kansas with the new reinforcing steel for more thorough testing. The research presented in this report involves comparing the corrosion properties of the new reinforcing steel with conventional reinforcing steel in the presence of sodium chloride, NaCl.

1.2 Background

Initially, steel in concrete is passive due to the high pH of the concrete pore solution. Passivation involves the formation of a tightly adhering iron-oxide layer to the reinforcing bar surface. This layer protects the iron from further corrosion. To reach a passive condition, the pH must be between 12.5 and 13.8 (Jones 1992). If the pH of the concrete pore solution is lowered, the iron-oxide layer becomes unstable and corrosion will occur.

The pH of concrete can be lowered in two ways: by carbonation, due to the penetration of CO_2 into the concrete; or, indirectly, by the presence of aggressive ions, like Cl^-, found in roadway deicing salts. Chloride ions also weaken areas of the iron-oxide layer, allowing chloride ions to react with available iron cations on the bar surface to form an iron-chloride complex. In the presence of hydroxyl ions, the iron-chloride reacts to form ferrous hydroxide and to release the chloride ions which in turn reacts with available iron cations. Therefore, chlorides initiate the corrosion process, and since the corrosion process reduces the pH of concrete, the passive iron-oxide layer is dissolved.

The increase in bridge deck maintenance costs can be tied to the increased use of deicing salts. Thus, the research presented in this paper will focus on the effect of deicers on corrosion of the new reinforcing steel. In particular, the effect of NaCl, the most common roadway deicer, is investigated. A more detailed description of the nature of corrosion of steel in concrete is given in the following paragraphs.

1.2.1 Electrochemistry

The corrosion of steel in concrete is an electrochemical process. There are four components of an electrochemical cell. For reinforcing steel in concrete that is corroding, they are:

a) The Anode, a region of a reinforcing bar or an entire bar where iron releases electrons, $Fe \rightarrow Fe^{++} + 2e^{-}$. This process is called oxidation.

b) The Cathode, a region of a reinforcing bar or an entire bar where oxygen combines with water and the released electrons from the anode to form hydroxyl ions, $1/2O_2 + 2H_2O + 2e^{-} \rightarrow 2OH^{-}$. This process is called reduction.

c) An Electronic Path. The reinforcing bar serves as an electronic path, so that the free electrons from the anode can flow to the cathode.

d) Ionic Solution. In concrete, the ionic solution is provided by the fluid in the concrete pores. The hydroxyl ions produced at the cathode move through the solution and react with the oxidized iron at the anode to produce rust.

Corrosion of reinforcing steel in concrete may occur on the same bar, where anode and cathode sites are adjacent to each other. This is called microcell corrosion. Also, large reinforced concrete structures often have entire layers or regions of steel that act as anodes and cathodes. This produces a more damaging type of corrosion called macrocell corrosion. To prevent corrosion, one of the four components of the electrochemical cell must be eliminated. For example, if oxygen or water were not available at the cathode, the reduction reaction would not occur and the corrosion process would stop.

This tendency of an electrochemical process is determined using the principles of thermodynamics. Thermodynamics gives an understanding of the energy changes involved in the electrochemical reactions of corrosion (Jones 1992). The energy of a metal is measured in volts and is called the potential. The potential of a metal changes as it is placed in different environments. Examples of different environments in reinforced concrete bridge decks are regular concrete, concrete with chloride ions present, concrete with admixtures,

and cracked concrete to name a few. The potential of the reinforcing bars will be different for each environment. Corrosion is more likely to occur when the potential of an anodic region becomes more negative with respect to the potential of a cathodic region.

The potential of the anode and cathode can be used to determine if corrosion will occur. These potentials are used in the Nernst and Gibbs equations (Uhlig and Revie 1985) to determine if the coupled reactions are spontaneous. If the equations show that energy is released (negative energy), corrosion will occur. However, these thermodynamic equations can only determine the tendency of corrosion, not the rate of the corrosion.

Chemical kinetics along with the laws of thermodynamics provide a means with which to determine the corrosion rate of an electrochemical cell. According to chemical kinetics, for every potential of an anodic or cathodic reaction there exists a rate for which that reaction will occur. The relationship between the potential and the rate of a reaction is logarithmic and is given by the Tafel equation (Uhlig and Revie 1985). The principles of chemical kinetics also state that when the anodic and cathodic reactions are coupled in an electrochemical cell, the potential and rate of the reactions will shift to equilibrium. At equilibrium, both the cathodic and anodic reactions will have the same potential and rate, known as the corrosion potential and corrosion rate, respectively, of the electrochemical cell.

For analysis of corrosion of reinforcing steel in concrete, it is easier to directly measure corrosion potential and rate than to predict them using the equations of thermodynamics and chemical kinetics. Oxidation of the iron in reinforcing bars in concrete and the reduction of oxygen at the bar surface are thermodynamically favorable reactions, thus steel corrodes in concrete. However, it is the rate of corrosion that is of concern. If the steel is passive (the normal state in concrete that has not carbonated or been penetrated by chlorides), the corrosion rate is so low that corrosion is considered to have stopped. If the steel is not passive, the corrosion rate may be great enough to effect the integrity of the structure. Several methods used to determine the corrosion potential and corrosion rate of reinforcing steel in concrete are presented in section 1.2.5 of this report.

As discussed earlier, there are two types of electrochemical cells that may form during corrosion of reinforcing steel in concrete, a microcell and a macrocell. Microcell corrosion occurs on a single bar with anode and cathode sites adjacent to each other. Macrocell corrosion occurs when large regions of reinforcing bars develop different corrosion potentials, setting up larger electrochemical cells that effect microcell corrosion. In effect, the corrosion rate of the bars with the higher (more positive) corrosion potential will be reduced and the corrosion rate of the bars with the lower (more negative) corrosion potential will be increased. Overall, corrosion of the reinforcing steel will be increased due to the formation of a macrocell. Therefore, in the analysis of corrosion of reinforcing steel in concrete, both microcell and macrocell corrosion should be investigated.

1.2.2 Chlorides

Corrosion of reinforcing steel can be initiated due to the presence of chloride ions. Chlorides break down isolated areas of the protective iron-oxide layer on the bar surface, allowing chloride ions and water to react with the steel (Fontana 1986). Reactions similar to the following are believed to occur at the anode:

$$Fe^{++} + 2Cl^- \rightarrow FeCl_2 + 2e^-$$

$$FeCl_2 + 2OH^- \rightarrow Fe(OH)_2 + 2Cl^-$$

The presence of oxygen will result in the further oxidization of iron. The corrosion is sustained due to the end reaction, which releases the chloride ions that initiated corrosion in the beginning. After a period of time, the protective iron-oxide layer will dissolve and pitting or general corrosion will occur.

The service life of reinforced concrete structures subject to corrosion due to the presence of chloride ions may be broken down into two stages:

a) The initiation period. This stage represents the time that it takes for chlorides to move through the concrete to the steel. The rate of chloride transport is effected by concrete quality, concrete cover, environment, temperature, and degree of cracking.

b) The corrosion period. This stage is the time from initial corrosion until the structure can no longer serve its intended purpose.

1.2.3 Testing Techniques - Bench Scale Tests

The focus of this research is to determine the corrosion rate of different types of steel in concrete. Therefore, tests that reduce the initiation time are desirable. Two short-term (one year) tests that provide for rapid chloride ion transportation and are widely used by industry in the U.S. are the "Southern Exposure" (SE) and the "Cracked Beam" (CB) tests. These small-scale tests reproduce macrocell type corrosion found in large reinforced concrete structures and, particularly, in bridge decks. The tests differ in that the SE test simulates a non-damaged bridge deck, while the CB test simulates a bridge deck cracked to the reinforcing steel. The SE tests were used extensively in previous research by Pfeifer, Landgren, and Zoob (1987) for the Federal Highway Administration. The CB tests are modified SE tests and were used in research done by McDonald, Pfeifer, Krauss, and Sherman (1994). A test similar to the SE test is ASTM G 109, "Standard Test Method for Determining the Effects of Chemical Admixtures on the Corrosion of Embedded Steel Reinforcement in Concrete Exposed to Chloride Environments." The test specimen and test procedure differ slightly for the two tests: the G 109 test specimen is half the width and has half the steel of the SE test specimen; and the relative aggressiveness of exposure to saltwater in the G 109 test is less severe than the SE test. Recent research using the SE, CB, or G 109 tests has been done by Berke and Tourney (1993), Berke, Dallaire, Hicks, and Hoopes (1993), and Nmai, Bury, and Farzam (1994).

In the SE and CB tests, rapid chloride ion transport is facilitated by: a low concrete cover over the reinforcing bars; a higher water/cement ratio than used in practice for higher permeability; and a unique "weathering" scheme. The weathering scheme involves ponding saltwater on the SE and CB specimens for a period of time and then drying the specimen to evaporate the water and deposit the salt. The ponding and drying is repeated, leaving additional deposits of salt after each cycle, thus creating high concentrations of chloride ions

in the concrete over a short period of time. A cycle starts by ponding the specimens with a 15% sodium chloride solution for 100 hours (four days) at 16°C to 27°C (60°F to 80°F). At the end of the 100 hours, the salt water is removed. The specimens are then heated to 38°C (100°F) for sixty-eight hours (three days). This weekly cycle is repeated 48 times.

The Southern Exposure specimen is shown in Fig. 1.1. The specimen is 305 mm (12 in.) wide, 305 mm (12 in.) long, and 178 mm (7 in.) high. The top of the specimen is crowned by a dam that retains salt water. The sides of the specimen are coated with epoxy to prevent salt intrusion from the sides. Two mats of steel are cast in the concrete. The top layer of steel serves as the anode, and the bottom layer of steel serves as the cathode. The cathode layer has twice as much steel so that the macrocell corrosion rate is not limited by the cathodic reaction. The top and bottom layers of steel extend from the sides of the concrete, so that an external electrical connection can be made between the two layers. This connection is made across a 10 ohm resistor. The protruding ends of the bars are epoxy-coated to prevent crevice corrosion at the exterior concrete/steel interface. The macrocell corrosion current is monitored weekly by measuring the voltage drop across the resistor.

The Cracked Beam specimen is shown in Fig. 1.2. The CB specimen is half the width of the SE specimen, 152 mm (6 in.), and has a load-induced transverse crack across the top of the specimen. The crack extends down past the top bar, providing a 0.13 to 0.38 mm (0.005 to 0.015 in.) gap at the bar. This test shows how the steel and concrete react to direct contact with chlorides. The testing procedure for the CB test is identical to that for the SE test.

SE and CB specimens are tested every week to determine the macrocell corrosion rate. The corrosion rate of a macrocell may be determined by using Faraday's law (Fontana 1986). Faraday's law gives the relationship between reaction rate and current density:

$$\text{Rate} = (i \cdot a) / (n \cdot F \cdot D)$$

in which the corrosion rate is the depth of metal loss over time (μm/yr), i is current density of the macrocell (mA/cm^2), a is the atomic weight of the metal (55.8 gram/gram-atom for iron), n is the number of ion equivalents exchanged (2 equivalent/gram-atom for iron), F is Faraday's

constant (96,500 amp·sec/equivalent), and D is the density of the metal (7.87 gram/cm^3 for iron). The current density is determined by dividing the current (obtained from the voltage drop) by the surface area of the anodic bars. If desired, other measurements such as bar potential, polarization resistance, and mat-to-mat resistance, may be made along with the corrosion rate measurements.

1.2.4 Testing Techniques - Rapid Tests

A rapid (4 month) test that determines the corrosion potential and macrocell corrosion rate of reinforcing bars in mortar was developed in previous research at the University of Kansas by Martinez, Darwin, McCabe, and Locke (1990). This test uses a specimen referred to as a "lollipop". To minimize the initiation stage of the corrosion process, the lollipop specimen has a very small mortar cover (7 mm), so that the full salt water concentration will reach the reinforcing bar in approximately one month. In contrast, the SE and CB specimens have a 25 mm (1 in.) cover that allows only about one fourth of the salt concentration to reach the reinforcing bars at the end of one year.

The specimen is shown in Fig. 1.3. A reinforcing bar is cast in mortar in a cylindrical mold, that allows for the small (7 mm) concrete cover. The mortar has a water/cement ratio of 0.5 to increase the permeability of the mortar. Admixtures may be added to the mortar, if desired. After casting, the specimen is cured for 14 days in lime saturated water. The specimens is used for two tests: the potential test and the macrocell test.

The potential test measures the corrosion potential of the specimen when it is exposed to different molal ion concentrations of roadway deicers. The deicing chemicals are measured on an isomolal basis, since the ion concentration, in moles per unit volume of water, controls ice melting capacity (Martinez et al. 1990). The test setup is shown in Fig. 1.4. A specimen is placed in a solution containing a simulated concrete pore solution (Farzammehr 1985) and a specific concentration of deicing chemicals. The corrosion potential is measured with respect to a saturated calomel electrode in a saturated potassium chloride solution, connected to the

solution surrounding the specimen with a salt bridge, and monitored as soon as the setup is made. A typical test is run for 40 days.

The macrocell test measures the macrocell corrosion rate between two sets of specimens placed in different concrete environments. The test setup is shown in Fig. 1.5. Two specimens are placed in a solution containing the concrete pore solution. These specimens passivate and act as the cathode in the macrocell. One specimen is placed in a solution containing concrete pore solution and a specific concentration of deicing chemicals. This specimen corrodes and acts as the anode in the macrocell. To assure that the macrocell corrosion is not limited by the cathodic reaction, twice as many specimens are used at the cathode and oxygen is supplied to the pore solution at the cathode. As with the potential test, the solutions at the cathode and anode are connected by a salt bridge to provide the ionic path necessary in an electrochemical cell. The two sets of specimens are connected electrically, across a 10 ohm resistor, to allow the free electrons at the anode to flow to the cathode. The corrosion current is determined by measuring the voltage drop across the resistor. The corrosion rate is then determined using Faraday's law as described for the SE and CB tests.

1.2.5 Corrosion Monitoring Methods

The following corrosion monitoring methods may be used with the Bench-Scale and Rapid tests.

a) *Metal Potential* - Potential is measured with respect to a reference electrode. Although the absolute amount of energy in a metal cannot be directly measured, the difference in energy between two reactions can be measured. Therefore, a standard reaction has been chosen to have zero potential and all other reaction potentials are defined as the difference in potential from the standard (Jones 1992). The standard reaction is $2H^+ + 2e^- \leftrightarrow H_2$. An electrode is used to produce the standard reaction. The electrode for the hydrogen reaction is called the standard hydrogen electrode (SHE). By setting up an electrochemical

cell between a metal and the electrode, the potential difference can be measured using a voltmeter.

Other electrodes that have more stable reactions are often used instead of the SHE. For bridge decks, the copper-copper sulfate electrode (CSE) is often used and has a potential difference of +0.318 V with respect to the SHE. ASTM C 876 is a standard test method for determining the corrosion potential of uncoated reinforcing bars in concrete using the CSE. ASTM C 876 is used to determine the corrosion potential of the reinforcing steel in the SE and CB tests. The saturated calomel electrode (SCE) is often used for testing in the laboratory and has a potential difference of +0.241 V with respect to the SHE. The SCE is used in the rapid potential tests.

Previous work has been done to find the range of potential values over which corrosion of conventional reinforcing steel in concrete is likely (Page and Treadway 1982, Schiessl 1988, and Clear 1989). Reinforcing bars are considered to be passive in concrete when the corrosion potential is between +100 mV to -200 mV versus the saturated calomel electrode (SCE). Corrosion potentials between -200 mV and -500 mV (vs. SCE) indicate pitting is occurring, and corrosion potentials between -450 mV and -600 mV (vs. SCE) indicate general corrosion is underway.

b) *Macrocell Corrosion* - The corrosion rate of a macrocell may be determined by measuring the voltage drop across a resistor placed in series with the electron path between the anode and the cathode, as described earlier. The macrocell corrosion rate can be easily measured in the laboratory using specially designed specimens like the bench scale and rapid macrocell test specimens. However, macrocell corrosion may be impossible to measure in actual reinforced concrete structures where access to the reinforcing bars is limited.

The macrocell corrosion rate is a good measure for comparing corrosion in different types of reinforcing steels in concrete, but it does not always give the absolute corrosion rate; the actual total corrosion rate may be higher than the macrocell corrosion rate. As discussed earlier, macrocell corrosion is created by electrochemically connecting two areas of steel with

different corrosion potentials. Typically, the smaller the corrosion potential difference, the smaller the macrocell corrosion rate and the larger the difference between the macrocell corrosion rate and total corrosion rate. Conversely, the larger the corrosion potential difference, the greater the macrocell corrosion rate and the closer the macrocell corrosion rate is to the total corrosion rate. For small differences in corrosion potential, microcell corrosion at the anode and cathode may be greater than macrocell corrosion.

c) *Polarization Resistance* - This test method determines the microcell corrosion rate on a reinforcing bar in concrete. Previous research has found a relationship between the resistance of a metal to microcell corrosion and the microcell corrosion rate (Stern and Geary 1958). The resistance of a metal may be approximated by a polarization curve. A polarization curve is made by imposing a range of potentials on the metal and measuring the corresponding corrosion currents. This process is carried out using a potentiostat. A portion of the polarization curve will exhibit a linear relationship. The slope of the linear region is proportional to the resistance of the metal. ASTM G 59, "Practice for Conducting Potentiodynamic Resistance Measurements," describes the procedure for generating polarization curves. The microcell corrosion current density is determined using the relationship (Berke and Hicks, 1990):

$$i_{corrosion} = B / R_p$$

in which i is the microcell corrosion current density (A/cm^2), B is a constant (that has been determined to be 26 mV for reinforced concrete), and R_p is the slope determined from the polarization curve ($k\Omega \cdot cm^2$). The microcell corrosion rate is determined by using Faraday's law.

d) *Electrochemical Impedance Spectroscopy (EIS)* - This test method determines the microcell corrosion rate of a reinforcing bar in concrete. This test method uses a potentiostat, like the polarization resistance method, but instead of a direct current being applied to the system an alternating current is applied. This is done to obtain more mechanistic information about the concrete. The different constituents that make up reinforced concrete may be

thought of as a network of capacitances and resistances (Berke and Hicks 1990). By applying a variable current to the reinforced concrete, the various constituents within the concrete may be isolated and quantified for their respective effect on resistance to corrosion. For example, the resistance due to an epoxy coating on a reinforcing bar or the reinforcing bar itself, may be directly measured, whereas for the polarization resistance method, the resistance of the coating and concrete are measured together and are indistinguishable.

This method is complex and expensive due to the need for specialized equipment and careful interpretation of data. Computer software is needed to run the test and to retrieve, compute, and display the data. A wide range of software applications are available (Munn 1992), but they require a thorough understanding of how they were written to interpret the results correctly.

e) *Chloride Ion Content* - The relationship between chloride ion content in the concrete and corrosion of conventional reinforcing steel has been researched by Slater (1983) and Schiessl (1989). If the chloride ion concentration can be determined at the bar, the corrosion rate can be estimated. Usually, destructive testing is necessary to find the chloride ion content at the bar. A small concrete sample, approximately 3 grams, is necessary for a laboratory analysis. The removal of a small sample of concrete will not endanger the service life of a large reinforced concrete structure but may compromise a small test specimen.

AASHTO T 260-84 is the most common laboratory method used to determine the chloride ion content of concrete. The technique involves titration of a sample. The sample is prepared by sieving and diluting a small portion of the concrete. Then measured amounts of titrant, $AgNO_3$, are added to the solution. The potential change of the solution is recorded with a specific ion probe for each increase in titrant. The recorded data is then used to calculate the chloride ion concentration in the concrete.

A newer laboratory method that determines the chloride ion content in concrete is, "The Standard Test Method for Chloride Content in Concrete Using the Specific Ion Probe," developed by Cady and Gannon (1992). The specific ion probe method is less time

consuming than the AASHTO method, if more than one sample is being evaluated. This method requires that the specific ion probe be calibrated by recording the millivolt response to different concentrations of chloride ion solutions. Each concrete sample is mixed with a digestion solution and then a stabilizing solution. After the mixture has settled, the probe is used to measure the potential of the solution. The chloride ion content is calculated from the relationship developed in the calibration process. The probe should be calibrated once a month, but may be used as many times as needed during that month.

Destructive testing is not always necessary. For common concrete mixes where standard reinforcing steel is used, researchers have developed chloride ion diffusion constants (Berke and Hicks 1994) needed to use Fick's Law, which estimates the concentration of chlorides in concrete at different depths with respect to time. If the salt water ponding concentration, the depth of concrete cover, the concrete mix design, and time involved are known, the chloride content can be estimated. If the chloride ion content and corrosion potential of the bar are known, the corrosion rate may be estimated.

f) *Mass Loss or Visual Inspection* - Visual inspection is a destructive method to evaluate the end effects of corrosion on the reinforcing bars in concrete. To make a visual inspection, the concrete must be destroyed to remove the bar. Total metal loss can be calculated if the bar was weighed before casting. The metal loss can be checked against non-destructive techniques that may have been used to estimate corrosion during the testing of the specimen. Also, visual inspection will show the type of corrosion that has occurred: pitting, crevice, or general corrosion.

1.3 Previous Work

The Tata Steel and Iron Company has developed a corrosion resisting reinforcing bar for concrete. Tata's goal was to select a steel chemistry for a new reinforcing bar that would maintain strength, lower its susceptibility to corrosion, and be cost effective to manufacture (Jha, Singh, and Chatterjee 1992). In the development of a new microalloyed steel, Tata Steel used two different rolling processes: the standard hot-rolling process and a quenching

and tempering heat treatment, also known as the Thermex/Tempcore process. The microalloy that worked best for Tata Steel was called TISCON-CRS. Tiscon is the product name and CRS is the abbreviation for corrosion resistant steel. Two grades of steel were tested, 42 and 50 (yield strengths of 420 MPa and 500 MPa, respectively). The main alloying elements were copper (0.5% max.), phosphorus (0.12% max.), and chromium (0.8% max.). The minimum total of the three elements was 0.9% (see Table 1.1).

Tata Steel and Iron Co. states that the improved corrosion resistance of the new microalloy is due to the corrosion products formed by the increased amounts of copper, chromium, and phosphorus. In the presence of a saline solution, the copper in the alloy reacts with chlorine and water to form a $CuCl_2 \cdot 3Cu(OH)_2$ layer, which is less soluble than $Fe(OH)_2$ (rust product for conventional steel). The corrosion layer retards corrosion, and the copper appears to plug pores in the rust, reducing the amount of oxygen and water reaching the steel surface. In the oxide form, phosphorus acts as an inhibitor to the formation of iron oxide and, as a result, slows the corrosion process. The chromium forms a spinal oxide layer with the iron, $FeO \cdot Cr_2O_3$, which is a poor conductor and thus reduces the corrosion rate. The $CuCl_2 \cdot 3Cu(OH)_2$ and $FeO \cdot Cr_2O_3$ form a compact, dense corrosion layer that further prevents the movement of oxygen and water to the steel surface (Jha, Singh, and Chatterjee 1992).

Tata performed five different tests on eight types of bare steel: salt spray test; alternate immersion test; sulfur dioxide chamber test; atmospheric corrosion test; and a polarization study. The steel types involved combinations of the hot-rolled and quenched and tempered rolling processes, conventional steel and CRS, and steel grades 42 and 50. The first four tests measured the total metal loss from 51 mm x 51 mm x 8 mm (2"x 2" x 0.3") metal coupons in a corrosive environment. The polarization study measured the microcell corrosion rate of the steel. The salt spray test consisted of placing a coupon in a fog created with a 3% NaCl solution for 96 hours. The alternate immersion test cycled a coupon through a 3% NaCl solution and the open air. The coupon was placed on a wheel rotating at 3 rpm and ran for 96 hours. The sulfur dioxide chamber test involved placing a coupon in a

gas chamber with high humidity and sulfur dioxide gas for 96 hours. The atmospheric corrosion test placed the coupons in coastal environments at different geological locations around India for two months to two years. The polarization study consisted of finding the polarization resistance of the metal in a 1 N H_2SO_4 solution.

The results of the five tests showed that both the microalloying and the quenching and tempering rolling process improved the corrosion resistance of the bars. The combination of the two provided the best resistance for both the 42 and 50 grade steels. The test results showed that TISCON-CRS has two to three times better corrosion resistance than standard reinforcing bars (Tata 1991).

One test was completed with the reinforcing steel in concrete, the accelerated corrosion test. The test specimen consisted of two steel bars (uncoupled) in a concrete block. The test involved cycling the specimen through a wet/dry environment. One cycle included 24 hour submersion in a 3% NaCl solution, followed by drying for 48 hours at room temperature, then drying at 60^{o}C for 48 hours. A total of 60 cycles were performed. The results of the test showed that the percentage weight loss of the TISCON-50-CRS bars was 33 to 42 percent less than conventional reinforcing bars.

Tata Steel performed mechanical tests on the eight different steels. Mechanical testing is necessary due to the increased amounts of phosphorus in the microalloyed steel. Phosphorus tends to make steel brittle. All of the bar types met the mechanical strength and ductility requirements. Quenching and tempering greatly improved the ductility of the conventional and CRS bars.

The weldablility and the bond strength for the different steels was determined. The weld joint strength for butt, single lap, and double lap welds of TISCON-CRS were found to be greater that 90 percent of the original bar strength. The bond strength between the steel and concrete was measured after corrosion. A pullout (bond strength) specimen was corroded by a similar accelerated corroding process described in the accelerated corrosion test. The test results showed that the bond strength increased over time for all steels.

1.4 Objective and Scope

The goal of this study is to evaluate a concrete reinforcing steel that has shown superior corrosion-resistant properties in the presence of chloride ions. Tata Iron and Steel Co. has developed a microalloyed reinforcing steel that has improved corrosion resistance. However, the testing completed by Tata was limited. The accelerated corrosion test used by Tata allowed the mass loss of the steel due to microcell corrosion in concrete to be measured after one year. These results showed that the CRS bars had less metal loss than the conventional steel bars. However, total metal loss does not provide the history of corrosion rate versus time, which would provide detail on how the metal loss occurred. The previous efforts did not measure the corrosion potential of the steel or the resistance of the corrosion product over time, which would provide information on why the corrosion rate was different. The response of the steel to macrocell corrosion was not tested, even though macrocell corrosion may be more damaging than microcell corrosion.

This study includes a detailed experimental analysis of how microalloying and the quenching and tempering heat treatment effect macrocell corrosion. Florida Steel Company has manufactured and supplied this project with four types of reinforcing steel: conventional hot-rolled steel (H), corrosion resistant hot-rolled steel (CRSH), conventional quenched and tempered (Thermex/Tempcore) steel (T), and corrosion-resistant quenched and tempered steel (CRST). The metal compositions for the four steels are given in Table 1.1. The four steel types were evaluated over time using the rapid and bench scale test methods described earlier in this chapter. The common roadway deicing salt, NaCl, was used in the tests. In addition, two corrosion inhibiting concrete admixtures, Rheocrete 222 (organic), developed by Master Builders Inc., and DCI-S (inorganic) developed by W.R. Grace & Co., were evaluated for their effectiveness with the CRS steels.

The rapid tests were used to determine the corrosion potential and macrocell corrosion rate of the four types of reinforcing bars for four molal ion concentrations of NaCl: 0.4 m, 1.0 m, 1.6 m, and 6.04 m (15%). Two potential tests and two macrocell tests were completed

for each steel type at each concentration of salt (4 macrocell tests were completed for 6.04 m). Two macrocell tests were made for each corrosion inhibitor for the CRSH and CRST bars. These tests gave an early (45-100 day) comparison of the relative corrosion resistance of the reinforcement and the ability of the two corrosion inhibitors to add to the corrosion protection.

The SE and CB tests were monitored once a week to determine the macrocell corrosion rate, corrosion potential of the anode and cathode, and the electrical resistance of the macrocell. The SE and CB tests were used to evaluate the eight combinations of materials studied for the rapid tests plus combinations of H and CRST steel to study the effects of combining the new reinforcement with conventional steel. In addition, epoxy-coated H, CRSH, and CRST bars were evaluated using the SE test. A portion of the epoxy coating was removed to simulate problems that occur in the field to establish the effectiveness of a combination of the new reinforcement with epoxy coating. Three replications for each combination of variables were carried out, for a total of forty two SE tests and thirty three CB tests.

Mechanical testing was done according to ASTM A 615 on all four steels. In particular, the percent of elongation, yield strength, and tensile strength were measured and a bend test was performed. A minimum of three tests were completed for each steel.

CHAPTER 2

EXPERIMENTAL WORK

This chapter includes a description of the experimental work performed in this study. The test methods include updated versions of the corrosion potential and macrocell tests developed by Martinez, Darwin, McCabe, and Locke (1990) and the Southern Exposure and Cracked Beam tests used by Pfeifer, Landgren, and Zoob (1987) and McDonald, Pfeifer, Krauss, and Sherman (1994). The tests are not standardized, therefore a full description of the test specimens, specimen fabrication, and test procedures are given for each of the test methods.

2.1 Rapid Corrosion Testing (4 months)

The rapid tests were used to measure the corrosion potential and macrocell corrosion rate of the four reinforcing steels, H, T, CRSH, and CRST, for four different molal ion concentrations of NaCl: 0.4 m, 1.0 m, 1.6 m, and 6.04 m (15%). The potential and macrocell tests use a similar test specimen and have similar setup procedures. The test specimen and fabrication are described first, followed by the corrosion potential and macrocell test procedures.

2.1.1 Materials

a) *Reinforcing Steel* - The chemical compositions of the four types of steel (H, T, CRSH, CRST) are shown in Table 1.1. The hot-rolled steels, H and CRSH, meet the mechanical testing standards of ASTM A 615 for Grade 300 (40) steel, and have a horizontal (bamboo) bar deformation pattern. The quenched and tempered steels, T and CRST, meet the mechanical testing standards of ASTM A 615 for Grade 400 (60) steel. Two sets of T and CRST steel reinforcing bars were rolled, each with a different deformation pattern; one set has a bamboo pattern, and the other set has a criss-cross (diamond) pattern. ASTM A 615 states that the phosphorus content shall not exceed 0.06%. The CRSH and CRST steels have a phosphorus content of 0.08%, exceeding the allowable phosphorus content of ASTM A 615, but less than the suggested phosphorous content of 0.12% by Tata Steel.

b) *Mortar* - Three mortar mix designs were used: one for conventional mortar and two incorporating corrosion inhibiting concrete admixtures. The conventional mortar is made with Type I Portland cement, ASTM C 778 graded Ottawa sand, and deionized water. The mortar has a water-cement ratio of 0.5 and a sand-cement ratio of 2.0, by weight, and represents the mortar constituent of concrete with a design strength of 4000 psi at 28 days.

The two corrosion inhibiting concrete admixtures are Rheocrete 222, provided by Master Builders Inc., and DCI-S (calcium nitrite), provided by W.R. Grace Company. The suggested dosages by the respective manufacturers are 5 l/m^3 (1 gal/yd^3) Rheocrete 222 and 19.8 l/m^3 (4 gal/yd^3) of DCI-S. The three mortar mix designs are given in Table 2.1.

c) *Epoxy Coating* - Two types of epoxy patching compounds were used: Scotchkote (Product No. 312), manufactured by 3M, and Corvel Epoxy Patch Compound (Product No. 10-6071 PC), manufactured by Morton Powder Coatings International.

2.1.2 Test Specimen

The test specimen used for the corrosion potential and macrocell test (Fig. 1.3) is 152 mm (6 in.) long and resembles a "lollipop". It consists of a 127 mm (5 in.) long 16 mm (No. 5) reinforcing bar, symmetrically embedded 76 mm (3 in.) into a 30 mm (1.18 in.) diameter mortar cylinder. The mortar cylinder is 102 mm (4 in.) long and provides a mortar cover of 7 mm over the reinforcing bar. The specimen configuration is based on research done by Martinez, Darwin, McCabe, and Locke (1990). The specimen was modified in this study by using a No. 5 bar instead of a No. 4 bar. This reduced the mortar cover over the steel reinforcement by 2 mm (0.0625 in.).

2.1.3 Specimen Fabrication

The specimen fabrication process is completed in the following order:

a) *Reinforcing Bar Preparation* - The reinforcing bars are cut to a length of 127 mm (5 in.), and one end of the bar is drilled and tapped for a 10-24 threaded bolt to a depth of 13 mm (0.5 in.). The threaded hole is needed to make a solid electrical connection. The bar is then cleaned in an acetone bath to remove oils, grease, and dirt. The mill scale is left on

the bar surface. An epoxy band, 15 mm (0.6 in.) wide and centered 51 mm (2 in.) from the tapped end of the bar, is then applied to the bar. The epoxy band is necessary to protect the mortar-steel interface from crevice corrosion. The epoxy is mixed according to manufacturer's recommendations. Two coats are applied, and each coat is dried for 24 hours at 38^{o}C (100^{o}F) after application.

b) *Mold Assembly* - The mold for the specimen is made from standard commercial materials that are available at the local hardware store. The specimen mold and mold container are shown in Fig. 2.1. The mold container holds a total of eight specimens and may be modified to hold more, if desired. The individual parts of the mold are labeled on the figure and detailed in Table 2.2. The assembly is explained in the following steps [This assembly procedure is taken from Martinez et al. (1990)]:

1. The tapped end of the prepared reinforcing bar is inserted through the hole of the small rubber stopper, A, beginning at the widest end of the stopper. The distance between the untapped end and the rubber stopper is 76 mm (3 in.).
2. The rubber stopper is inserted in the machined end of the small connector, B. The widest end of the small rubber stopper has to be in contact with the shoulder (an integral ring) on the internal surface of the small connector.
3. The large rubber stopper, C, is inserted in the cut end of the larger connector, D, until it makes contact with the shoulder on the inside surface of the connector.
4. The turned end of the small connector, B, is inserted in the free end of the large connector, D. At the same time, the tapped end of the reinforcing bar is inserted through the hole of the large rubber stopper, C.
5. The longitudinal slice along the side of the PVC pipe, E, is taped with masking tape. The pipe is then inserted in the free end of the small connector.
6. The assembled mold is placed between the wooden boards, F, in the holes provided. The threaded rods, G, are then inserted between the wooden boards. The rods are used

to hold the molds together and center the reinforcing bar by tightening or loosening the nuts on the rods.

c) *Mortar Mixing* - The mix designs given in Table 2.1 provide enough mortar to make eight specimens and provide fill for six specimen containers. The mortar is mixed by hand. The sand and cement are mixed together first. The water is then added to the cement-sand mixture and mixed for 5 minutes. Admixtures are mixed with the water before being placed in the cement-sand mixture. Specimens are cast within 10 minutes of mixing.

d) *Casting* - The specimens are cast in three layers. Each layer is rodded 25 times with a 3.2 mm (0.125 in.) diameter rod, 305 mm (12 in.) long. The rod is used to work the mortar between the mold and reinforcing bar. The rod is allowed to penetrate the previous layer of mortar to work the layers of mortar together, but the rod is not allowed to forcibly strike the bottom of the mold. Each layer is vibrated for 15 seconds after rodding, using a vibration table with an amplitude of 0.15 mm (0.006 in.) and a frequency of 60 Hz.

e) *Curing* - After the specimens are cast, the molds are covered with a moist towel and a plastic sheet for 24 hours at room temperature, $23^{o}C \pm 1^{o}C$ ($74^{o}F \pm 2^{o}F$). The specimens are then removed from the molds and placed in lime-saturated water for 13 days. The total curing time is two weeks.

2.1.4 Corrosion Potential Test Procedure

This test measures the corrosion potential of different types of concrete reinforcing bars exposed to various concentrations of NaCl. The corrosion potential of the reinforcing bar is measured with respect to a saturated calomel electrode. The test configuration is shown in Fig. 1.4. The test period is 40 days.

This section includes descriptions of the test components and how they are assembled.

a) *Specimen* - The specimen is fabricated according to the procedures described in section 2.1.3.

b) *Mortar Fill* - The specimen is surrounded by a fill material made out of the mortar used to make the test specimen. The mortar fill provides a buffer for the test specimen, as the pore

solution is highly basic and is introduced in large quantities relative to regular concrete. Also, the fill saves on the amount of concrete pore solution needed and secures the specimen in an upright position. The fill is cast in metal baking sheets, 25 mm (1 in.) deep, at the same time the test specimens are fabricated. The mortar is air cured for 14 days and then crushed into 25 mm to 50 mm (1 in. to 2 in.) pieces.

c) *Concrete Pore Solution* - Based on an analysis by Fazammehr (1985), the solution in the pores of concrete contains potassium hydroxide (KOH), sodium hydroxide (NaOH), and sodium chloride (NaCl). To match his analysis, one liter of simulated pore solution, contains 974.8 g of distilled water, 18.81 g of KOH, 17.87 g of NaOH, and 0.14 g of NaCl. For this study, the sodium chloride was not included in the pore solution.

d) *NaCl Solution* - Four molal ion concentrations of NaCl were used for this study: 0.4 m, 1.0 m, 1.6 m, and 6.04 m. To produce these concentrations, 11.4 g, 28.5 g, 45.6 g, and 172.1 g of NaCl, respectively, are used per liter of pore solution.

e) *Container (with lid)* - The specimen, fill, and solution are held in a 5 liter container. The container is circular, measuring 197 mm (7.75 in.) in diameter and 216 mm (8.5 in.) in height, and is made of high density polyethylene, so that it will not react with the NaCl or the pore solution.

f) *Salt Bridge* - To measure the corrosion potential of the specimen, an ionic path must connect the solution containing the specimen and the solution containing the SCE. The ionic path is provided by a salt bridge. A salt bridge is a salt "gel" cast in a flexible tubing. The gel is made with 4.5 grams of agar, 30 grams of potassium chloride (KCl), and 100 grams of distilled water, enough to produce three salt bridges with a total length of 3 m (9 feet). The constituents are mixed together and heated over a burner at 200°C (400°F) for five minutes and then siphoned into three flexible latex tubes, each 1 m (3 feet) long, with inner diameters of 9.5 mm (0.375 in.). The salt bridges are then placed in a pot of boiling water for one hour to finish the gel process.

g) *Terminal Box* - A terminal box was constructed to ease the process of taking electrical measurements for a large number of test specimens. The box is 178 mm (7 in.) x 102 mm (4 in.) x 51 mm (2 in.) and is purchased from Radio Shack. Eight binding posts (also from Radio Shack) are attached to the top of the box.

h) *Wire* - A 16 gage stranded copper wire, 1.3 m (4 feet) long, is used to connect the test specimen to the terminal box.

i) *Saturated Calomel Electrode (SCE)* - The potential of the specimen is measured with respect to a SCE. The SCE is easily maintained and widely available. The SCE is submerged in a saturated potassium chloride (KCl) solution (50 g of KCl per 100 g of distilled water). With the current test setup, eight potential tests are connected to the KCl solution with salt bridges.

j) *Voltmeter* - The voltmeter used was a Hewlett Packard 3455A digital voltmeter.

After the test specimen has cured for 14 days, the test is initiated. The specimen is removed from the lime water and the tapped end of the specimen is dried with compressed air. The copper wire is then attached to the specimen with a 6 mm (1/4 in.) 10-24 machined steel screw. The other end of the wire is threaded through the container lid and attached to a binding post on the terminal box. The specimen is placed in the center of the container and fill is placed around the specimen. To prevent crevice corrosion, the wire connection on the specimens is epoxy coated. The pore solution and the desired amount of NaCl are mixed together and then poured into the container until the solution is 13 mm (0.5 in.) from the top of the mortar/steel interface of the specimen (approximately 1.5 liters of solution). One end of the salt bridge is placed in the pore/salt solution and the other end is threaded through the lid and placed in the KCl solution used for the SCE.

The potential reading may be taken as soon as the test is assembled. To obtain a reading, the lead from the SCE is inserted into the positive terminal on the voltmeter, a wire is connected between the negative terminal on the voltmeter and the binding post (specimen of

interest), and the voltage (corrosion potential) is recorded. The corrosion potential is measured every day for 40 days.

2.1.5 Corrosion Potential Tests Performed

The corrosion potential was measured for the four types of steel provided by Florida Steel in regular mortar and mortar with corrosion inhibiting concrete admixtures, when exposed to four different molal ion concentrations of NaCl. Two batches of steel were delivered from Florida Steel. The CRSH and CRST steels for both batches came from the same heat, but the H and T steels from the first batch came from a different heat than the second batch. Therefore, the H and T steels used early in the project have a slightly different chemical composition than the same types of steel used later.

Two sets of tests were run for the steel in regular mortar: one using the first batch of steel and the other using the second batch of steel. For the first batch of steel, three tests were performed for each steel type with only a 6.04 m NaCl solution (i.e., no pore solution). This was done to severely test the new steel. For the second batch of steel, two tests were done on each steel type for four concentrations of NaCl in pore solution: 0.4 m, 1.0 m, 1.6 m, and 6.04 m. The lower concentrations and the addition of the pore solution provide a closer representation of actual field conditions of reinforcing bars in concrete than the first set of tests. Two additional potential tests were completed for each steel type from the second batch of steel in pore solution only.

Crevice corrosion at the mortar-steel interface was a significant problem for the tests using the first batch of steel. Therefore, the epoxy band on the reinforcing bar was modified by using a different type of epoxy and by applying more layers of epoxy for the second set of tests. For the first batch of steel, the Scotchkote epoxy compound, manufactured by 3M, was used and only one layer of epoxy was applied to make the epoxy band. For the second batch of steel, the Corvel epoxy compound, manufactured by Morton Powder Coatings, was used and two or more layers of epoxy were applied.

Mortar with Rheocrete 222 and DCI-S were also evaluated with both batches of steel. In the first batch, only the CRSH and CRST steels were tested. The first batch of steel was used in three tests with Rheocrete 222 in 6.04 m (15%) NaCl solution and three tests with DCI-S in 1.0 m NaCl both with pore solution. For the second batch of steel, the corrosion potential was measured for all four steel types in both the Rheocrete 222 and DCI-S mortar in a 1.6 m NaCl concentration with pore solution. However with this second batch, corrosion potential tests as described here were not made; instead, potential was measured using the cathode from the macrocell tests. Two macrocell tests were completed for each steel and admixture for the 1.6 m NaCl concentration. Potential measurements were taken each week by disconnecting the macrocell test for two hours and then measuring the corrosion potential of the anode and the cathode with respect to a SCE .

2.1.6 Macrocell Test Procedure

This test measures the macrocell corrosion rate of different types of concrete reinforcing bars, when exposed to various concentrations of NaCl. Two sets of test specimens are placed in separate solutions to create a potential difference between the steel, causing macrocell corrosion. One solution contains only pore solution and the other solution contains NaCl in pore solution. The two solutions are ionically connected by a salt bridge and are electrically connected by a wire across a 10 ohm resistor. The macrocell test setup is shown in Fig. 1.5.

This section includes a description of the test components and how they are assembled. Many of the materials necessary for the macrocell test are similar to the corrosion potential test, therefore the components shown here are in addition to the components listed in section 2.1.4.

a) *Wire* - 16 gage copper wire: two at 1.3 m (4 feet), and one at 102 mm (4 in.).

b) *Terminal Box* - The terminal box is the same size as the box described for the potential test. Eight pairs of binding posts are attached to the top of the terminal box. Each

pair of binding posts has a red and black colored post. The posts are closely spaced, so that a resistor may be connected between them.

c) *Resistor* - A 10 ohm resistor with ± 2 % accuracy.

d) *Air Scrubber* - Compressed air is used to supply the cathode solution with oxygen. An air scrubber is used to remove the carbon dioxide in the compressed air, since CO_2 lowers the pH of the pore solution. The air scrubber consists of a 19 liter (5 gallon) plastic container filled with a 1 M NaOH solution. The compressed air is channeled into the container with plastic tubing. The end of the tubing in the container is sealed and punctured with hundreds of pin holes along its final four feet. Before the NaOH solution is placed in the container, the punctured tubing is coiled on the bottom of the container and weighted down with trap rock. The container is then filled with the 1M NaOH solution. The CO_2 is removed as the compressed air rises through the solution in hundreds of small air bubbles. The container is sealed at the top and the filtered air is channeled out of the container through flexible tubing. One air scrubber serves up to 32 macrocells at an air pressure of 15 psi. The maintenance of the air scubber consists of replacing the NaOH solution once a month. The pH of the solution was checked during testing on a weekly basis for one month and the pH never dropped below 14; however, approximately half the solution evaporated over the month, thus the need to replace the solution.

After the test specimens finish curing, two containers with specimens are assembled, similar to those used for the potential test. The cathode is assembled by placing two specimens inside a container and wiring the specimens together with the 102 mm (4 in.) long wire. Then the 1.3 m (4 feet) long wire is used to connect the two specimens to the black binding post on the terminal box. The cathode container is then assembled using the same procedure as for the corrosion potential test, but only pore solution is placed in the container. The anode has one specimen and is connected to the corresponding red binding post on the terminal box. The assembly procedure is the same as for the cathode, except NaCl in pore solution is used. A salt bridge connects the solution in the anode container to the solution in

the cathode container. The 10 ohm resistor is placed between the red and black binding posts on the terminal box to complete the electrical connection. A steady supply of air is then channeled to the cathode from the air scrubber. Deionized water is added to the cathode on a regular basis to account for evaporation.

The macrocell corrosion rate may be measured as soon as the test setup is complete. To determine the corrosion rate, the voltage drop across the resistor is measured by connecting wires from the negative terminal on the voltmeter to the black binding post and from the positive terminal to the red binding post. The voltage drop is recorded in millivolts. By converting the voltage reading into current density, Faraday's law may be used to calculate the macrocell corrosion rate (see Appendix A for the detailed calculation). For this test setup, the corrosion rate in μm/yr equals 32 times the voltage drop recorded in millivolts. Measurements are taken on a daily basis for 100 days.

2.1.7 Macrocell Tests Performed

This test was used to measure the macrocell corrosion rate of the four types of steel in regular mortar and mortar with corrosion inhibiting concrete admixtures, when exposed to four different molal ion concentrations of NaCl. As discussed in section 2.1.5, two batches of steel were used in this study. The first batch of steel was used in a series of macrocell corrosion tests done to modify the macrocell test procedure detailed by Martinez et al. (1990). The macrocell corrosion rates measured by Martinez et al. were unstable or non-existent. Therefore, modifications to the test setup were necessary to produce reliable corrosion rates. Initial modifications to the setup were the addition of oxygen to the cathode pore solution and the use of a 10 ohm resistor, instead of a 100,000 ohm resistor. Other modifications were made to the setup in a series of tests described below. The second batch of steel was used in a series of macrocell corrosion tests made using the modified test setup described in this chapter.

Modifications to the test setup included changing the corrosive solution at the anode and placing more test specimens at the cathode than the anode. The first set of tests were

modified by changing the solution at the anode by using only a 6.04 m (15%) NaCl solution (no pore solution). Four tests were completed for each type of steel (H, T, CRSH, CRST) cast in regular mortar. For these tests, three specimens were used at both the anode and the cathode, as done by Martinez et al. (1990). Due to an error in making these macrocells, the first two tests for each steel were made with a different pore solution than suggested by Farzammehr (1985). The incorrect pore solution consisted of 0.2 N NaOH and 0.34 N KOH, when it should have consisted of 0.45 N NaOH and 0.34 N KOH. Removing the pore solution from the anode solution provided a more severe condition than would realistically occur in the field, due to the fact that corroding reinforcing steel is surrounded by concrete and would, therefore, still have concrete pore solution present.

For the rest of the macrocell tests in this study, concrete pore solution was included in the anode solution, as originally designed by Martinez et al. (1990), so that the test setup would resemble actual field conditions. Two more tests were made with steel types H and CRST, so that a comparison could be made between tests with pore solution at the anode and tests without.

The test setup was then modified by placing twice as many test specimens at the cathode than at the anode; a 2:1 ratio. This modification was done to assure that the cathodic reaction was not controlling the corrosion rate of the macrocell. Even though an ample supply of oxygen is available in the cathode solution, there was still a concern that the oxygen may not be able to move through the mortar fast enough to meet the demand for oxygen. Two tests were made with steel types H and CRST. One test had 4 specimens at the cathode and 2 specimens at the anode, and the other test had 2 specimens at the cathode and 1 specimen at the anode.

The final set of tests in regular mortar were made with the second batch of steel and were assembled using the modified test setup, described in this chapter. Two tests were made for each steel at NaCl concentrations of 0.4 m, 1.0 m, and 1.6 m. Three tests of the T and CRSH steels and one test of the H and CRST steels were made at the 6.04 m NaCl concentration.

Only one test was necessary for the H and CRST steel, since two identical tests were completed for these steels in the last test setup for the first batch of steel.

Specimens made with mortar containing Rheocrete 222 and DCI-S were also evaluated with both batches of steel. In the first batch of steel, only the CRSH and CRST steels were tested. Four tests with Rheocrete 222 in 6.04 m (15%) NaCl and four tests with DCI-S in 1.0 m NaCl were completed. These tests used pore solution in both the anode and cathode and had three specimens at both the anode and cathode. The second batch of steel tested all four steel types in both the Rheocrete 222 and DCI-S mortar, with 1.6 m NaCl. These tests were assembled using the modified test setup, described in this chapter.

In the original scope of this study, only the CRS steels were to be evaluated with the admixtures in a 6.04 m (15%) salt concentration. Therefore, rapid tests were made with the CRSH and CRST steels cast with the Rheocrete 222 admixture in a 6.04 m salt concentration. After fabrication of these tests, the amount of salt used was reconsidered and a more realistic concentration of NaCl was chosen to be give the admixtures a fair test. Thus, the salt concentration was reduced to 1.0 m for the DCI-S admixture. Since H and T steels were never evaluated and the two admixtures were tested at different salt concentrations, new tests for the admixtures were made with all four steels at one salt concentration, 1.6 m.

2.2 Bench-Scale Tests

The Southern Exposure and the Cracked Beam tests were used to evaluate the corrosion resistance of the new reinforcing steels in concrete, when exposed to NaCl. The test specimens were measured for macrocell corrosion rate, corrosion potential, and mat-to-mat resistance. The specimens were designed so that macrocell corrosion could be easily monitored. The tests take one year to complete and are widely accepted by U.S. industry as an effective short-term test to study macrocell corrosion of reinforcing bars in concrete.

2.2.1 Materials

a) *Reinforcing Steel* - The steel used is described in Section 2.1.1.

b) *Concrete* - Three concrete mix designs were used: one for conventional concrete and two incorporating corrosion inhibiting concrete admixtures. The concrete was air entrained, with 6% air (± 1%), and a 3 inch slump (± 0.5 in.). The mix designs are shown in Table 2.3. The concrete materials were:

1. Cement, Type-I Portland cement, manufactured by Lonestar.
2. Coarse aggregate, 19 mm (3/4") Crushed Limestone, from Folgel Quarry, KS (bulk specific gravity ssd = 2.54, absorption dry = 3.33%).
3. Fine aggregate, from Lawrence Sand Pit, KS (bulk specific gravity ssd = 2.62, absorption dry = 0.32%).
4. Air Entraining Agent, Vinsol Rison, from Master Builders Inc.
5. Concrete Admixtures: Rheocrete 222, provided by Master Builders Inc., and DCI-S (calcium nitrite), provided by W.R. Grace Company.

c) *Epoxy Coatings* - The epoxy patching compound, Scotchkote (Product No. 312) by 3M, was used on the reinforcing bars. The concrete epoxy, Ceilguard 615 provided by Master Builders Inc., was used to coat the outside of the test specimens.

d) *Silicone Caulk* - The caulk, 100 percent silicone (30 year guarantee) manufactured by Macklenburg-Duncan, was used to seal the wooden dams to the concrete surface

2.2.2 Test Specimens

The Southern Exposure test specimen is shown in Fig. 1.1. It consists of 6 reinforcing bars embedded in a concrete block, 305 mm (12 in.) wide, 305 mm (12 in.) long, and 178 mm (7 in.) high. Two reinforcing bars are cast 25 mm (1 in.) from the top of the specimen, spaced 64 mm (2.5 in.) on center, and centered across the width. Four reinforcing bars are cast 25 mm (1 in.) from the bottom, spaced 64 mm (2.5 in.) center to center, and centered across the width. Each bar is 457 mm (18 in.) long and extends 76 mm (3 in.) from both sides of the concrete block. This enables an external connection to be made from the top mat of steel to the bottom mat. A wooden dam is placed around the top of the specimen to hold salt water.

The Cracked Beam test specimen is shown in Fig. 1.2. The specimen is similar to the SE specimen, with two differences: the CB specimen is half the width of the SE specimen, and a crack is initiated in the concrete through the top mat of steel. The specimen width is 152 mm (6 in.) with one bar in the top mat of steel and two bars in the bottom mat of steel. The crack is transverse to the reinforcing bar and has a width of 0.25 mm to 0.38 mm (10 to 15 mils) at the bar. The SE and CB tests were modeled after work by Pfeifer, Landgren, and Zoob (1987) and McDonald, Pfeifer, Krauss, and Sherman (1994).

2.2.3 Test Specimen Fabrication

The specimen fabrication process is completed in the following order:

a) *Reinforcing Bar Preparation* - Each reinforcing bar is cut to 457 mm (18 in.) in length. One end of the bar is drilled and tapped for a 10-24 threaded bolt to a depth of 13 mm (0.5 in.). The bar is then cleaned in an acetone bath to remove oils, grease, and dirt and the mill scale is left on the bar. Each end of the bar is completely covered with epoxy for 89 mm (3.5 in.), except for the surface of the tapped end, to prevent crevice corrosion from occurring where the reinforcing bar exits the concrete. The epoxy is mixed and applied according to manufacturers recommendations. Two coats are applied, and each coat is dried for 24 hours at 38°C (100°F) after application.

To evaluate the effectiveness of fusion-bond epoxy coating on the corrosion resistant steel, epoxy-coated bars are prepared with a deliberately damaged coating. After cutting, drilling, tapping, and cleaning the bars, as described above, the epoxy is penetrated at four evenly spaced locations using a 3 mm (1/8 in.) diameter drill. The drill penetrates only far enough to remove the epoxy coating. The bars are positioned in the SE specimens so that the holes face in the horizontal direction.

b) *Mold Assembly* - The molds are made so that the specimen is cast upside down. Each mold is made out of 19 mm (3/4 in.) thick plywood and consists of four sides and a bottom. Holes are cut in two side molds so that the reinforcing bars can extend from the mold (see Figs. 1.1 and 1.2 for dimensions). The mold pieces are held together with clamps and

the inside corners are sealed with caulk rope. Once the mold is assembled, the reinforcing bars are inserted and centered in the holes provided. Space left between the bars and mold at the holes is sealed with modeling clay.

c) *Concrete Mixing* - Concrete is mixed following the requirements of ASTM C 192 for mechanical mixing.

d) *Specimen Casting* - The specimens were cast in two layers. Each layer was vibrated according to ASTM C 192. The final layer was finished with a wooden float.

e) *Specimen Curing* - After the specimens were cast, the molds were covered with plastic and cured for 24 hours at room temperature, $23^{o}C \pm 1^{o}C$ ($74^{o}F \pm 2^{o}F$). The specimens were then removed from the mold and cured in a plastic bag with 2 liters of water for 48 hours at room temperature. The specimen was then removed from the bag and air cured for 28 days at 50 percent relative humidity. The total curing time was 31 days.

f) *Cracking the Cracked Beam Specimen* - The Cracked Beam specimen must be cracked before final preparation of the specimen. Seven days after casting, the specimen is cracked so that a transverse crack, approximately 0.3 mm wide, is placed at the top bar. To create a transverse crack, a notch is made using a transverse saw cut across the top center of the specimen. An 8 mm (0.25 in.) deep cut with a 3 mm (1/8 in.) wide blade is sufficient. Three point bending is used to initiate the crack, with the load located at the bottom center of the specimen, and the two reactions located at the top of the specimen, 25 mm (1 in.) from each end. The loads are distributed by using 25 mm (1 in.) wide, 152 mm (6 in.) long, and 6 mm (0.25 in.) thick metal plates. For this study, the load is applied using a 60 kip hydraulic universal testing machine. The load rate is 100 lb per second until the crack appears, then the loading rate is reduced by one third. Loading continues until the crack width is at least 0.4 mm at the level of the bar on both sides of the specimen.

g) *Dams and Concrete Epoxy* - Seven days before testing begins, wooden dams and concrete epoxy are placed on the SE and CB specimens. The wooden dams are 19 mm (0.75 in.) x 13 mm (0.5 in.) parting stop. The parting stop is cut into 292 mm (11.5 in.) and

140 mm (5.5 in.) long pieces. To make a dam around the top of the specimens, the SE specimen needs four long pieces and the CB specimen needs two long and two short pieces. The tops of the specimens are brushed with a wire brush to open the concrete pores on the surface of the specimen, then the dams are sealed to the top perimeter of the specimen with silicone caulking material. The silicone is allowed to dry for one day. Then the concrete epoxy is applied to all four sides of the specimen and the wooden dam. The epoxy is mixed and applied according to manufacturer's recommendations. The bottom of the concrete specimen is not epoxy coated, so that oxygen may reach the bottom mat of steel.

h) *Wiring* - Wiring for both specimens is similar.

1. A terminal box. Twelve specimens are wired to a terminal box, 203 mm (8 in.) x 152 mm (6 in.), purchased from Radio Shack. Three binding posts, two black and one red, are needed for each specimen (a total of 36 binding posts per box) and are attached in the order of black-black-red to the top of the box. A 10 ohm (± 2%) resistor is attached to the red and interior black binding posts. A 16-gage copper wire, 102 mm (4 in.) long, with a banana plug on one end and a stackable banana plug on the other end attaches the interior black post to the exterior black post.

2. 16-gage copper wire. Each specimen needs two 3 m (9 feet) long wires to attach each mat of steel on the specimen to the terminal box. 102 mm (4 in.) long wire connectors are needed to link together bars in the same mat: 4 for the SE test and 1 for the CB test.

The bars in the same mat are connected using the short connector wires and 6 mm (0.25 in.) 10-24 machined steel bolts. The long wire is then used to connect the top mat of steel to a red post on the terminal box. The other long wire connects the bottom mat of steel to the exterior black binding post that corresponds to the red post. Two coats of reinforcing bar epoxy are applied to the exposed connections on the bars.

2.2.4 Bench-Scale Test Procedures

The test procedure is the same for both the Southern Exposure and the Cracked Beam tests. The specimens are placed on wooden skids to allow for air circulation under the specimen. After the specimens have cured, a wetting and drying cycle is started to accelerate the transport of chloride ions through the concrete to the top mat of steel. The first part of the cycle consists of pouring a 15% salt water solution into the dam around the top of the specimens. The solution is ponded on the top of the specimen for 100 hours at room temperature 23°C ± 1°C (74°F ± 2°F). The dams are covered with pieces plywood to reduce evaporation. After 100 hours, the voltage drop across the 10 ohm resistor and the mat-to-mat resistance of the specimen are measured. The saltwater is removed and the corrosion potentials of the anode and the cathode are measured. The specimens are heated to 38°C ± 1.5°C (100°F ± 3°F) for 68 hours. To heat the specimen, a portable heating tent is placed over the specimen. The tent is of such a size that it can hold 6 SE and 6 CB specimens at once. Specimens undergo 48 cycles (weeks) of testing.

The heating tent is designed to be mobile. The tent is an oblong structure, 1.2 m (3.5 feet) high, 1.33 m (4 feet) wide, and 2.67 m (8 feet) long. The roof and ends are made of 19 mm (3/4 in.) thick plywood and are connected together by six 2.67 m (8 ft), studs. The sides of the tent are covered in two layers of plastic, separated by a 25 mm (1 in.) dead space. Three heating lamps (250 watts) are evenly spaced along the roof of the tent. When the tent is placed over the specimens, the lamps are 450 mm (18 in.) over the specimens. A thermostat with a temperature probe senses the temperature within the tent and maintains a temperature range of 38°C ± 1.5°C (100°F ± 3°F).

The macrocell corrosion rate is obtained each week at the end of the ponding cycle. The voltage drop is measured across the resistor at the terminal box with the use of a voltmeter. Two wires are attached from the voltmeter to the terminal box: one wire connects the negative terminal on the voltmeter to the red binding post, and the other wire connects the positive terminal to the interior black binding post with the stackable banana plug. The voltage drop is

recorded in millivolts, and by converting the voltage reading into current density, Faraday's law may be used to calculate the macrocell corrosion rate (see Appendix A for the detailed calculations). The corrosion rates in μm/yr for the SE and CB specimens are determined by multiplying the voltage drop recorded in millivolts by 4.16 and 8.32, respectively.

The mat-to-mat resistance is the total resistance between the two layers of reinforcing steel and is measured after the macrocell corrosion rate. To measure the mat-to-mat resistance, the macrocell circuit must be broken, therefore the wire connecting the two black binding posts on the terminal box is removed. The resistance is then measured using an AC-Ohm meter. The meter is connected to the red post and the exterior black post on the terminal box and the resistance is measured.

The corrosion potentials of both mats of steel are taken after the macrocell has been disconnected for 2 hours and the saltwater has been removed. The CSE test procedure described in ASTM C 876 is used to obtain the corrosion potential. The electrode is centered on top of the specimen and connected by a wire to the negative terminal on the voltmeter. Another wire is used to connect the positive terminal on the voltmeter to either the red post, which would measure the corrosion potential of the anode, or the outer black post, which would measure the corrosion potential of the cathode.

The chloride ion concentration in the concrete at the top mat of steel is determined for the SE test specimens at the initiation of corrosion and at the end of the test. The initiation of corrosion is assumed to have occurred when the corrosion potential of the anode becomes more negative than -0.35 V with respect to the CSE. A 3 gram concrete sample is removed from the specimen using a hand drill and a 6 mm (1/4 in.) concrete drill bit. To do this, the specimen is laid on its side and a hole was drilled 13 mm (1/2 in.) deep. The concrete powder is vacuumed away and discarded. The concrete bit is then cleaned with acetone. The concrete sample is obtained by drilling another 38 mm (1.5 in.) into the hole. The concrete powder is collected after every 13 mm (0.5 in) and stored in an air tight sample container.

Two samples are taken at both the initiation of corrosion and at the end of the test period for every SE specimen.

The chloride ion content is determined using the Standard Test Method for Chloride Content in Concrete Using the Specific Ion Probe (Cady and Gannon 1992). The test method does suggest that the results from this method be calibrated to the results from the AASHTO T 260 test method. Previous work has shown that measurements determined by the specific ion probe method are similar to measurements from the AASHTO method for chloride concentrations less than 1 kg/m^3, but for chloride concentrations greater than 1 kg/m^3, the measurements from the specific ion probe method underestimate the chloride concentration.

2.2.5 Bench-Scale Tests Performed

The SE and CB tests were used to measure the corrosion resistance of the four types of steel in regular concrete and concrete containing corrosion inhibiting admixtures when exposed to a NaCl solution. The first batch of steel was used in all of the specimens, except for the epoxy coated hot-rolled steel which was supplied by Chapparral Steel. There were 14 combinations of materials that were tested. A total of 42 SE and 33 CB tests were completed for this study.

This section describes the material combinations and the number of specimens cast.

1. Steel Type H, Regular Concrete, 3 SEs and 3 CBs.
2. Steel Type T, Regular Concrete, 3 SEs and 3 CBs.
3. Steel Type CRSH, Regular Concrete, 3 SEs and 3 CBs.
4. Steel Type CRST, Regular Concrete, 3 SEs and 3 CBs.
5. Steel Type H at anode and CRST at cathode, Regular Concrete, 3 SEs and 3 CBs.
6. Steel Type CRST at anode and H at cathode, Regular Concrete, 3 SEs and 3 CBs.
7. Steel Type H at anode and CRST at cathode, Regular Concrete, 3 SEs and 3 CBs.
8. Steel Type CRSH, Concrete w/Rheocrete 222, 3 SEs and 3 CBs.
9. Steel Type CRST, Concrete w/Rheocrete 222, 3 SEs and 3 CBs.
10. Steel Type CRSH, Concrete w/DCI-S, 3 SEs and 3 CBs.

11. Steel Type CRST, Concrete w/DCI-S, 3 SEs and 3 CBs.

12. Steel Type epoxy coated CRSH at anode and CRSH at cathode, Regular Concrete, 3 SEs only.

13. Steel Type epoxy coated CRST at anode and CRST at cathode, Regular Concrete, 3 SEs only.

14. Steel Type epoxy coated H at anode and H at cathode, Regular Concrete, 3 SEs only.

2.3 Mechanical Tests

The four types of steel used in this study were tested in tension to determine the percent of elongation, yield strength, and tensile strength, and in bending tests to determine compliance with the requirements of ASTM A 615. The H and T steels from the first batch (heat K4-3064) was tested by Florida Steel. The H and T steels from the second batch (heat K5-5546) and the CRSH and CRST steels (heat K3-1725) were tested at the University of Kansas. The tests were carried out to evaluate the effect of the high phosphorus content of the CRS steels on ductility.

CHAPTER 3

RESULTS AND EVALUATION

This chapter presents the test results from this study and the evaluation of those results. The chapter is divided into four sections, covering 1) the rapid corrosion potential, macrocell corrosion, Southern Exposure, and Cracked Beam tests for the four steel types cast in conventional mortar and concrete, 2) the steels cast in mortar and concrete with corrosion inhibiting admixtures, 3) the Southern Exposure tests for damaged epoxy-coated reinforcing bars, and 4) the results of the mechanical tests.

3.1 Regular Concrete or Mortar

The bulk of the experimental work focused on comparing the corrosion resistance of the four types of steel in regular concrete. The test results are presented in the first part of this section, followed by a general discussion of the performance of the individual steel types.

3.1.1 Corrosion Potential Tests

The test results show that the corrosion potentials for all four steels placed in identical concentrations of NaCl are approximately equal. The individual tests are averaged for each steel type at each salt concentration and are shown in Fig. 3.1. After 40 days, the average corrosion potentials of the reinforcing steels at each concentration of NaCl with pore solution are, approximately: -0.4 V, 0.0 m (pore solution only); -0.375 V, 0.4 m; -0.425 V, 1.0 m; -0.4 V, 1.6 m; and -0.5 V, 6.04 m (the potentials given throughout this chapter are with respect to the SCE). The average corrosion potential for the steels in a 6.04 m NaCl solution with no pore solution is -0.575 V. The number of tests averaged for each steel is shown in parenthesis by the steel abbreviation in the legends in Fig. 3.1. The tests show that the corrosion potential of the reinforcing steels become more negative as the salt concentration is increased. The individual test results for H, T, CRSH, and CRST steels are shown in Figs. 3.2 - 3.5.

The corrosion potentials observed in these tests are similar to the corrosion potentials of conventional reinforcing steel in concrete reported in other research (discussed in Section 1.2.5), with the exception of the values obtained for most specimens in pore solution and a

few specimens in the salt solutions. For steel to be passive, the corrosion potential should be more positive than -0.3 V. Only one test for the H steel and two tests for the CRSH steel show passivation in pore solution. Data from the SE and CB tests, discussed later, clearly show that all four steels passivate. Conversely, six of the specimens in contact with the salt solutions passivated when they should have had potentials more negative than -0.3 V: one H test at 1.6 m; two T tests at 0.4 m; one T test at 1.6 m; one CRSH test at 1.0 m; and one CRSH test at 1.6 m.

The reasons for the unexpected behavior are unknown. The specimens were examined after testing and crevice corrosion was found under the epoxy band at the steel-mortar interface in all cases. The crevice corrosion was so excessive that most of the specimens showed corrosion through the epoxy band. General corrosion was also observed on the exposed surface of the steel on all test specimens. How these phenomena effect the test results requires further study.

The problem of crevice corrosion under the epoxy is due to the infiltration of water through the epoxy to the steel surface. The epoxy on the specimen is softened due to being submerged in lime-saturated water during curing, thus allowing water to reach the steel surface. Less crevice corrosion was observed for the specimens with the Morton epoxy than for specimens with the Scotchkote epoxy and for specimens with two layers of epoxy than for specimens with one layer of epoxy. For most of the specimens made with one layer of Scotchkote epoxy, corrosion was so extensive that the epoxy band was blistered. For the specimens made with two layers of the Morton epoxy, crevice corrosion was present on all the specimens, but only about one third of the specimens exhibited corrosion as extensive as observed on the previous specimens. One observation on the difference in performance between the two epoxies is that the Morton epoxy band did not soften in the lime water as much as the Scotchkote epoxy: an indentation could be made with a fingernail in the Scotchkote epoxy, but not in the Morton epoxy.

3.1.2 Macrocell Tests

The average corrosion rates for the macrocell corrosion tests with no pore solution at the anode are shown in Fig. 3.6. The cathode:anode specimen ratio is 1:1. The figure has two graphs; one for the tests with the incorrect pore solution at the cathode, and one for the tests with the correct pore solution. After 100 days, the average macrocell corrosion rates for all steel types with the incorrect pore solution at the cathode are approximately the same at 4 μm/yr. The average macrocell corrosion rates for the steels with the standard pore solution at the cathode are not the same: 3.5 μm/yr for T steel, 4.5 μm/yr for CRST steel, and 6 μm/yr for H and CRSH steels. In this case, the specimens with the quenched and tempered reinforcing bars, T and CRST, have lower corrosion rates than the hot-rolled bars. The individual macrocell test results for the H, T, CRSH and CRST steels are shown in Figs. 3.7 - 3.10.

The difference in results between the tests with the standard pore solution and the incorrect pore solution may be due to a change in potential differences. The incorrect pore solution has a lower amount of NaOH than the standard pore solution. Lower NaOH causes the pH to drop. Since a lower pH makes the potential of steel more negative, the potential difference between the cathode and the anode in the macrocell is reduced, and the corrosion rates for the tests with the now nonstandard pore solution are lower than the tests with the standard pore solution.

The average macrocell corrosion rates for the H and CRST tests with the pore solution added to the anode are shown in Fig. 3.11. After 100 days, the average corrosion rates for the CRST and H tests are 2 μm/yr and 3 μm/yr, respectively. The average corrosion rate for the H steel may have been closer to 5 μm/yr, but the rate of one H test suddenly dropped 4 μm/yr at the 85th day of testing, which may indicate a faulty test. Comparing these test results with the results of the H and CRST steels without a pore solution at the anode (Fig. 3.6b) at 100 days, both steels show lower corrosion rates due to the presence of a pore solution at the anode; the average corrosion rates of both steels drop 3 μm/yr.

This reduction in the corrosion rates is partially due to a smaller potential difference between the cathode and anode. The addition of a pore solution to the salt solution at the anode, increases the pH, thus reducing the potential difference between the anode and cathode, which reduces the macrocell corrosion rate. The significant drop in corrosion rate of the CRST steel throughout the test period may indicate that a high pH must be present for the corrosion products on the corrosion resistant steel to be effective. The same cannot be said of the H steel due to the unstable result from one of the tests. The individual test results for the H and CRST steels are shown in Figs. 3.12 and 3.13.

For the macrocell test configuration with a cathode:anode specimen ratio of 2:1 and pore solution at both the cathode and the anode, the test results show that the corrosion resistant steels consistently performed better than the conventional steels at each concentration of salt. The average macrocell corrosion rates for each steel type at each salt concentration are shown in Fig. 3.14. A test was not used in the average if the rate never reached 1 μm/yr.; the actual number of tests averaged is indicated in the legends in Fig. 3.14. The individual test results for the H, T, CRSH, and CRST steels at the different salt concentrations are shown in Figs. 3.15 - 3.18, respectively.

The individual test results for each steel type varied considerably at each salt concentration. For example, the H test (Fig. 3.15) at a salt concentration of 1.0 m shows one test initially rising to a corrosion rate of 3 μm/yr at 45 days and then leveling off at a rate of 1.25 μm/yr at 100 days. The other test shows virtually no macrocell behavior until the 68th day, at which time the corrosion rate increases to 10 μm/yr and then levels off to 5 μm/yr. The varied behavior may be explained by the results of the corrosion potential tests described in section 3.1.1 in which certain steels would passivate when placed in salt solutions or corrode when placed in a simulated pore solution. If similar behavior occurs in the macrocells, the potential difference between the anode and cathode will be affected, thus affecting the macrocell corrosion rate. All specimens were examined after completion of the macrocell test. Every specimen showed crevice corrosion and general corrosion along the

exposed surface of the steel. General and pitting corrosion was found under the mortar at the anode for all steels.

Due to the low number of tests for each combination of steel type and NaCl concentration and the wide range of test results, quantifying the corrosion rate for each steel type at each concentration would be misleading. Therefore, a relative relationship was established by averaging the macrocell test rates for all four salt concentrations for each steel type (specimens for which rates never reached 1 μm/yr are not averaged). The results are shown in Fig. 3.19. At 40 days, the CRS steels are clearly corroding at a lower rate than the conventional steels, and at 100 days, the CRSH steel has the lowest relative macrocell corrosion rate followed by CRST, T, and H steels. At the end of the tests, the results show that macrocell corrosion rates of the corrosion resistant reinforcing steels are approximately half of the corrosion rates of the conventional reinforcing steels.

In future testing, the corrosion potential of the specimens at the anode and cathode should be monitored. If the cathode specimens do not passivate or if the anode specimens passivate, a potential test will be able to monitor this behavior and the test may be terminated.

3.1.3 Bench-Scale Tests

The Southern Exposure test results show that, after 48 weeks of testing, the average macrocell corrosion rate of the CRST steel is half of the corrosion rates of the other three steels. The average macrocell corrosion rates are approximately 2.25 μm/yr for the CRST and 4.5 μm/yr for the H, T, and CRSH steels (see Fig. 3.20). The individual test results for the H, T, CRSH, and CRST are given in Figs. 3.21, 3.22, 3.23, and 3.24, respectively.

The Cracked Beam test results show that, after 48 weeks of testing, the conventional steel, H, has the lowest average macrocell corrosion rate of 3 μm/yr (see Fig. 3.20). The T and CRST steels have an average macrocell corrosion rate of 4 μm/yr, and the CRSH steel has a macrocell corrosion rate of 13 μm/yr. One CB test for the T reinforcing steel is not averaged because the potential at the cathode shifted to -0.425 V (Fig. 3.26), meaning the cathode is corroding. The reinforcing bars were removed from this specimen and corrosion

was observed on the cathode bars. This behavior is believed to be due to the intrusion of salt to the cathode steel. The individual test results for the H, T, CRSH, and CRST steels are given in Figs. 3.25, 3.26, 3.27, and 3.28, respectively.

The SE and CB test results for the specimens cast with the H and CRST steel combinations show that lower macrocell corrosion rates occur when H steel is at the anode and CRST steel is at the cathode (H/CRST) compared to the same tests cast with conventional steel only, and that higher macrocell corrosion rates occur when CRST is at the anode and H steel is at the cathode (CRST/H) compared to the tests done with conventional steel. The average macrocell corrosion rates for these tests are shown in Fig. 3.29. After 41 weeks, the H/CRST and CRST/H steel combinations for the SE tests have average macrocell corrosion rates of 2 and 6 μm/yr, respectively. Not all of the SE tests completed the 48 week test period due to time constraints on this research. After 48 weeks, the H/CRST and CRST/H steel combinations for the CB tests have average macrocell corrosion rates of 3 and 7.5 μm/yr, respectively. Reasons for these differences will be discussed later in this section. The individual test results are shown in Figs. 3.30 - 3.33.

The corrosion potentials of the anodes and cathodes are approximately the same for all steel types in both the SE and CB tests. The corrosion potential of the cathode is between -0.1 V and -0.2 V with respect to the SCE. The potential of the anode is between -0.4 V and -0.5 V with respect to the SCE. Therefore, potential difference is not the primary reason for the difference in macrocell corrosion rates. The individual corrosion potential values of the cathode and anode for the H, T, CRSH, and CRST steels are shown on Figs. 3.21 to 3.24 for the SE tests and Figs. 3.25 to 3.28 for the CB tests, along with the individual macrocell corrosion rates.

The mat-to-mat resistances show that the corrosion products have a direct effect on the macrocell corrosion rate. For tests on the same steel type, the difference in corrosion rates is directly related to the resistance of the macrocell: the higher the mat-to-mat resistance; the lower the corrosion rate. This is true for all steel types for the SE and CB tests. The

individual mat-to-mat resistances for the H, T, CRSH, and CRST steels are shown in Figs. 3.21 to 3.24 for the SE tests and Figs. 3.25 to 3.28 for the CB tests, along with the individual macrocell corrosion rates and corrosion potentials.

This relationship, the higher the mat-to-mat resistance, the lower the corrosion rate, does not always hold when comparing the mat-to-mat resistance and macrocell corrosion rates of different types of steel. To compare the macrocell corrosion rate to the mat-to-mat resistance for the different steels, average mat-to-mat resistances are determined for all four reinforcing steel types for the SE and CB tests and shown in Fig. 3.34. After 48 weeks, the mat-to-mat resistance for the SE tests is the highest for the CRST steel at 3500 ohms, followed by the H, CRSH, and T steels at 3000 ohms, 2500 ohms, and 2000 ohms, respectively. After 48 weeks, the mat-to-mat resistance for the CB tests is highest for the H steel at 3000 ohms, followed by the CRST, CRSH, and T steels at 2000 ohms, 1250 ohms, and 1000 ohms, respectively.

In both the SE and CB tests, the steel with the highest mat-to-mat resistance has the lowest macrocell corrosion rate, but for the other steels in both the SE and CB tests, the trend ends. The SE tests show that the CRST steel is the most resistive and has the lowest corrosion rate. If this trend is to continue, the H steel should have the next lowest corrosion rate followed by the CRSH and T steels. The corrosion rates of the three steels are higher, but they are all the same, even though there is definite difference in resistance. The CB tests show that the H steel is the most resistive and has the lowest corrosion rate. Once again if this trend is to continue, the CRST steel should have the next lowest corrosion rates followed by the CRSH and T steels, but the CRST and T steel have the next have lowest corrosion rates, followed by the CRSH steel which has a very high corrosion rate.

Thus, there is not a consistent pattern between the average mat-to-mat resistance and the average macrocell corrosion rates for the different types of steel. It may be surmised that, for multiple tests done on a particular steel type, the corrosion rate will differ due to the change in resistance of the corrosion product, but when two different steel types are being

compared, the resistance of the corrosion product only plays a partial role in the difference in corrosion rates.

The corrosion product of reinforcing steel does more than just provide macrocell mat-to-mat resistance. The product also reduces the rate of at which oxygen, water, and chloride ions reach the steel surface. The effects of this rate reduction can be seen in the SE and CB test results for the steel combinations H/CRST and CRST/H. The H/CRST steel combination has corrosion rates less than half of the CRST/H corrosion rates for both the SE and CB tests. When comparing the H/CRST combination to the same tests done with H steel, the average corrosion rate for the SE tests decreases 2 μm/yr, and the average corrosion rate for the CB test stays at 3 μm/yr. When comparing the CRST/H tests to the H steel tests, the average corrosion rate for the SE test increases 2.5 μm/yr, and the average corrosion rate for the CB test increases 4.5 μm/yr. The reduction in corrosion rate (versus conventional steel) only occurs when the CRST acts as a cathode. This indicates that the rate of reaction at the cathode is reduced due to the presence of the corrosion resistant steel. It is important to note that for the CRST/H steel combination corrosion increases, therefore CRS steel should not be mixed with regular steel in structures.

The chloride ion content in kilograms per cubic meter of concrete is given for all southern exposure test specimens in Table 3.1. The average chloride ion concentrations at the initiation of corrosion for H, T, CRSH, CRST, H/CRST, and CRST/H steel tests are 0.6 kg/m^3, 0.6 kg/m^3, 0.7 kg/m^3, 1.1 kg/m^3, 0.7 kg/m^3, and 1.7 kg/m^3, respectively. Earlier studies have shown that for conventional steel corrosion will start at chloride concentrations between 0.6 kg/m^3 and 0.9 kg/m^3 (Berke and Hicks 1994). These test results show that the corrosion resistant steels begin corrosion at slightly higher chloride ion concentrations.

3.1.4 Discussion

The effect of quenching and tempering reinforcing steel on the macrocell corrosion rate has been positive for most of the tests. The T steel has lower initial macrocell corrosion rates than the H steel for both the SE and CB tests (Fig. 3.20). For the first 28 weeks, the T steel

for the SE test has a macrocell corrosion rate about 2 μm/yr less than the H steel, before leveling off to the same corrosion rate as the H steel at 48 weeks. For the first 16 weeks, the T steel for the CB test has a corrosion rate that is 1 to 2 μm/yr less than the H steel test. After 16 weeks, the T steel has a higher corrosion rate than the H steel, but this is the only test in which the T steel performs worse than the H steel, and the difference in corrosion rate for this test is very small, 1 μm/yr. In the relative average macrocell corrosion results (Fig. 3.19), T steel shows a lower corrosion rate than the H steel.

The reason for the slight improvement in the macrocell corrosion rate may be that the heat treatment reduces the number of available corrosion initiation sites on the steel surface, due to the outer layer of steel on the reinforcing bar being in compression. It is theorized that the microcracks on the steel surface may be squeezed together, thus reducing the total number and size of microcracks. Further research is needed to determine if this is actually what happens on the bar surface.

The full effect of the microalloying on the CRS reinforcing steels may have yet to be determined. Since the corrosion product formed by the corrosion of the CRS steel is what presumably provides the reduced macrocell corrosion rate, testing over a period of one year may not be enough time for the corrosion product to fully form. The corrosion product is reported (Jha, Singh, and Chatterjee 1992) to reduce the corrosion rate in two ways: 1) by increasing the macrocell mat-to-mat resistance; and 2) by slowing the rate at which oxygen, water, and chlorides reach the iron at the reinforcing bar surface. Therefore, a corrosion product must be fully developed before most of these mechanisms may be assessed.

The results obtained so far do raise certain concerns about using only the microalloying as a corrosion resistant steel. The CRSH steel in the CB tests has a higher macrocell corrosion rate than any other test in the entire study. This may indicate that the CRS steel needs the high pH of the concrete to form its protective oxide film. Therefore, any factors that would reduce pH, like cracked concrete or carbonation, may create higher corrosion rates in the corrosion resistant steel than conventional steel.

However, the combination of both microalloying and quenching and tempering provide the lowest overall macrocell corrosion rates. In the SE tests, the CRST steel has half the macrocell corrosion rate of the other steels. The CB tests show that the CRST steel has a slightly higher corrosion rate than the H steel, 1 to 2 μm/yr, but significantly lower corrosion rates than the CRSH steel. In the relative average macrocell corrosion results (Fig. 3.19), the CRST and CRSH steels have half the macrocell corrosion rate of the T and H steels. Therefore, the CRST steel is the most corrosion resistant steel in this study. However, the CRSH and CRST steels should be evaluated for longer periods of time to study the long-term behavior of the CRS corrosion product.

3.2 Corrosion Inhibiting Concrete Admixtures

The effects of the corrosion inhibiting concrete admixtures were evaluated for all four steels using the rapid corrosion potential and macrocell tests and for the CRS steels using the Southern Exposure and Cracked Beam tests. It is important to note that the water-cement ratio used in this study, 0.5, is generally acknowledged to provide good performance for the organic corrosion inhibitor (Berke, Dallaire, Hicks, and Hoopes 1993). However, it is higher than recommended for use with calcium nitrite (Berke, Dallaire, Hicks, and Hoopes 1993). Concrete with a water-cement ratio of 0.5 was selected to increase the rate at which sodium chloride reached the upper mat of steel; it does not, however, represent the high quality concrete that should be used in transportation structures.

3.2.1 Corrosion Potential Tests

The corrosion potential results for the CRSH and CRST steels cast with the inorganic inhibitor, DCI-S (calcium nitrite), and exposed to a 1.0 m NaCl concentration are shown in Fig. 3.35. The approximate average potentials of the CRSH and CRST tests are -0.4 V and -0.525 V, respectively. The potential of the CRSH steel is less negative than the potential of the CRST steel in the presence of the DCI-S, which indicates that the macrocell corrosion rate of the CRSH steel may be lower than the CRST steel.

For the 1.6 m NaCl solution, the corrosion potentials for all four steels were obtained from the macrocell corrosion test specimens. The corrosion potentials for the H, T, CRSH, and CRST steels are plotted in Figs. 3.36, 3.37, 3.38, and 3.39, respectively, along with the macrocell corrosion rates. The corrosion potentials of the cathodes for all four steels are approximately the same, -0.25 V to -0.3 V. The corrosion potentials of the anodes for all four steels are also approximately the same, -0.5 V to -0.55 V.

The corrosion potential results for the CRSH and CRST steels cast with the organic inhibitor, Rheocrete 222, and exposed to a 6.04 m salt concentration are shown in Fig. 3.40. The approximate corrosion potential of both the CRSH and CRST steels is -0.575 V. For the 1.6 m NaCl solution, the corrosion potentials for all four steels were obtained from the macrocell corrosion test specimens. The corrosion potentials for the H, T, CRSH, and CRST are plotted in Figs. 3.41, 3.42, 3.43, and 3.44, respectively, along with the macrocell corrosion rates. The corrosion potentials of the cathodes for all four steels are approximately the same, -0.25 V to -0.3 V. The corrosion potentials of the anodes for all four steel are approximately the same, -0.5 V to -0.6 V. As will be explained in the next section, problems encountered in curing the specimens used for these measurements may have produced data that does not reflect normal behavior.

3.2.2 Macrocell Tests

The macrocell corrosion results for the CRSH and CRST steels cast with the inorganic inhibitor, DCI-S (calcium nitrite), and exposed to a 1.0 m salt concentration are shown in Fig. 3.45. The CRSH steel shows no corrosion in two tests, and one test reaches a corrosion rate of 1 μm/yr after 100 days. The CRST steel shows higher initial corrosion than the CRSH steel at 40 days, with three tests at 1 to 2 μm/yr, but at the end of the 100 days, only one test is above 1 μm/yr. Therefore, the DCI-S proves to be a very effective corrosion inhibitor at this concentration of NaCl.

The macrocell corrosion results for the CRSH and CRST steels cast with the organic inhibitor, Rheocrete 222, and exposed to a 6.04 m salt concentration are shown in Fig. 3.46.

After 100 days, the approximate average macrocell corrosion rates for the CRSH and CRST steel are 3.5 and 3 μm/yr, respectively. The organic inhibitor corrosion rates are similar to the corrosion rates of the CRS steels in conventional mortar given in Fig. 3.14. For the CRSH and CRST steels in 6.04 m NaCl in regular mortar, the corrosion rates are 2 and 4 μm/yr, respectively. Therefore, the organic inhibitor did not provide additional protection against chlorides at the 6.04 m NaCl concentration in these tests.

In curing the specimens for the macrocell tests for the 1.6 m NaCl solution, the pH of the water in the curing tank was 10 instead of 13. Since the specimens were not properly cured, the test results (corrosion potential and macrocell currents) may not reflect normal behavior. The macrocell tests for the H and CRST steels completed 95 days of testing and the T and CRSH steels completed 100 days of testing. The approximate macrocell corrosion rates at the end of testing for H, T, CRSH, and CRST with the inorganic inhibitor are 6.5, 6 , 3, and 7.5 μm/yr, as shown in Figs. 3.36, 3.37, 3.38, and 3.39, respectively. The approximate macrocell corrosion rates at the end of testing for H, T, CRSH, and CRST with the organic inhibitor are 7.5, 10, 11, and 7.5 μm/yr, as shown in Figs. 3.41, 3.42, 3.43, and 3.44, respectively. These corrosion rates are higher than the corrosion rates for the steels in regular mortar at the 1.6 m NaCl concentration, which range from 0.25 to 6.5 μm/yr (Fig. 3.14), and the corrosion rates from the initial tests using the admixtures, which range from 0.25 to 3.25 μm/yr.

The reason for the difference in corrosion rates may be because the low pH of the water in the curing tank caused KOH, NaOH, and $Ca(OH)_2$ to leach out of the mortar during the curing period. This would result in a lower pH in the mortar and lower deposits of $Ca(OH)_2$ at the steel surface, both of which would be expected to result in a loss of passivation and an increase in corrosion. Thus, the specimens would be more susceptible to corrosion, regardless of the use of admixtures.

3.2.3 Bench-Scale Tests

The average macrocell SE and CB test corrosion rates for the corrosion resistant steels in concrete containing the two corrosion inhibiting admixtures are shown in Fig. 3.47. A more complete analysis would have included tests of all four steel types. The symbols used in Fig. 3.47 indicate the type of corrosion inhibitor, using the letter "O" for organic and "I" for inorganic (calcium nitrite), following the basic designation of the steel. The organic inhibitor results represent 42 weeks of testing, while the inorganic inhibitor results represent 38 weeks. The average macrocell corrosion rate of CRST steel for both admixtures in the SE tests is 1 μm/yr at the end of testing. The average macrocell corrosion rate of CRSH in the SE test is 5 μm/yr for the inorganic inhibitor and 1 μm/yr for the organic inhibitor at the end of testing. Thus for the SE tests, the inhibitors significantly reduce the macrocell corrosion rates of the CRS steels compared to the same steel in regular concrete (Fig. 3.20), except for the CRSH steel cast with the DCI-S admixture, which does only marginally better; the steels with the organic inhibitor have lower corrosion rates than the steels with inorganic inhibitor. The individual test results for the SE tests are shown in Figs. 3.48 - 3.51.

The CB tests show similar results to the SE tests. The average corrosion rate of both the CRSH and CRST steels with the organic inhibitor is 4 μm/yr at 4 weeks and 1.5 μm/yr at 42 weeks. The CRST steel with the inorganic inhibitor has an average corrosion rate of 3 μm/yr at 4 weeks that rises to 4 μm/yr at 38 weeks. The CRSH steel with the inorganic inhibitor starts with an average macrocell corrosion rate of 8 μm/yr at 4 weeks, that climbs to 11 μm/yr at 38 weeks. The average macrocell corrosion rate of CRSH steel in regular concrete after 38 weeks is 16 μm/yr, thus the inorganic inhibitor did reduce the macrocell corrosion rate, but not as much as the organic inhibitor. For the CB tests, the inhibitors significantly reduce the macrocell corrosion rates of the CRS steels compared to the same steel in regular concrete (Fig. 3.20), except for the CRSH steel cast with the DCI-S admixture which does only marginally better; the steels cast in concrete with the organic inhibitor have lower corrosion

rates than the steels cast in concrete with the inorganic inhibitor. The individual test results for the CB tests are shown in Figs. 3.52 - 3.55.

The potential differences between the anode and cathode for the SE and CB tests are slightly greater for the inorganic inhibitor than for the organic inhibitor. The potential of the cathode is the same for all tests, -0.1 V to -0.2 V. For the SE and CB tests with the inorganic inhibitor, the potential of the anode is the same for all tests, -0.4 V to -0.5 V, except for the SE tests with the CRST steel, which have a potential between -0.3 V and -0.4 V. For the SE and CB tests with the organic inhibitor, the potential of the anode is the same for all tests, -0.3 V to -0.4 V. Therefore, the potential difference is 0.1 V greater for the inorganic admixture than for the organic admixture, except for the CRST steel in the SE test which has the same potential difference for both admixtures. This may partially explain why the steels cast in concrete containing the organic inhibitor have a lower corrosion rate than the steels cast in concrete containing the inorganic inhibitor.

The mat-to-mat resistances are different for the CRS steels in the two admixtures. After 48 weeks, the average mat-to-mat resistance for the CRS steels in both the SE and CB tests with the inorganic inhibitor is 500 ohms. This resistance is one-half to one-fifth of the resistance measured for similar tests without an admixture (Fig. 3.34). The average mat-to-mat resistances for the CRS steels in the SE and CB tests with the organic inhibitor are 1500 and 2000 ohms, respectively. These resistances are comparable to the resistances measured in the CB tests without the admixture and approximately one half the resistances measured in the SE tests without the admixture. The lower mat-to-mat resistances of the specimens with the inorganic inhibitor may contribute to a higher corrosion rate in those specimens compared to that obtained with the organic inhibitor.

The average chloride ion concentrations at the initiation of corrosion for the CRSH and CRST steels with the inorganic inhibitor are 1.7 kg/m^3 and 3.1 kg/m^3, respectively. The concentration for the CRSH and CRST steels with the organic inhibitor are 3.0 kg/m^3 and 0.2 kg/m^3, respectively. The average chloride ion concentration for the CRSH steel with the

organic inhibitor may be misleading because, at this writing, only two out of the three test specimens had started to corrode. One of those specimens had a concentration of 5.8 kg/m^3, which is very high and may mean that the specimen sample used in the chloride ion test was contaminated. The other specimen had a chloride ion concentration of 0.3 kg/m^3.

Both inhibitors increased the "time to corrosion" for the SE test specimens. The time to corrosion for the CRS steels cast with regular concrete is 7 weeks or less (Fig. 3.20). The times for the CRSH and CRST steels are 16 and 25 weeks, respectively, with the organic inhibitor and 7 and 11 weeks, respectively, with the inorganic inhibitor.

3.3 Epoxy-Coated Reinforcing Bars with Damage

The corrosion resistance of the new steel with a damaged epoxy-coating was evaluated using the SE test. Only the anode bars were epoxy-coated and the H, CRSH, and CRST steels were tested. The tests are denoted as EH, ECRSH, and ECRST. The average macrocell corrosion rates are shown in Fig. 3.56. The rates are based on the area of epoxy-coating removed for the test (28 mm^2 per bar), not the total bar surface. After 28 weeks, the H steel has an approximate corrosion rate of 55 μm/yr. After 45 weeks, the CRSH and CRST steels have approximate average corrosion rates of 30 μm/yr and 60 μm/yr, respectively. For the CRSH tests, only two of the three tests are averaged, because one specimen has salt contamination at the cathode. Also, corrosion had not initiated in one CRSH specimen as of 45 weeks. For the CRST tests, only one of the three tests are averaged, because two tests have salt contamination at the cathode. The reinforcing bars from the contaminated test specimens were removed from their specimens and corrosion was observed at the cathode bars. The individual test results for the EH, ECRSH, and ECRST steels are shown in Figs. 3.57 - 3.59.

The time to corrosion of the epoxy-coated corrosion resistant steels is greater than the time to corrosion of the epoxy-coated H steel. The EH steel began to corrode after 10 to 14 weeks. The two ECRSH specimens began to corrode after 24 and 41 weeks, respectively. The one ECRST specimen began to corrode after 32 weeks. The overall corrosion rates of

these specimens are much higher than observed for the uncoated steel specimens (Fig. 3.20). This may be due, in part, to the size of the anode relative to the cathode and the fact that the rates are based only on the exposed area of steel (28 mm^2).

The average chloride ion concentrations at the initiation of corrosion for the EH, ECRSH, and ECRST steels are 0.4 kg/m^3, 2.3 kg/m^3, and 3.7 kg/m^3, respectively. The EH value is about the same as obtained for H steel, while the ECRSH and ECRST values are two to three times those measured for the CRSH and CRST specimens.

3.4 Mechanical Testing of the Reinforcing Bars

All four steel types were tested for their mechanical properties per ASTM A 615. The H and CRSH steels met the requirements of a Grade 300 (40) steel, while the T and CRST steels met the requirements of a Grade 400 (60) steel for yield strength, tensile strength, elongation, and bending test. A minimum of two tests were completed for each steel for each test. One bend test for the CRST steel did not meet the minimum bending requirement. The reinforcing bar cracked at the bar deformation due to a high stress concentration created by the bamboo deformation pattern. The test was repeated for the CRST bars with a diamond pattern, which met the bend test requirements. The fact that the CRSH and CRST steels passed these tests means that the microalloyed steel is a viable alternative to the standard ASTM A 615 reinforcing steel, and that the higher phosphorus content did not cause the steel to become brittle. The mechanical test results are shown in Table 3.2. The mechanical tests for the H and T steels from the K4-3064 heat were performed by Florida Steel. The balance of the tests were performed as part of this study.

CHAPTER 4

CONCLUSIONS AND RECOMMENDATIONS

4.1 Summary

The corrosion performance of a new reinforcing steel is compared with that of conventional steel. The effects of both microalloying and a special heat treatment are evaluated. The microalloying includes small increases in the percentages of copper, phosphorus, and chromium compared to conventional reinforcing steel (less than 1.5 percent total), and the heat treatment involves quenching and tempering after hot rolling. The increase in the phosphorus content exceeds the amount allowed in the ASTM specifications for reinforcing steel. The steels are evaluated using the Southern Exposure and Cracked Beam tests, which are generally accepted in United States practice, plus rapid corrosion potential and macrocell tests developed at the University of Kansas. Corrosion potential, macrocell corrosion rate, and macrocell mat-to-mat resistance are measured. Mechanical properties are compared with the requirements of ASTM A 615 to measure the affects of microalloying and heat treatment on the ductility and strength of the steel.

Four types of steel were evaluated: conventional steel, conventional steel rolled with the quenching and tempering heat treatment, microalloyed steel, and microalloyed steel with the quenching and tempering heat treatment. The test specimens consisted of the individual steel types cast in concrete for the Southern Exposure and Cracked Beam tests and in mortar for the rapid tests. A water-cement ratio of 0.5 was used for all specimens. The steels were tested in regular concrete/mortar and in concrete/mortar with corrosion inhibiting concrete admixtures. Combinations of conventional steel and corrosion resistant steel with the quenching and tempering heat treatment were tested in the Southern Exposure and Cracked Beam tests. Epoxy-coated conventional steel, microalloyed steel, and microalloyed steel with the quenching and tempering heat treatment were evaluated with holes in the coating using the Southern Exposure test.

4.2 Conclusions

The following conclusions are based on the test results and analyses presented in this report.

1. The quenched and tempered microalloyed steel exhibited half the macrocell corrosion rate of conventional reinforcing bars in the rapid macrocell corrosion and Southern Exposure tests. The CRST steel had a slightly higher macrocell corrosion rate than the H steel in the Cracked Beam test after 48 weeks, with a difference of 1 μm/yr, but the corrosion rate at the end of 48 weeks was only 4 μm/yr and decreasing.

2. The use of microalloying with the regular hot rolling process is not recommended at this time. The macrocell corrosion rate of the CRSH steel was five times that of H steel in the CB tests and had the same corrosion rate as H steel in the SE tests. Thus, microalloying did not appear to lower the macrocell corrosion rate of steel in the bench-scale tests. However, the CRSH steel had half the macrocell corrosion rate of H steel in the rapid macrocell corrosion tests, and the CRSH steel macrocell corrosion rates were steadily decreasing at the end of the CB tests. To evaluate the full effect of microalloying, the test period for the bench scale tests should be extended.

3. The use of the quenching and tempering heat treatment process following hot rolling appears to provide some corrosion resistance to reinforcing steel. The quenched and tempered regular steel had lower initial corrosion rates than conventional hot-rolled steel in the rapid macrocell corrosion and Southern Exposure tests. The only case in which the macrocell corrosion rate of T steel exceeded that of H steel was in the Cracked Beam tests, and then only marginally.

4. The corrosion potentials of all four steels in concrete, when exposed to identical concentrations of NaCl, were approximately the same.

5. The corrosion resisting mechanisms exhibited by the microalloyed steel appear to involve the deposition of protective corrosion products at both the anode and the cathode.

6. It is not recommended that the new steel be combined with conventional reinforcing steel in reinforced concrete structures. The macrocell corrosion rates were higher for the SE

and CB tests when CRST steel was placed at the anode and H steel was placed at the cathode compared to similar tests with conventional steel.

7. A phosphorus content in excess of 0.06 percent did not cause the microalloyed steel evaluated in this study to be brittle. However, the phosphorus content of the metal used in this study was 0.08% and not the 0.12% recommended by Tata Steel.

8. The corrosion inhibiting concrete admixture, Rheocrete 222 (organic), significantly reduced the macrocell corrosion rate of both the CRST and CRSH steels.

9. The corrosion inhibiting concrete admixture, DCI-S (calcium nitrite), reduced the macrocell corrosion rate of the CRST and CRSH steels, but after 36 weeks of testing, the CRSH steel in the SE tests exhibited a macrocell corrosion rate that approached the rates of steel cast in regular concrete.

10. Epoxy-coated corrosion resistant steel had a greater "time-to-corrosion" than epoxy-coated conventional steel.

11. The corrosion resistant steel had higher overall chloride ion concentrations at the initiate of corrosion compared to conventional steel.

4.3 Recommendations

1. The SE and CB test period should be extended to two years to fully evaluate the behavior of the CRS corrosion products. Over time, the corrosion products on regular steel expand, causing concrete to crack. The SE and CB tests did not run long enough to observe how the corrosion product of the microalloyed steel affect the concrete.

2. The quality of construction of the SE and CB specimens should be improved if longer testing periods are to be completed. After approximately 9 months, the wooden dams around the top of the specimens begin to leak, due seepage through the wood and the silicone losing its bond with the concrete and the wood. To eliminate this problem, the dam should be made of concrete. By modifying the specimen molds, a 51 mm (2 in.) wide by 51 mm (2 in.) high dam can be cast monolithically with the specimen.

3. Plastic wedges should be used to maintain the crack width in the Cracked Beam specimens. Alternatively, removable plastic inserts should be used to establish grooves of known width to serve as cracks in the CB specimens.

4. The concentration of the salt solution for use in the Cracked Beam test should be reduced from 15 to 3 or 4 percent. This would provide more realistic conditions, closer to what would be expected on a cracked bridge deck.

5. Once a month, polarization resistance measurements of the reinforcing bars should be taken for all tests. This would measure the microcell corrosion rate of the individual reinforcing bars, thus providing a more thorough analysis of the reinforcing steel.

6. A longer testing cycle is recommended for the SE and CB tests. A longer drying time would dry out more of the test specimen and end up drawing in the chlorides further during the ponding cycle. A two week test cycle would be sufficient, one week drying, one week ponding. Measurements could be made after every cycle or every month.

4.4 Future Work

Further work is necessary to understand the corrosion product developed by the corrosion resistant steel and to fully utilize the rapid macrocell tests.

1. The specimen used for the rapid potential and macrocell tests has problems with crevice corrosion. This may be the reason why reproducing test results is so difficult. Different materials should be evaluated to make an epoxy band that is less susceptible to water and adheres more tightly to the steel surface than the epoxies used in this study.

2. The Cracked Beam test should be modified to study the effects of a longitudinal crack along the length of the bar. Both transverse and longitudinal cracks appear on bridge decks, therefore, both should be studied.

3. Additional heats of corrosion resistant steel should be evaluated using the tests in this study, modified as suggested in this chapter. Of particular interest is an evaluation of microalloyed steel containing the maximum percentages recommended by Tata Steel.

4. New testing techniques should be implemented to gain greater insight into the corrosion inhibiting mechanisms provided by the microalloying and the quenching and tempering heat treatment process.

REFERENCES

AASHTO T 260-84. (1990). "Standard Method of Sampling and Testing for Total Chloride Ion in Concrete and Concrete Raw Materials," *Standard Specifications for Transportation Materials and Methods of Sampling and Testing*, Part II Tests, 15th Ed., American Association of State Highway and Transportation Officials, D.C., pp. 771-777.

ASTM A 615/A 615M-94. (1995). "Standard Specification for Deformed and Plain Billet-Steel Bars for Concrete Reinforcement," *1995 Annual Book of ASTM Standards*, Vol. 1.04, American Society for Testing and Materials, Philadelphia, PA, pp. 300-310.

ASTM C 192-90a. (1994). "Standard Practice for Making and Curing Concrete Test Specimens in the Laboratory," *1994 Annual Book of ASTM Standards*, Vol. 4.02, American Society for Testing and Materials, Philadelphia, PA, pp. 113-119.

ASTM C 778-92a. (1994). "Standard Specification for Standard Sand," *1994 Annual Book of ASTM Standards*, Vol. 4.01, American Society for Testing and Materials, Philadelphia, PA, pp. 323-325.

ASTM C 876-91. (1994). "Standard Test Method for Half-Cell Potentials of Uncoated Reinforcing Steel in Concrete," *1994 Annual Book of ASTM Standards*, Vol. 4.02, American Society for Testing and Materials, Philadelphia, PA, pp. 432-437.

ASTM G 59-91. (1994). "Practice for Conducting Potentiodynamic Resistance Measurements," *1994 Annual Book of ASTM Standards*, Vol. 3.02, American Society for Testing and Materials, Philadelphia, PA, pp. 230-237.

ASTM G 109-92. (1994). "Standard Test Method for Determining the Effects of Chemical Admixtures on the Corrosion of Embedded Steel Reinforcement in Concrete Exposed to Chloride Environments," *1994 Annual Book of ASTM Standards*, Vol. 3.02, American Society for Testing and Materials, Philadelphia, PA, pp. 465-469.

Berke, N. S., Shen, D. F., and Sundberg, K. M. (1990). "Comparison of the Polarization Resistance Technique to the Macrocell Corrosion Technique," *Corrosion Rates of Steel in Concrete*, ASTM STP 1065, American Society for Testing and Materials, Philadelphia, PA, pp. 38-51.

Berke, N. S., and Hicks, M. C. (1990). "Electrochemical Methods of Determining the Corrosivity of Steel in Concrete," *Corrosion Testing and Evaluation: Silver Anniversary Volume*, Babraiam/Deam editors, ASTM STP 1000, November, pp. 425-440.

Berke, N. S., and Tourney, P. (1993). "A Call for Standardized Tests for Corrosion-Inhibiting Admixtures," *Concrete International*, Vol. 22, No. 4, April, pp. 57-62.

Berke, N. S., Dallaire, M. P., Hicks, M. C., and Hoopes, R. J. (1993). "Corrosion of Steel in Cracked Concrete," *Corrosion Engineering*, Vol. 49, No. 11, November, pp. 934-943.

Berke, N. S., and Hicks, M. C. (1994). "Predicting Chloride Profiles in Concrete," *Corrosion Engineering*, Vol. 50, No. 3, March, pp. 234-239.

Cady, P. D., and Gannon, E. J. (1992). *Condition Evaluation of Concrete Bridges Relative to Reinforcement in Concrete*, Vol. 1, State of the Art of Mixing Methods, SHRP-S/FR-92-103; Strategic Highway Research Program, National Research Council, Washington, D.C., 70 pp.

Cady, P. D., and Gannon, E. J. (1992). "Standard Test Method for Chloride Content in Concrete Using the Specific Ion Probe," *Condition Evaluation of Concrete Bridges Relative to Reinforcement in Concrete*, Vol. 8, Procedure Manual, SHRP-S/FR-92-110; Strategic Highway Research Program, National Research Council, Washington, D.C., pp. 85-105.

Clear, K.C. (1989). "Measuring Rate of Corrosion of Steel in Field Concrete Structures," Transportation Research Record 1211 (Washington, D.C.: Transportation Research Board), pp. 28-37.

Fontana, M. G. (1986). *Corrosion Engineering,* 3rd. Ed., McGraw Hill, New York, 556 pp.

Farzammehr, H. (1985). "Pore Solution Analysis of Sodium Chloride and Calcium Chloride Containing Cement Pastes," *Master of Science Thesis*, University of Oklahoma, Norman, OK, 101 pp.

Jha, R., Singh, S. K., and Chatterjee, A. (1992). "Development of New Corrosion-Resistant Steel Reinforcing Bars," *Materials Performance*, NACE, Vol. 31, No. 4, April, pp. 68-72.

Jones, D. A. (1992). *Principles and Prevention of Corrosion.*, Macmillan Publishing Company, New York, 568 pp.

Locke, C. E. (1986). "Corrosion of Steel in Portland Cement Concrete: Fundamental Studies," *Corrosion Effect of Stray Currents and the Techniques for Evaluating Corrosion of Rebars in Concrete*, ASTM STP 906, American Society for Testing and Materials, Philadelphia, pp. 5-14.

Martinez, S. L., Darwin, D., McCabe, S. L., and Locke, C. E. (1990). "Rapid Test for Corrosion Effects of Deicing Chemicals in Reinforced Concrete," SL Report 90-4, University of Kansas Center for Research, Lawrence, Kansas, Aug., 61 pp.

McDonald, D. B., Pfeifer, D. W., Krauss, P., and Sherman, M. R. (1994). "Test Methods for New Breeds of Reinforcing Bars," *Corrosion and Corrosion Protection of Steel in Concrete,* Vol. II, Proceedings of International Conference held at the University of Sheffield, July, pp. 1155-1171.

Munn, R. S. editor. (1992). *Computer Modeling in Corrosion*, ASTM STP 1154, Philadelphia, PA, 291 pp.

Nmai, C. K., Bury, M. A., and Farzam, H. (1994). "Corrosion Evaluation of a Sodium Thiocyanate-Based Admixture," *Concrete International*, Vol. 24, No. 4, April, pp. 22-24.

Page, C. L., and Treadway, K. W. J. (1992). "Aspects of the Electrochemistry of Steel in Concrete," *Nature,* Vol. 297, No. 5862, May, pp. 109-115.

Pfeifer, D. W., Landgren, R. J., and Zoob, A. (1987). "Protective Systems for New Prestressed and Substructure Concrete," *Report* No. FHWA/RD-86/193, Federal Highway Administration, McLean, VA, April, 133 pp.

Pfeifer, D. W., and Landgren, R. J. (1992). "Corrosion Resistant Reinforcement For Concrete Components," *Technical Proposal - Part I,* DTFH61-93-R-00027, Federal Highway Administration, Washington D.C., July, 77 pp.

Schiessl, P. (1988). "Corrosion of Steel in Concrete" *Report of the Technical Commitee* 60-CSC, RILEM, Chapman and Hall, New York, 97 pp.

Slater, J. E. (1983). *Corrosion of Metals in Association with Concrete,* ASTM Special Technical Publication 818, America Society for Testing and Materials, Philadelphia, 83 pp.

Stearn, M. S., and Geary, A. J. (1985). *Journal of the Electrochemical Society*, Vol. 105, No. 638.

Tata Iron and Steel Co. (1991). "Development of New Corrosion Resistant Steel (CRS) at Tata Steel," *Report,* Jamshedpur, India, 32 pp.

Uhlig, H. H., and Revie, R. R. (1985). *Corrosion and Corrosion Control: An Introduction to Corrosion Science and Engineering*, John Wiley & Sons, New York, 441 pp.

W.R. Grace Construction Products (1993) "A Call for Standardized Tests For Corrosion Inhibiting Admixtures," *Report*, W.R. Grace & Co.-Conn., Cambridge, Mass, 6 pp.

Table 1.1 - Chemical Composition of 16 mm (No. 5) Steel Reinforcing Bars

Chemical Composition (%)

Steel Type	C	Mn	S	V	Si	Ni	Sn	Mo	P	Cr	Cu	P+Cr+Cu	*C.E.
Florida Steel H and T (Batch 1) Heat K4-3064	0.36	0.67	0.027	0.002	0.17	0.09	0.011	0.016	0.017	0.12	0.30	0.44	0.53
Florida Steel H and T (Batch 2) Heat K5-5546	0.32	0.72	0.044	0.000	0.22	0.14	0.011	0.018	0.026	0.14	0.34	0.51	0.50
Chaparral Steel H Heat 2-0977	0.43	0.75	0.017	0.000	0.30	0.09	0.000	0.019	0.018	0.11	0.23	0.36	0.60
Florida Steel CRSH and CRST Heat K3-1725	0.20	0.76	0.032	0.003	0.23	0.11	0.011	0.011	0.080	0.53	0.44	1.05	0.48
Tata Steel Recommended Chemistry for CRS	0.18 max.	0.85 max.	0.035 max.		0.45 max.				0.120 max.	0.80 max.	0.50 max.	0.90 min.	0.30 to 0.45

*Carbon Equivalent = C + Mn/6 + (Cu + Ni) / 15 + (Cr + Mo) / 5 + V / 0.5

Table 2.1 - Mortar Mix Design

Types of Mortar	Water (g)	Cement (g)	Sand (g)	Rheocrete 222 (mL)	DCI-S (mL)
Regular	2640	5280	10,560	---	---
Rheocrete 222	2607	5280	10,560	33	---
DCI-S (Calcium Nitrite)	2510	5280	10,560	---	130

Table 2.2 Parts Description of the Mold for the Test Specimen used for the Rapid Corrosion Potential and Time to Corrosion Tests.

A: No. 6.5 Rubber Stopper (Laboratory grade)
- A 16 mm (0.625in.) diameter hole is drilled into the center of the stopper.

B: 1 in. to 1 in. PVC Fitting (ASTM D 2466), internal diameter 33 mm (1.3 in.)
- At one end of the fitting, the external diameter is machined down to a 41 mm. (1.60 in.) so that it will fit into connector, D.

C: No. 9 Rubber Stopper (Laboratory grade)
- A 16 mm (0.625in.) diameter hole is drilled into the center of the stopper.

D: 1.25 in. to 1.25 in. PVC Fitting (ASTM D 2466), internal diameter 42 mm (1.65 in.)
- One end of the fitting is shortened 14 mm (0.55 in.).

E: 1 in. PVC Pipe (ASTM D 2466), internal diameter 30 mm (1.18 in.)
- The pipe is cut into 102 mm (4 in.) lengths and sliced longitudinally along one side through its thickness.

F: Two - 51 mm (2 in.) x 203 mm (8 in.) x 381 mm (15 in.) Pieces of CCA Treated Wood
- The bottom piece has eight holes on the top surface centered two wide and four deep. Each hole is 52 mm (2 in.) in diameter and 6mm (0.25 in.) deep.
- The top piece has eight holes centered two wide and four deep. Each hole is 33 mm (1-5/16 in.) in diameter through half of the thickness of the wood piece and 25 mm (1 in.) in diameter through the other half.
- Six holes are drilled through the thickness of the top and bottom pieces to recieve 6 mm (0.25 in.) diameter threaded rods.

G: Six - 6 mm (0.25 in.) x 305 mm (12 in.) Threaded Rods
- Each rod has one nut, one wing nut, and two washers.

Table 2.3 Concrete Mix Design

Type	Water (kg/m^3)	Cement (kg/m^3)	Coarse Aggregate (kg/m^3)	Fine Aggregate (kg/m^3)	Vinsol Resin (ml/m^3)	Rheocrete 222 (ml/m^3)	DCI-S (ml/m^3)
Regular Mix	169	338	824	882	167	---	---
Organic Inhibitor	164	344	824	879	2,057	3,785	---
Inorganic Inhibitor	145	322	824	911	97	---	15,140

Table 3.1 Chloride Ion Concentration of Southern Exposure Specimens

	At Initiation of Corrosion				At End of One Year			
	Test Number				Test Number			
	1 (kg/m^3)	2 (kg/m^3)	3 (kg/m^3)	Average (kg/m^3)	1 (kg/m^3)	2 (kg/m^3)	3 (kg/m^3)	Average (kg/m^3)
H	0.7	0.5	0.5	0.6	1.3	3.7	N.T.	2.5
T	0.9	0.1	0.7	0.6	5.0	9.7	N.T.	7.4
CRSH	0.1	1.1	0.8	0.7	7.8	3.7	N.T.	5.8
CRST	0.4	1.2	1.8	1.1	4.7	5.4	N.T.	5.0
H/CRST	0.8	0.5	0.7	0.7	N.T.	N.T.	N.T.	---
CRST/H	3.6	0.1	1.4	1.7	N.T.	N.T.	N.T.	---
EH	0.4	N.T.[1]	0.3	0.4	N.T.	N.T.	N.T.	---
ECRSH	C.S.[2]	N.C.[3]	2.3	2.3	C.S.	N.T.	N.T.	---
ECRST	5.4	C.S.	2.1	3.7	C.S.	C.S.	N.T.	---
CRSHO	N.C.	5.8	0.3	3.0	N.T.	N.T.	N.T.	---
CRSTO	0.2	0.2	0.2	0.2	N.T.	N.T.	N.T.	---
CRSHI	1.2	0.9	2.9	1.7	N.T.	N.T.	N.T.	---
CRSTI	4.3	3.1	2.1	3.1	N.T.	N.T.	N.T.	---

N.T.[1]: Not Taken: Indicates that a sample was not taken from the specimen.

C.S.[2]: Contaminated Specimen: Indicates that the test was stopped.

N.C.[3]: No Corrosion: Indicates that corrosion had not started for this specimen.

Table 3.2 Mechanical Test Results for 16 mm (No. 5) Steel Reinforcing Bars

Steel Type	Heat ID No.	Yield Strength MPa	Tensile Strength MPa	Elongation percent	Bend Test
H	K5-5546	384	612	17.3	pass
T	K5-5546	545	702	12.3	pass
H	K4-3064	---	---	---	pass
T	K4-3064	585	701	15.0	pass
CRSH	K3-1725	350	565	22.7	pass
CRST	K3-1725	570	700	12.0	pass

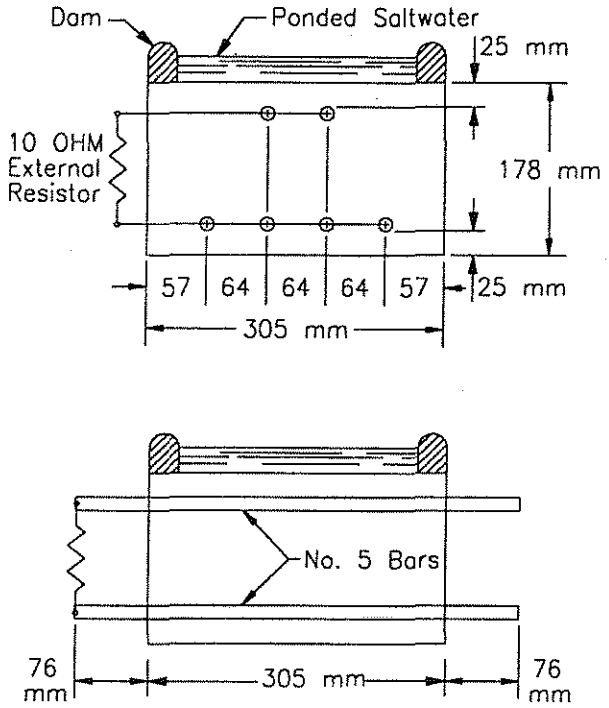

Figure 1.1 End and Side Views of the Southern Exposure Test Specimen

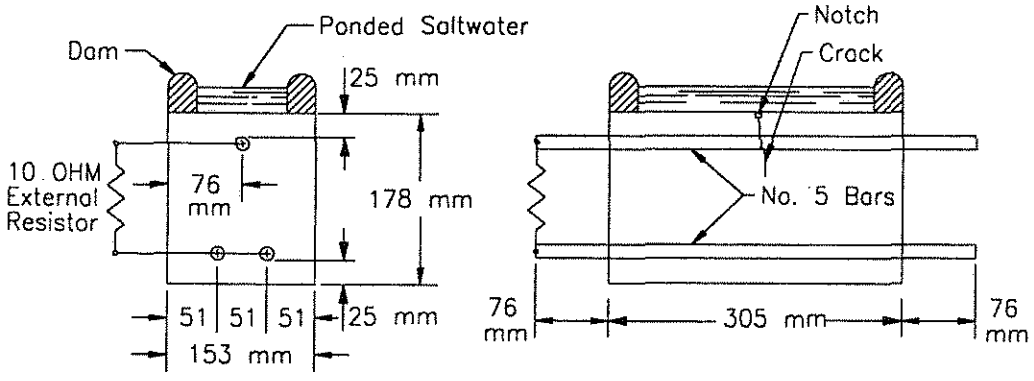

Figure 1.2 End and Side Views of the Cracked Beam Test Specimen

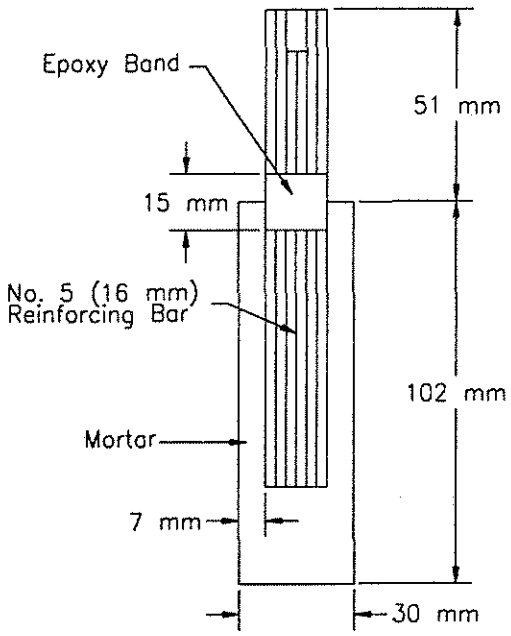

Figure 1.3 Cross Section of Test Specimen needed for Rapid Corrosion Potential and Time to Corrosion Tests

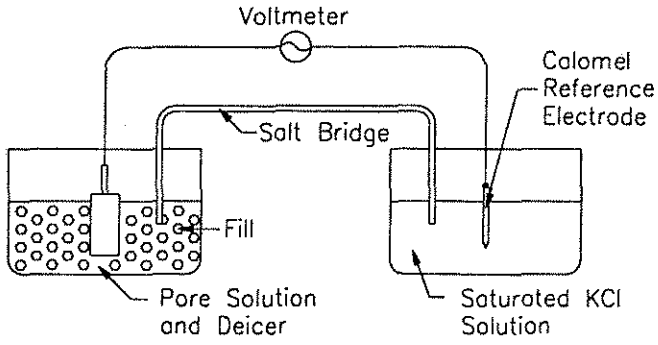

Figure 1.4 Schematic of Corrosion Potential Test

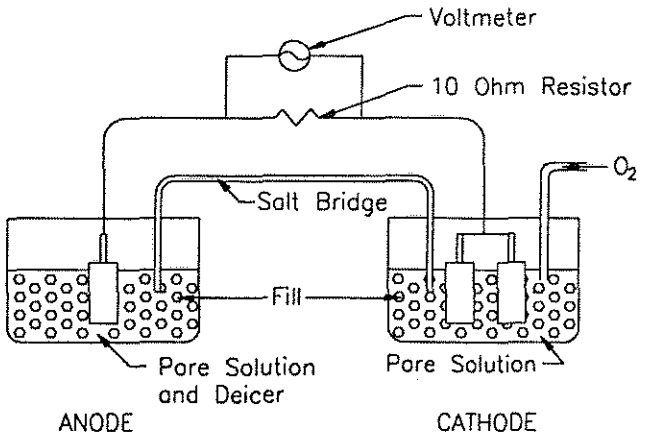

Figure 1.5 Schematic of Macrocell Corrosion Test

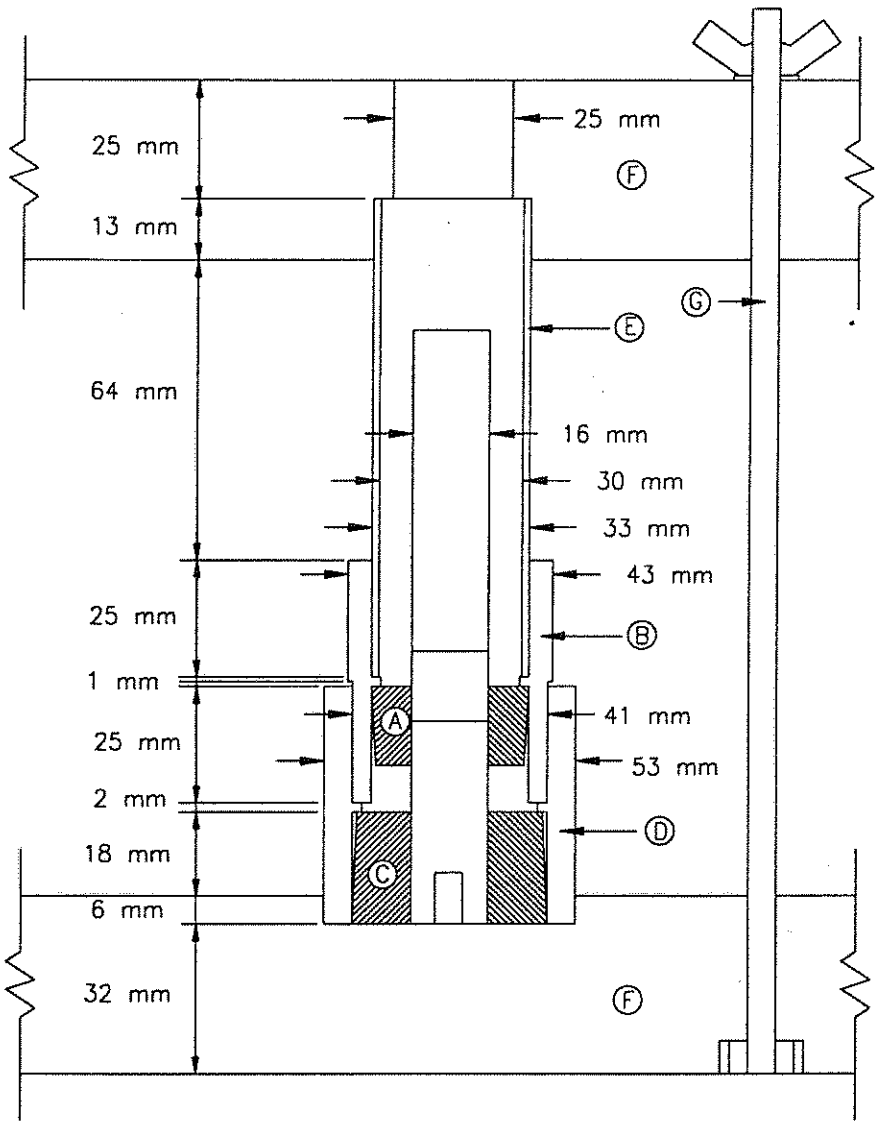

Figure 2.1 Cross Section of Mold for the Test Specimen needed for Rapid Corrosion Potential and Time to Corrosion Tests.

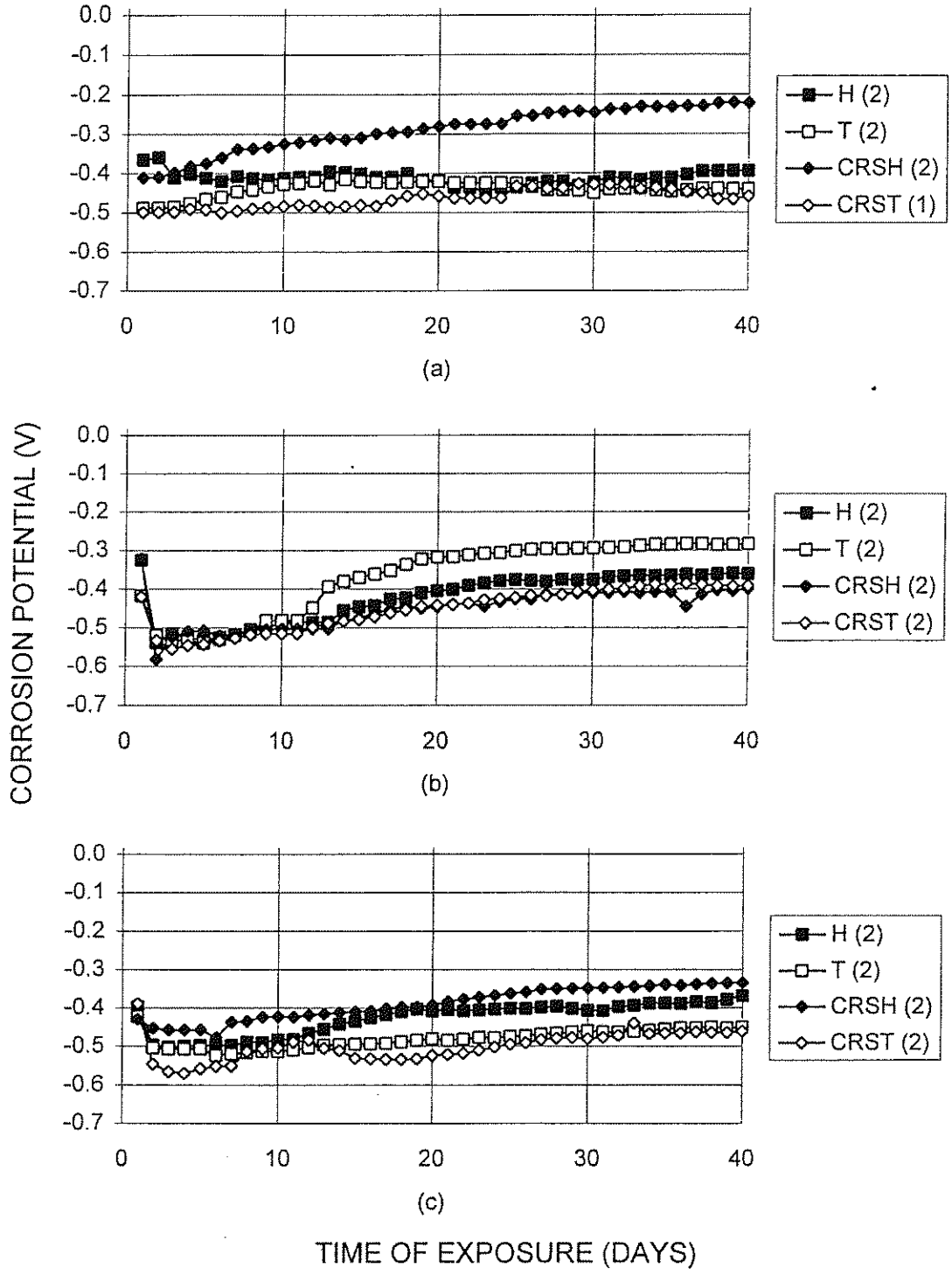

Fig. 3.1 Corrosion Potential Test: Average corrosion potential for different steels in different concentrations of NaCl. (a) 0.0 m, (b) 0.4 m, (c) 1.0 m, (d) 1.6 m, (e) 6.04 m, and (f) 6.04 m (no pore solution)

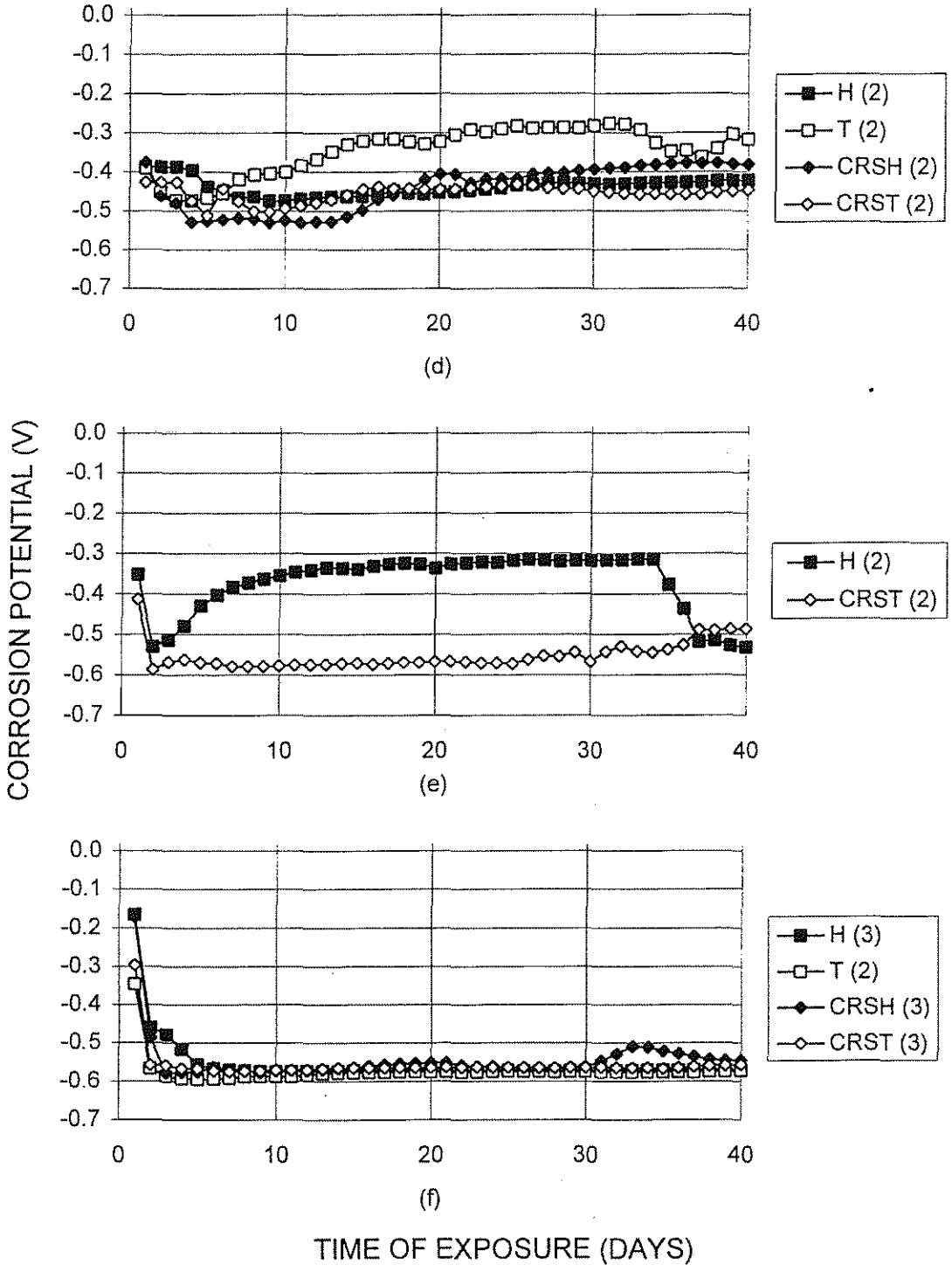

Fig. 3.1 (Continued) Corrosion Potential Test: Average corrosion potential for different steels in different concentrations of NaCl. (a) 0.0 m, (b) 0.4 m, (c) 1.0 m, (d) 1.6 m, (e) 6.04 m, and (f) 6.04 m (no pore solution)

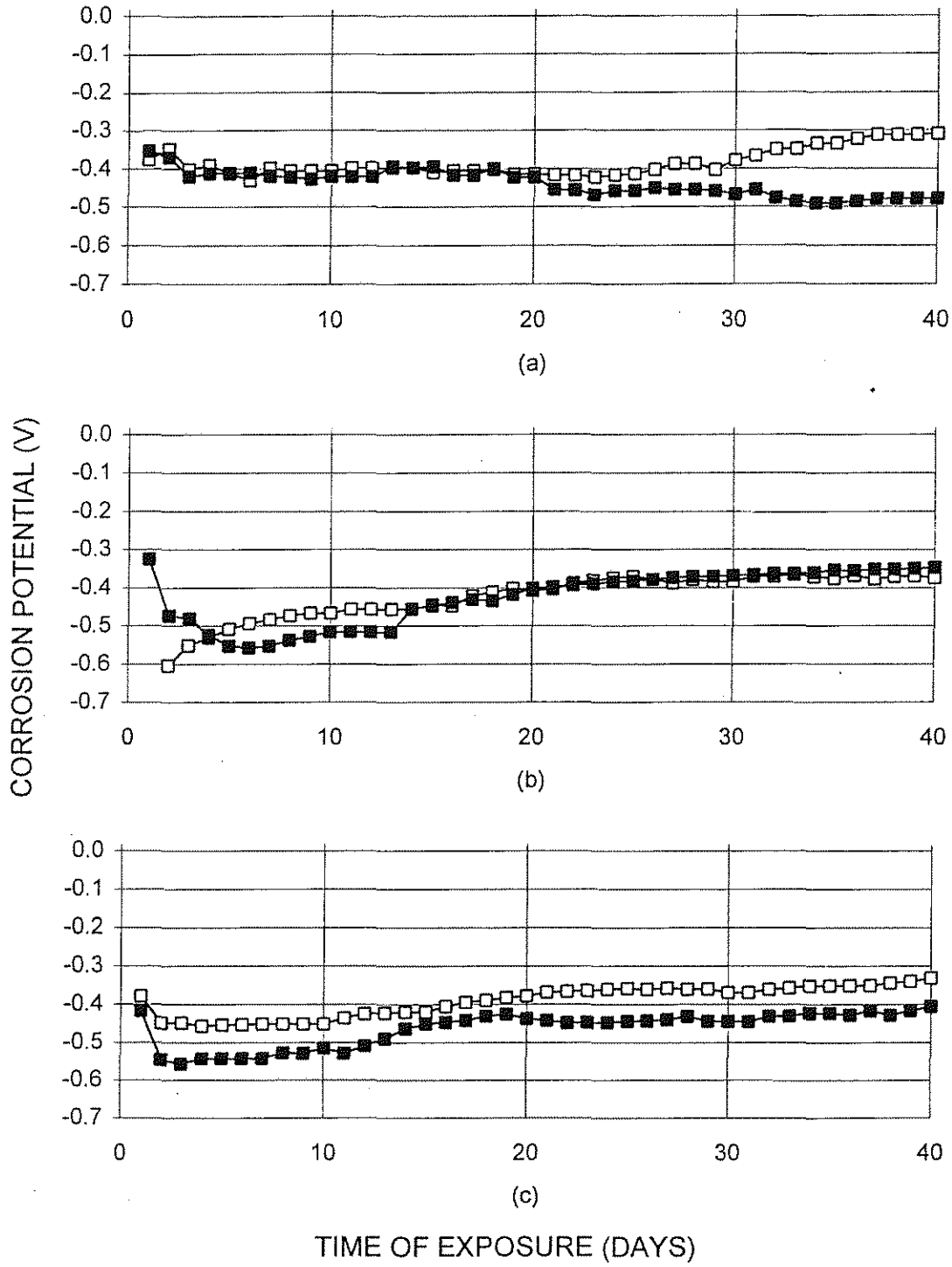

Fig. 3.2 Corrosion Potential Test: Corrosion potential for H steel in different concentrations of NaCl. (a) 0.0 m, (b) 0.4 m, (c) 1.0 m, (d) 1.6 m, (e) 6.04 m, and (f) 6.04 m (no pore solution)

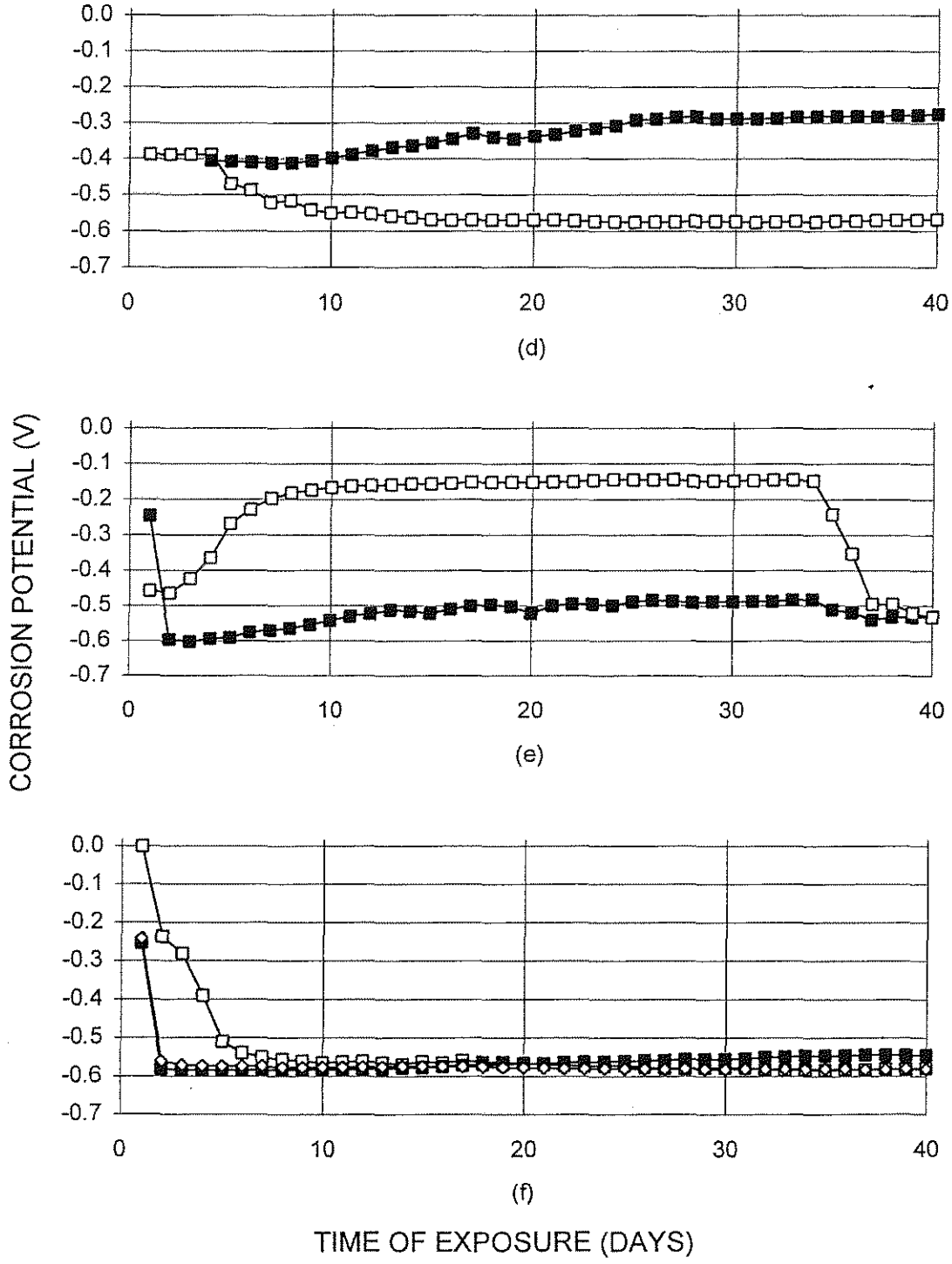

Fig. 3.2 (Continued) Corrosion Potential Test: Corrosion potential for H steel in different concentrations of NaCl. (a) 0.0 m, (b) 0.4 m, (c) 1.0 m, (d) 1.6 m, (e) 6.04 m, and (f) 6.04 m (no pore solution)

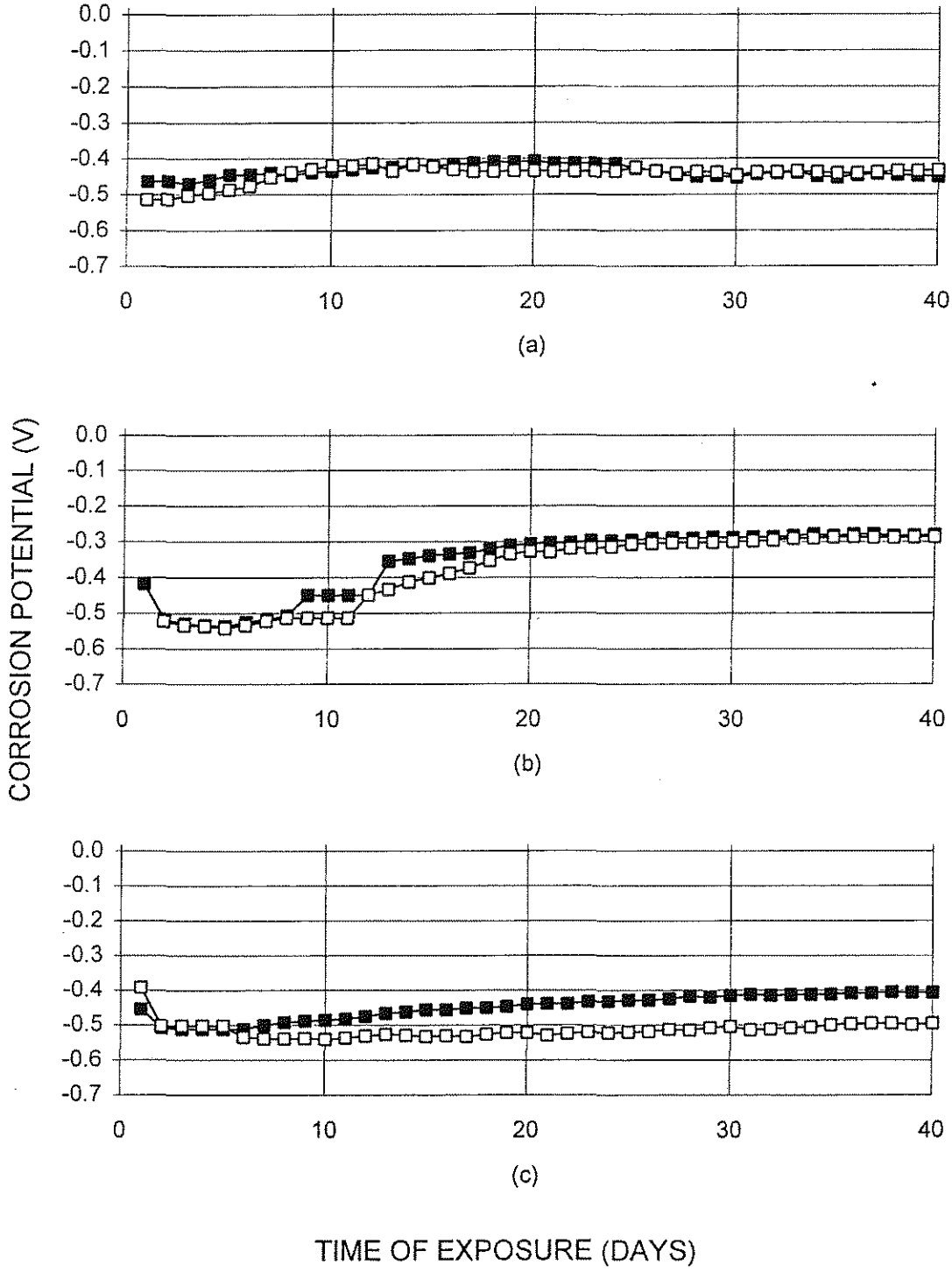

Fig. 3.3 Corrosion Potential Test: Corrosion potential for T steel in different concentrations of NaCl. (a) 0.0 m, (b) 0.4 m, (c) 1.0 m, (d) 1.6 m, and (e) 6.04 m (no pore solution)

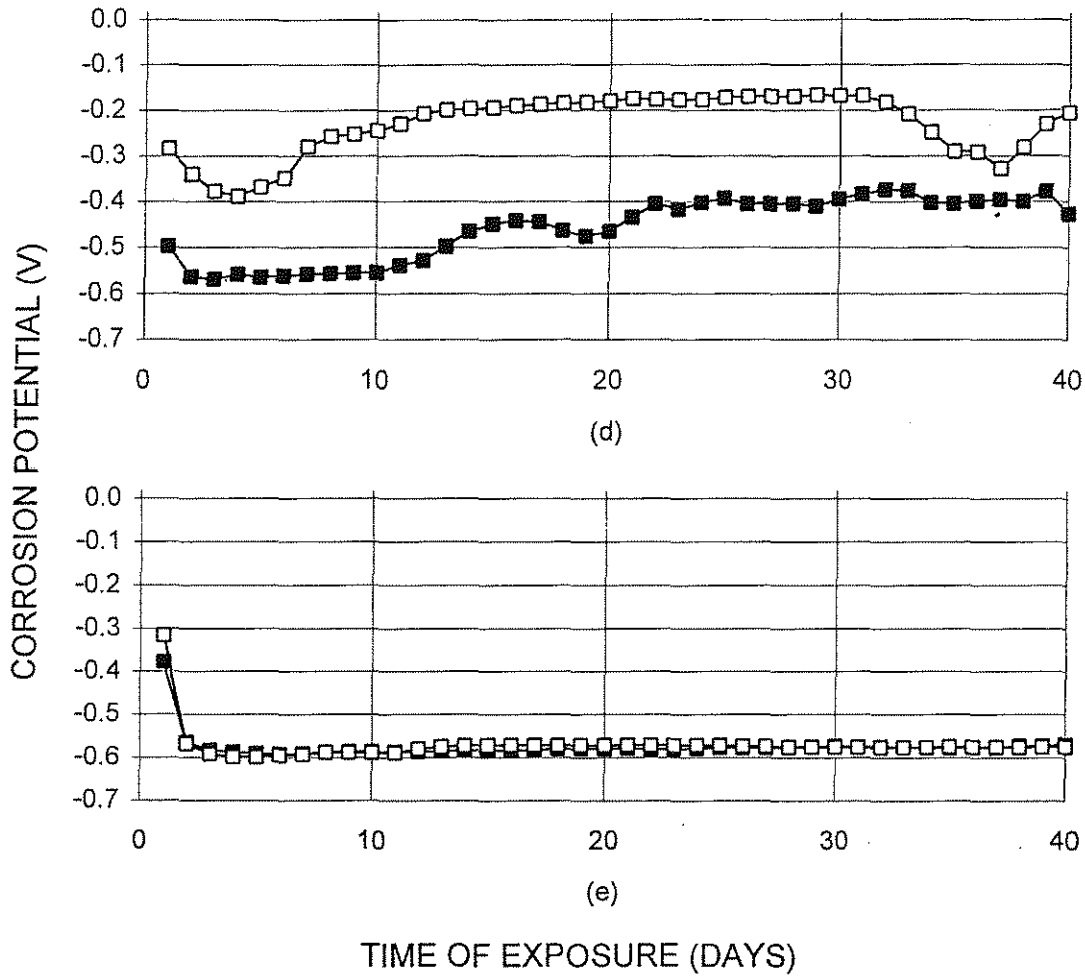

Fig. 3.3 (Continued) Corrosion Potential Test: Corrosion potential for T steel in different concentrations of NaCl. (a) 0.0 m, (b) 0.4 m, (c) 1.0 m, (d) 1.6 m, and (e) 6.04 m (no pore solution)

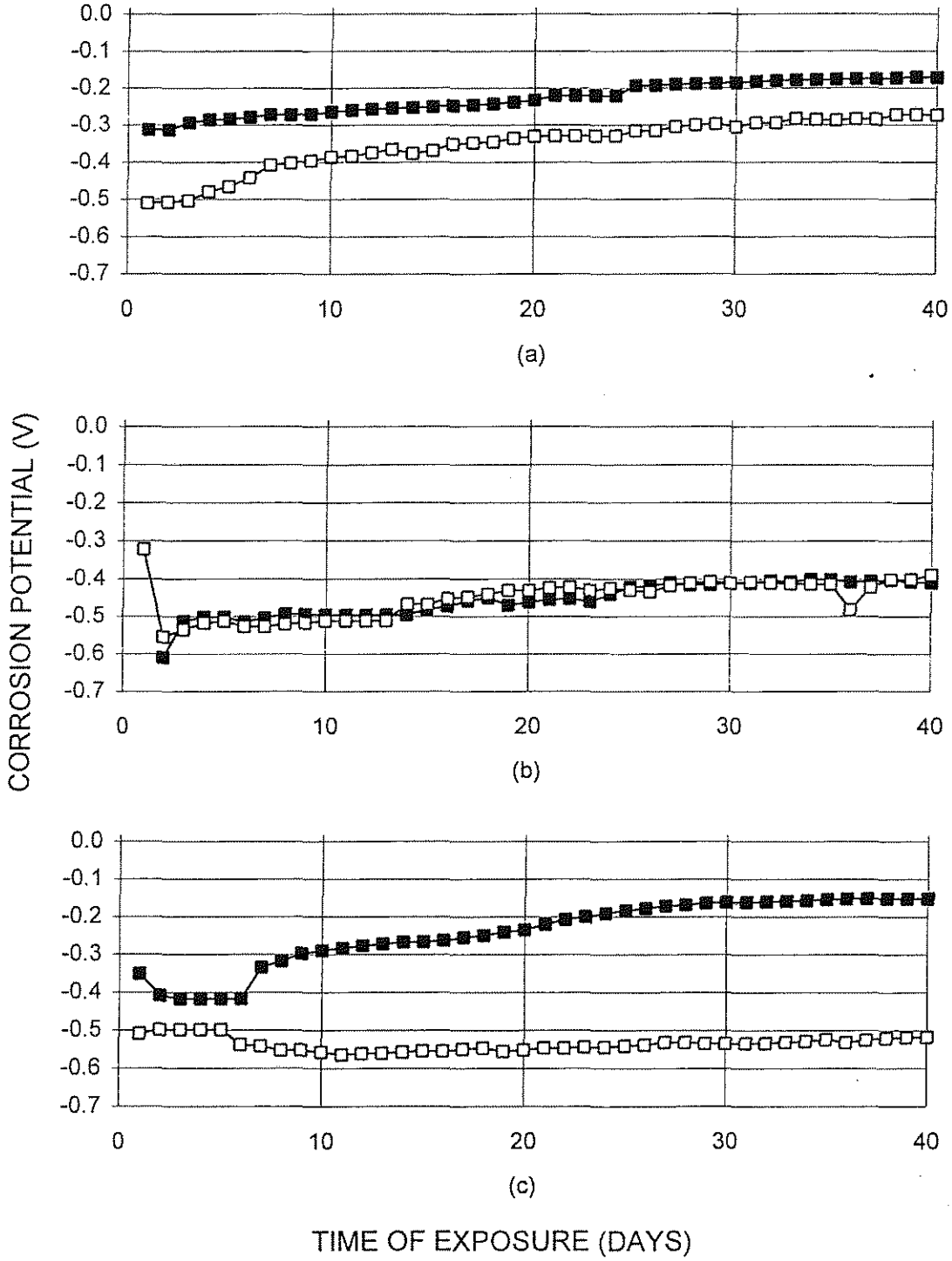

Fig. 3.4 Corrosion Potential Test: Corrosion potential for CRSH steel in different concentrations of NaCl. (a) 0.0 m, (b) 0.4 m, (c) 1.0 m, (d) 1.6 m, and (e) 6.04 m (no pore solution)

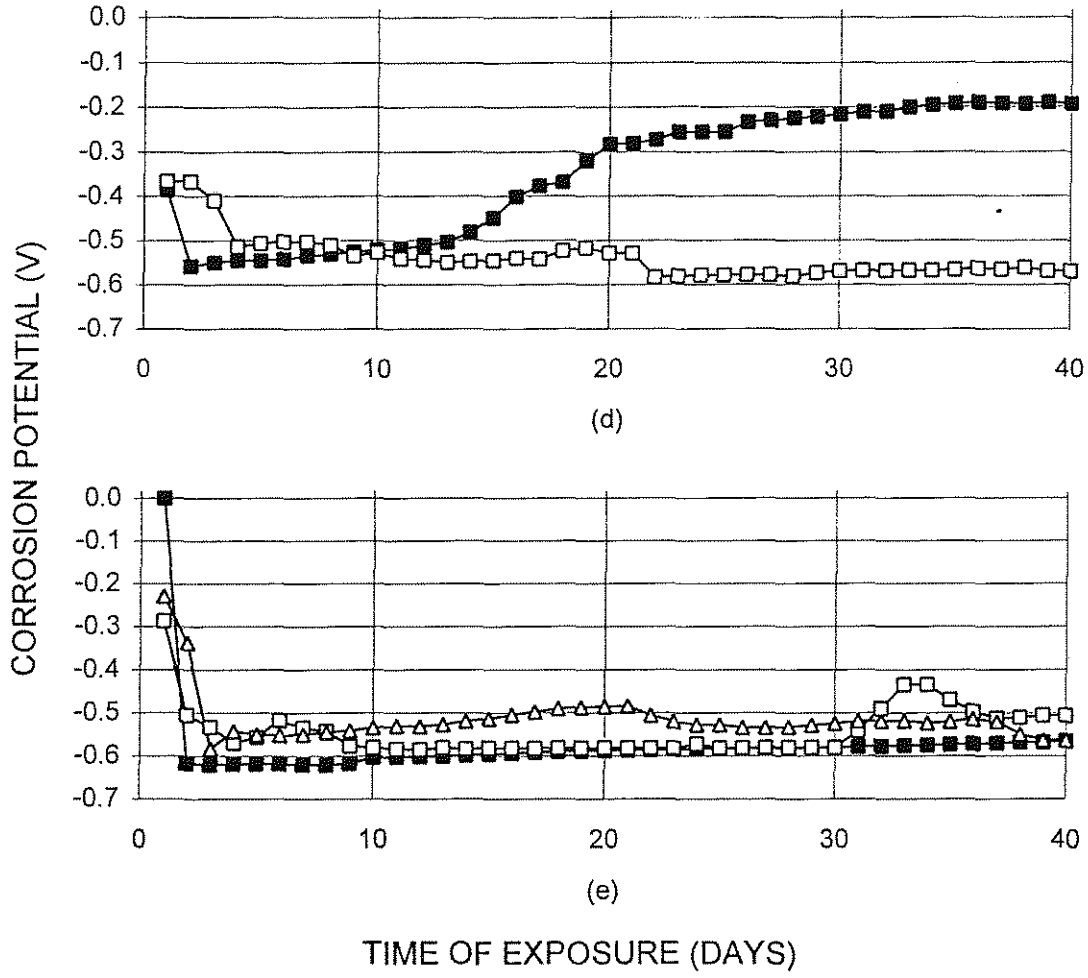

Fig. 3.4 (Continued) Corrosion Potential Test: Corrosion potential for CRSH steel in different concentrations of NaCl. (a) 0.0 m, (b) 0.4 m, (c) 1.0 m, (d) 1.6 m, and (e) 6.04 m (no pore solution)

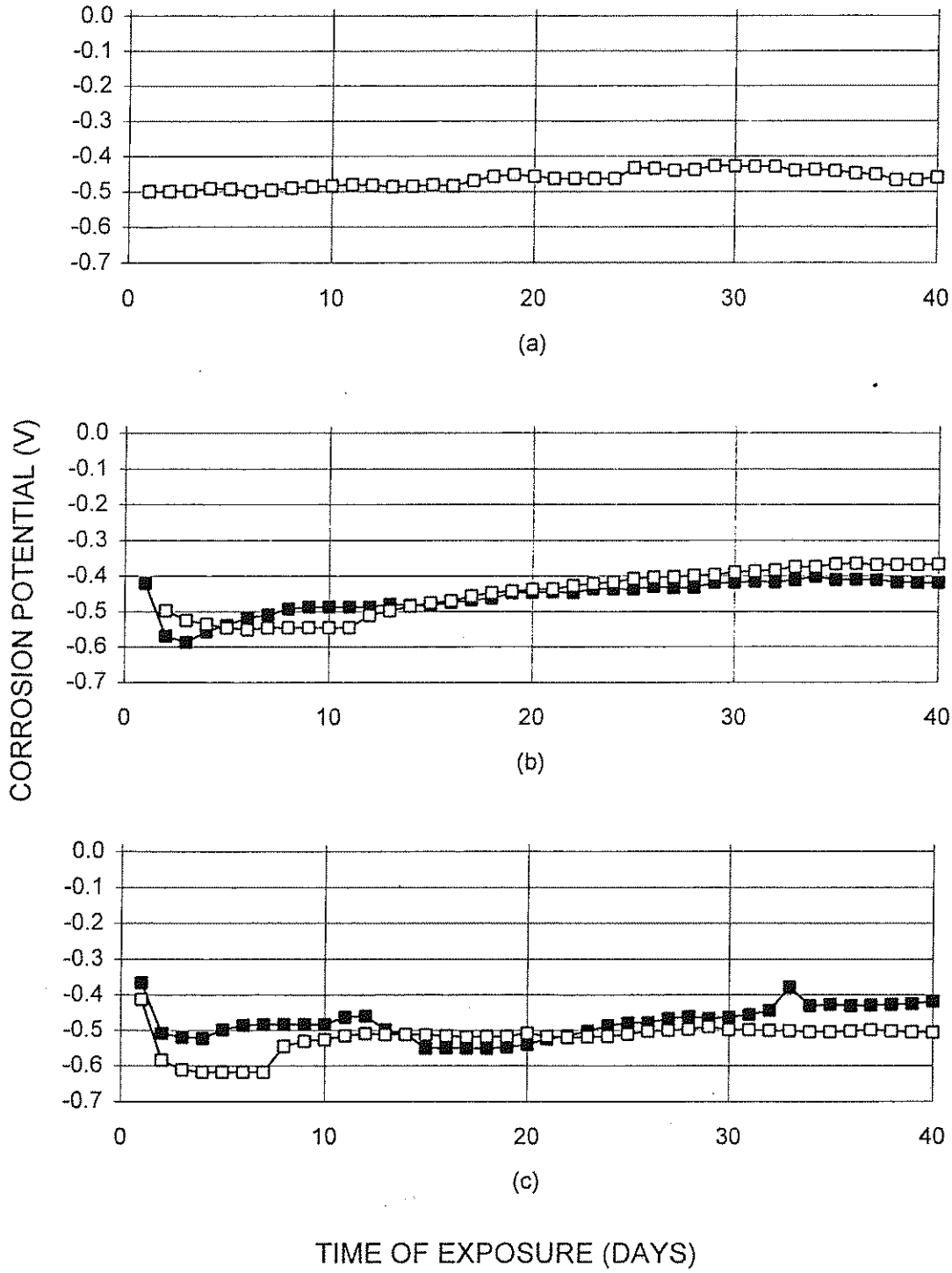

Fig. 3.5 Corrosion Potential Test: Corrosion potential for CRST steel in different concentrations of NaCl. (a) 0.0 m, (b) 0.4 m, (c) 1.0 m, (d) 1.6 m, (e) 6.04 m, and (f) 6.04 m (no pore solution)

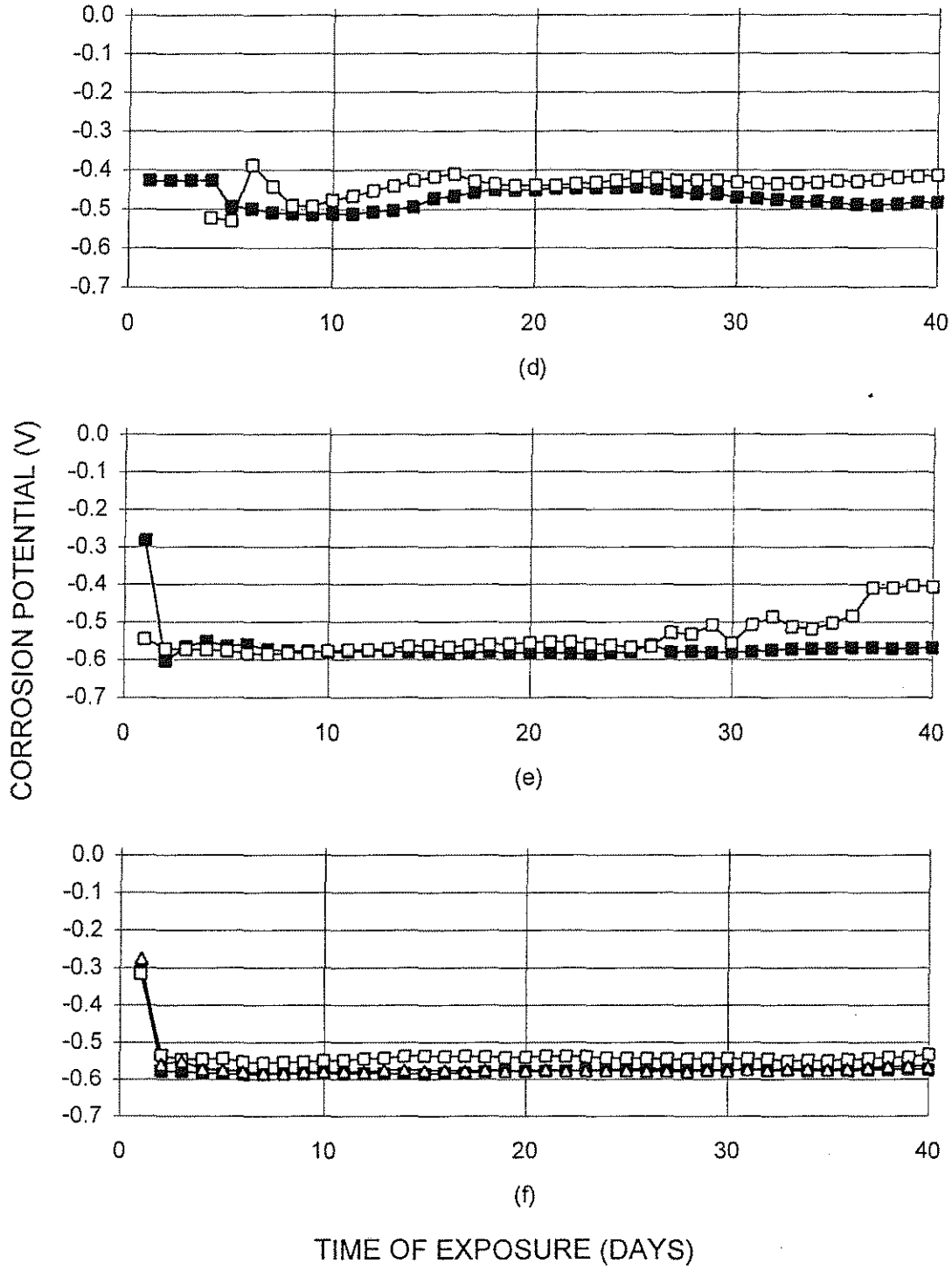

Fig. 3.5 (Continued) Corrosion Potential Test: Corrosion potential for CRST steel in different concentrations of NaCl. (a) 0.0 m, (b) 0.4 m, (c) 1.0 m, (d) 1.6 m, (e) 6.04 m, and (f) 6.04 m (no pore solution)

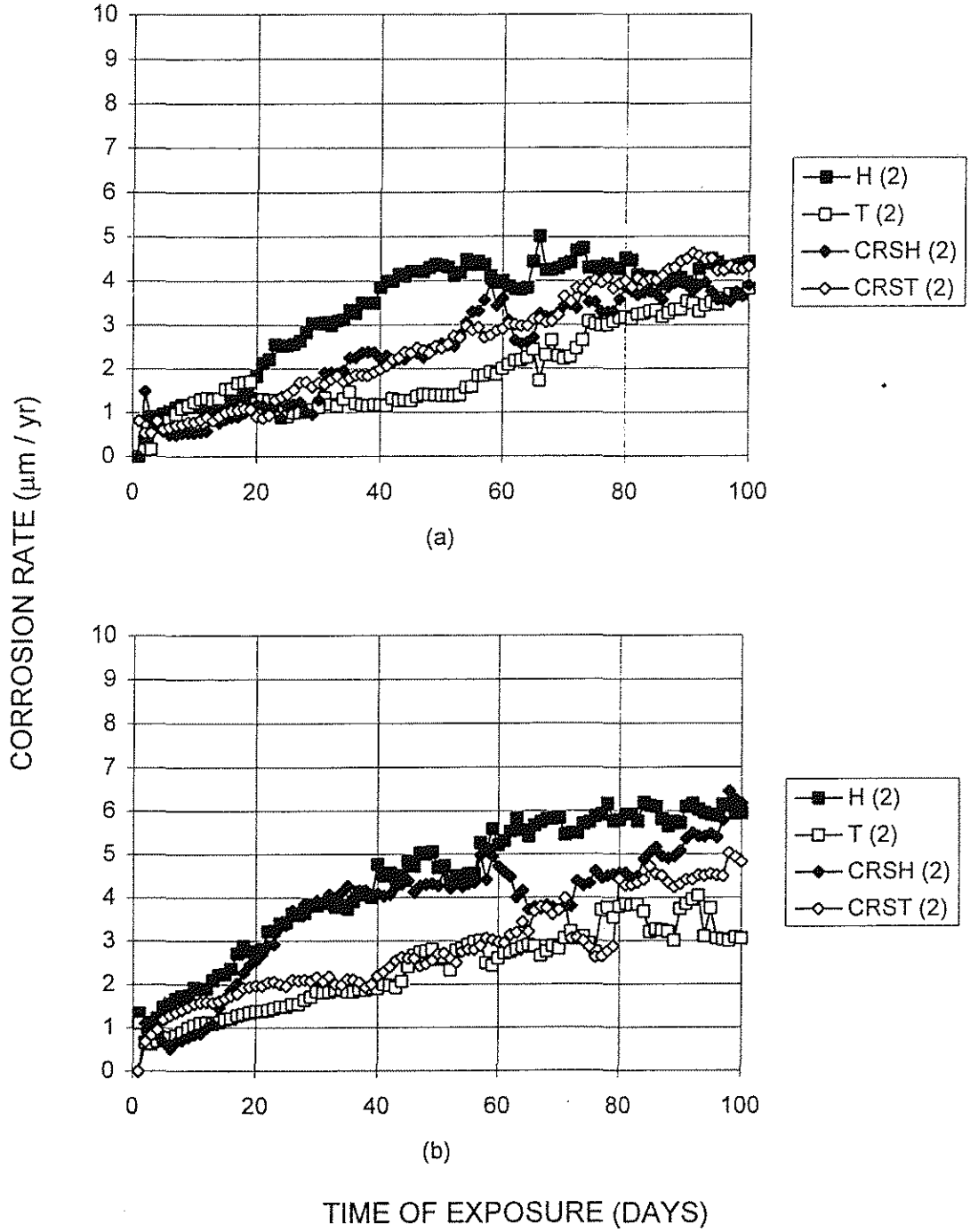

Fig. 3.6 Macrocell Test: Average corrosion rates for different steels in a 6.04 m NaCl solution (no pore solution at the anode) and a cathode:anode specimen ratio of 1:1. (a) Incorrect pore solution at the cathode and (b) Standard pore solution at the cathode

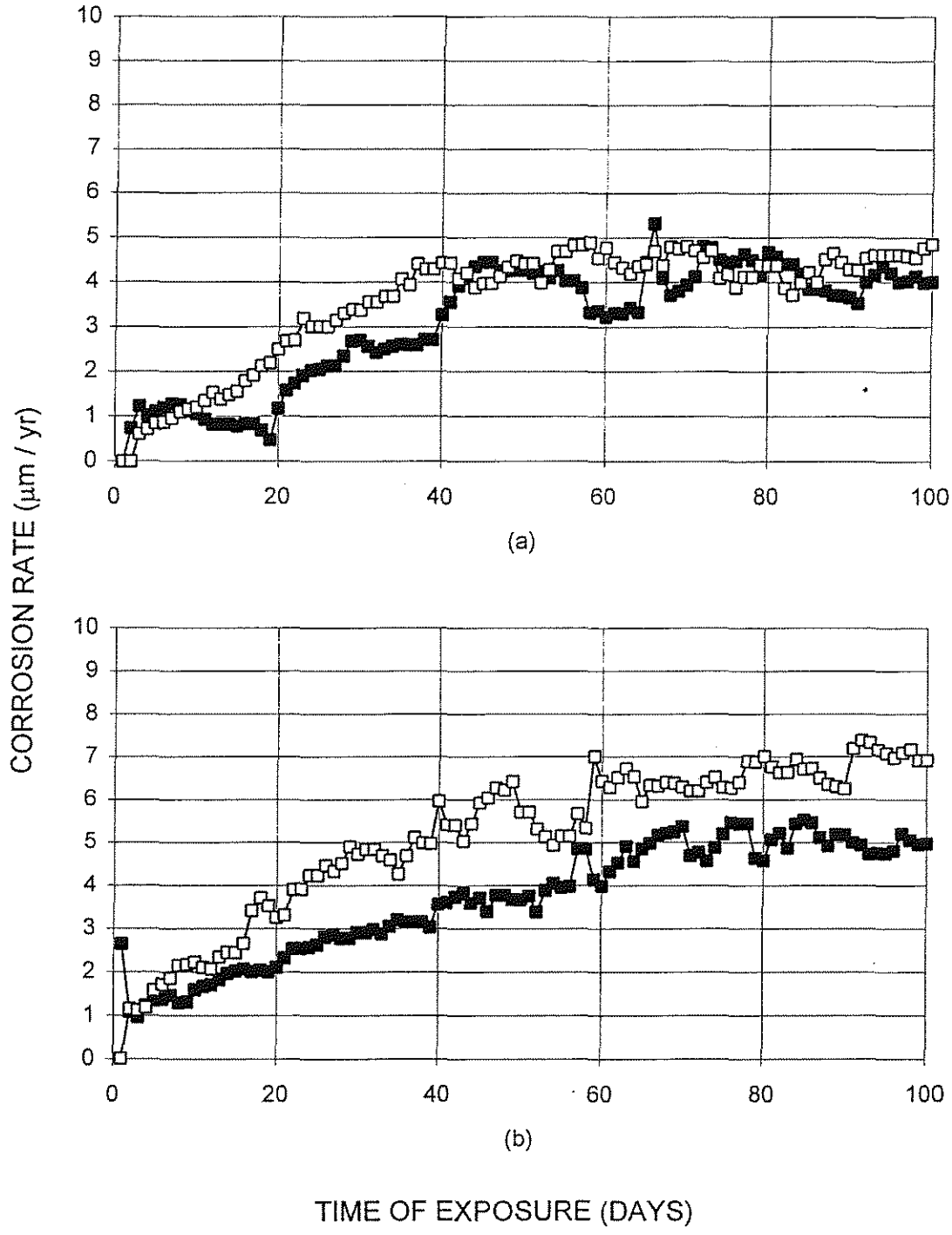

Fig. 3.7 Macrocell Test: Corrosion rate for H steel in a 6.04 m NaCl solution (no pore solution at the anode) and a cathode:anode specimen ratio of 1:1. (a) Incorrect pore solution at the cathode and (b) Standard pore solution at the cathode

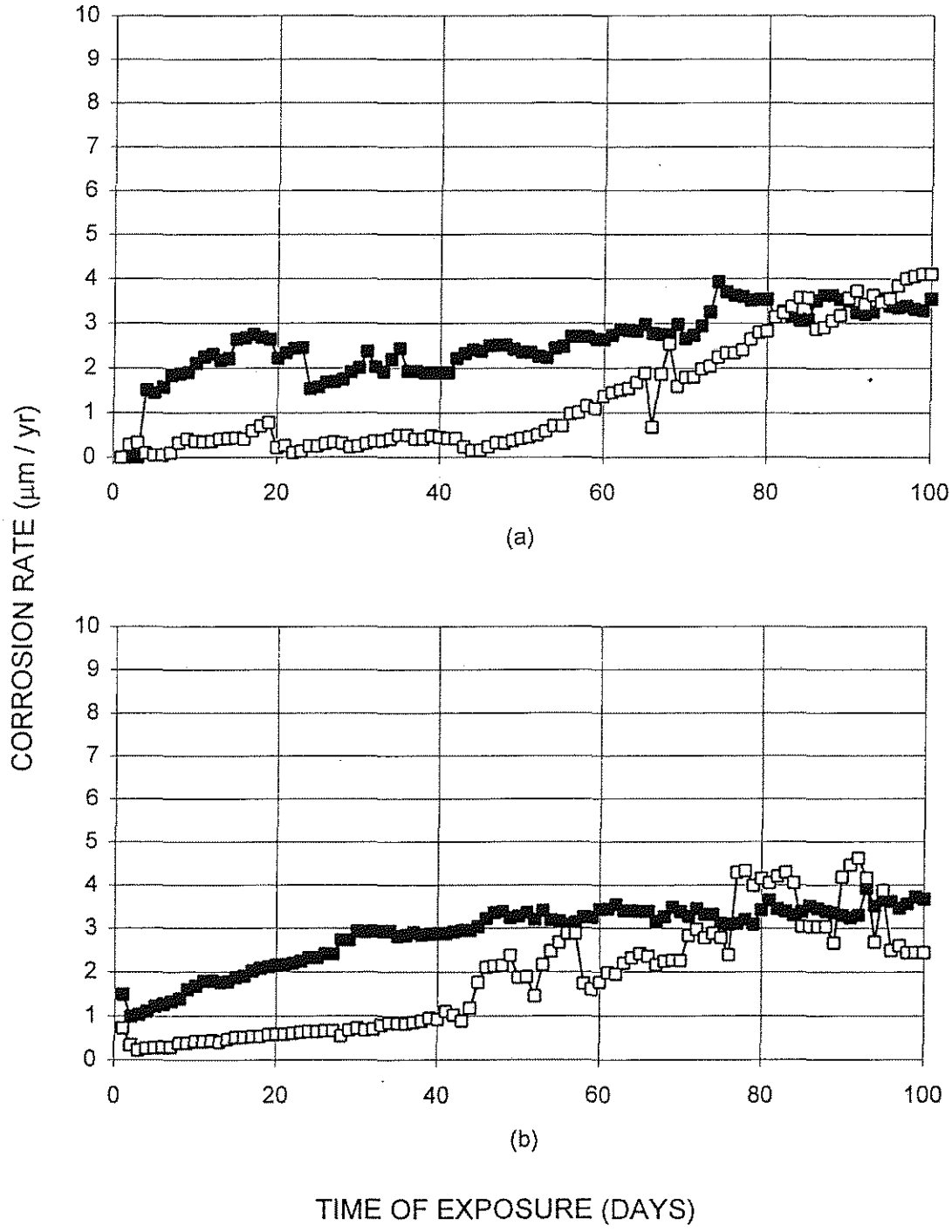

Fig. 3.8 Macrocell Test: Corrosion rate for T steel in a 6.04 m NaCl solution (no pore solution at the anode) and a cathode:anode specimen ratio of 1:1. (a) Incorrect pore solution at the cathode and (b) Standard pore solution at the cathode

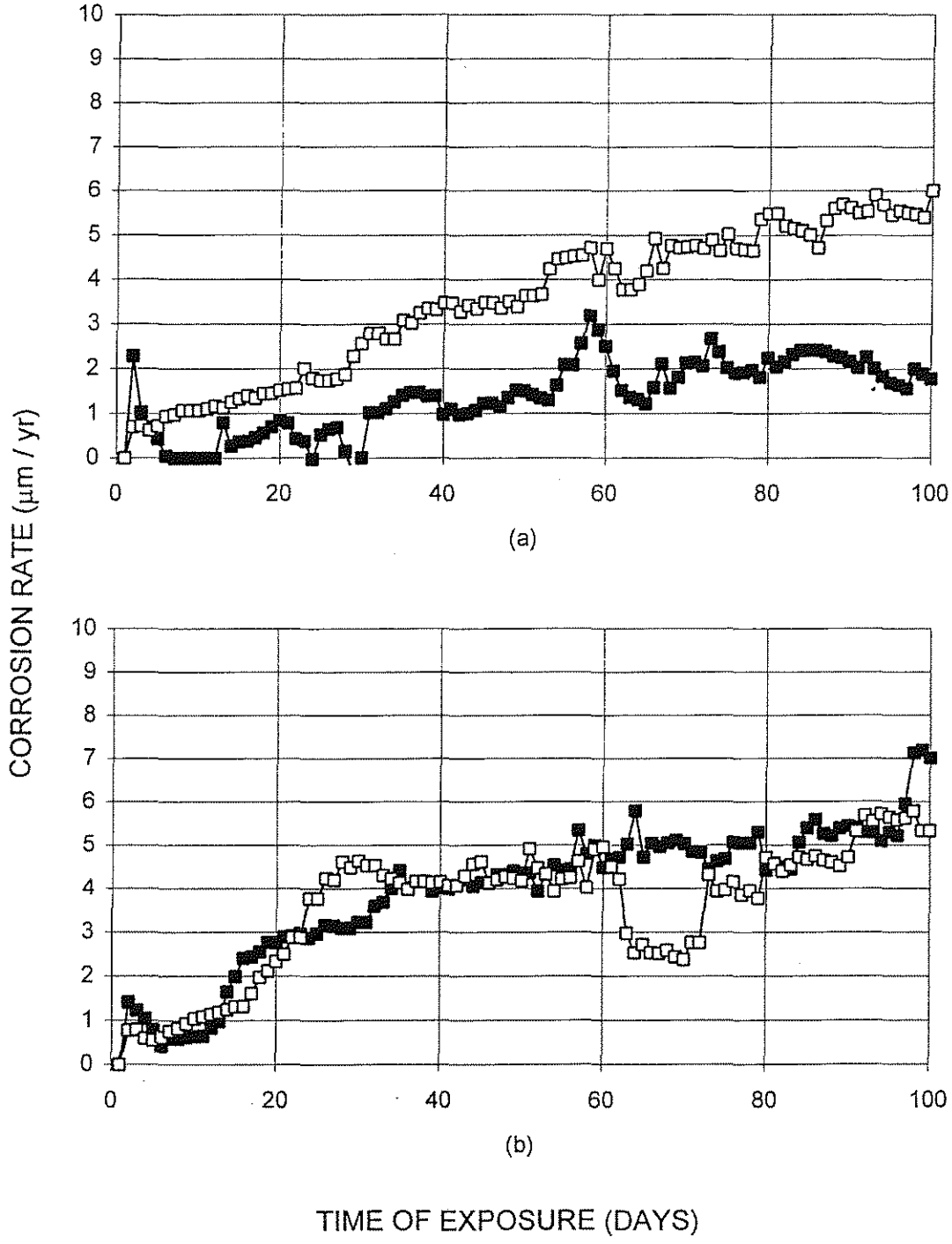

Fig. 3.9 Macrocell Test: Corrosion rate for CRSH steel in a 6.04 m NaCl solution (no pore solution at the anode) and a cathode:anode specimen ratio of 1:1. (a) Incorrect pore solution at the cathode and (b) Standard pore solution at the cathode

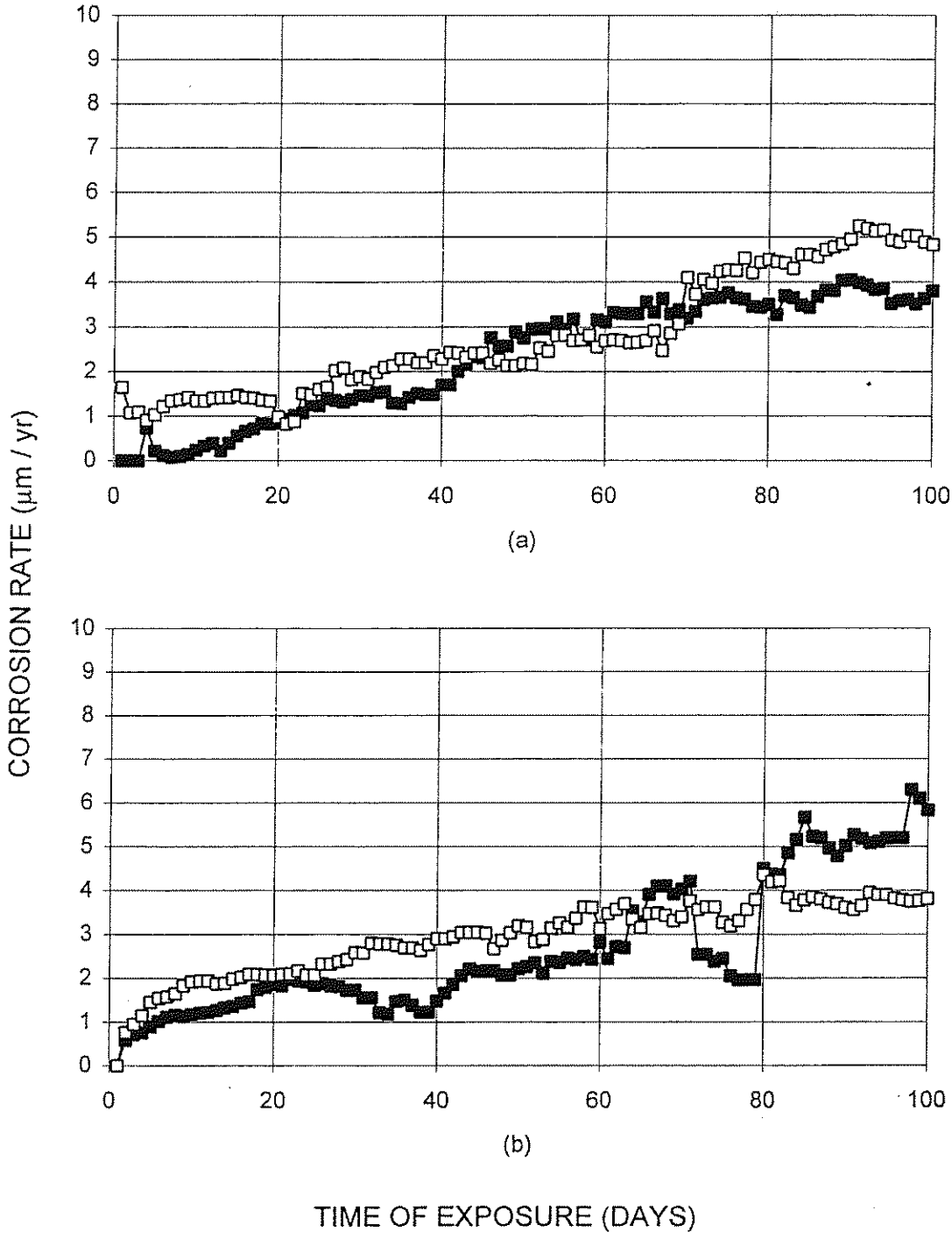

Fig. 3.10 Macrocell Test: Corrosion rate for CRST steel in a 6.04 m NaCl solution (no pore solution at the anode) and a cathode:anode specimen ratio of 1:1. (a) Incorrect pore solution at the cathode and (b) Standard pore solution at the cathode

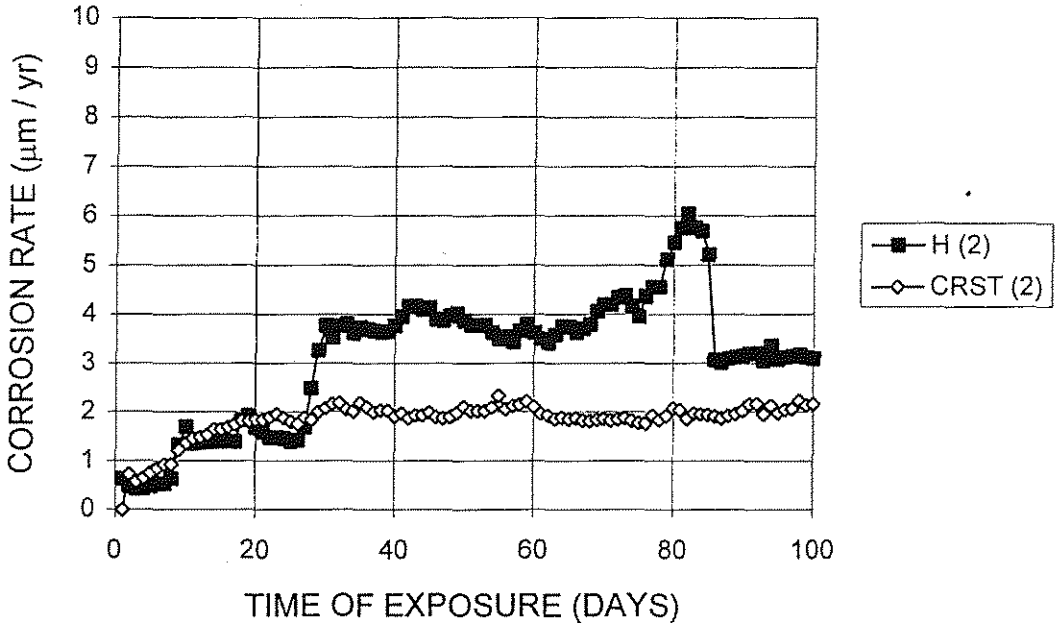

Fig. 3.11 Macrocell Test: Average corrosion rates for H and CRST steels in a 6.04 m NaCl solution and a cathode:anode specimen ratio of 1:1.

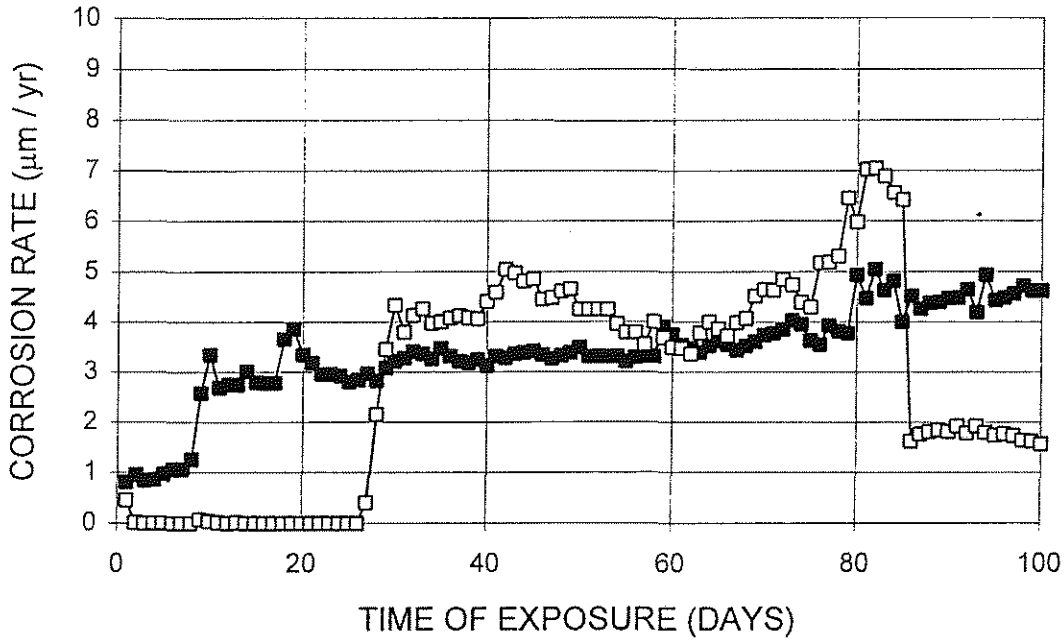

Fig. 3.12 Macrocell Test: Corrosion rate for H steel in a 6.04 m NaCl solution and a cathode:anode specimen ratio of 1:1.

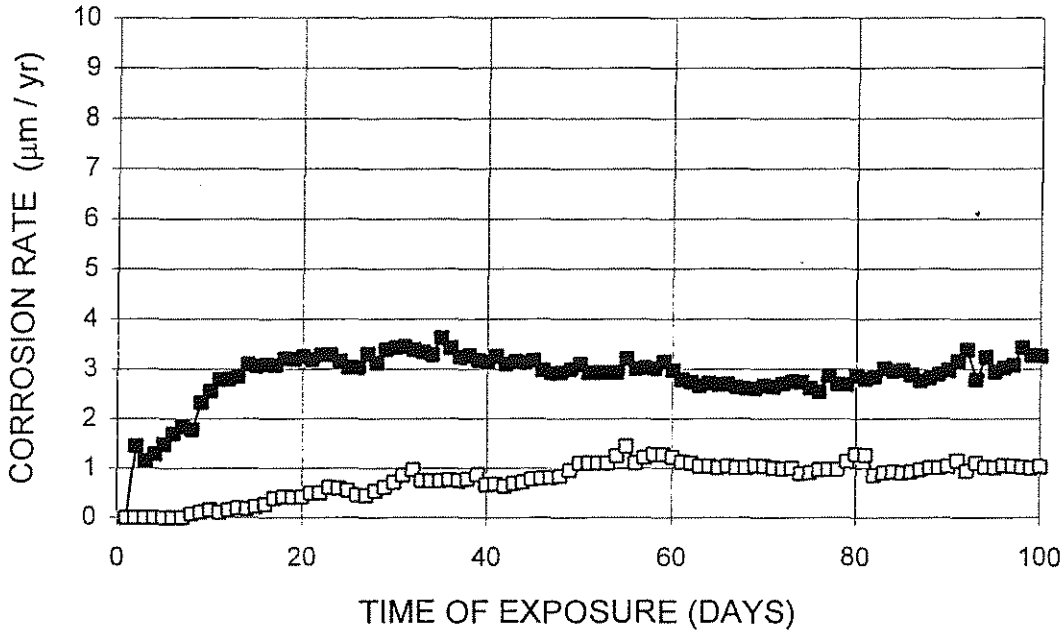

Fig. 3.13 Macrocell Test: Corrosion rate for CRST steel in a 6.04 m NaCl solution and a cathode:anode specimen ratio of 1:1.

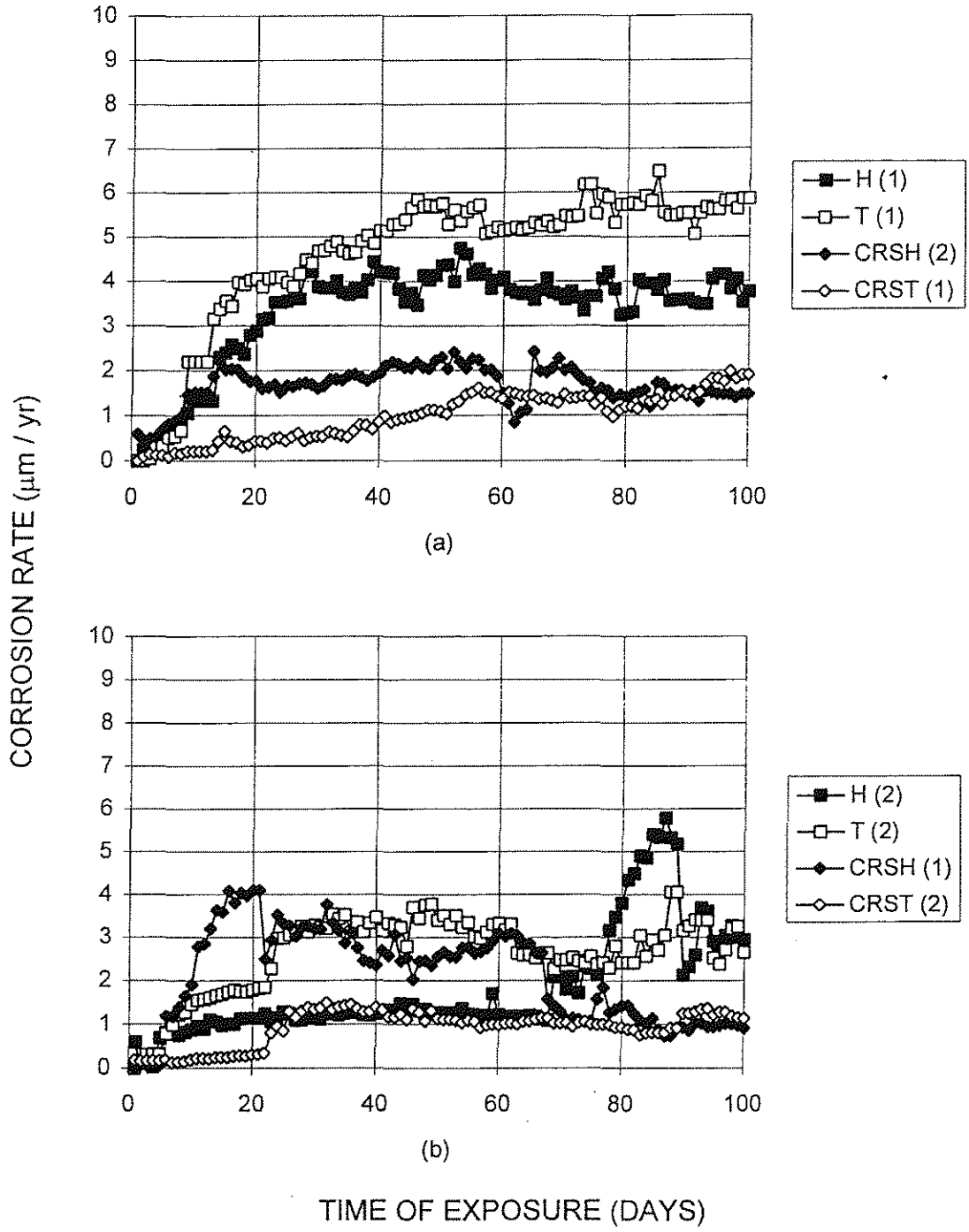

Fig. 3.14 Macrocell Test: Average corrosion rates for different steels in different concentrations of NaCl and a cathode:anode specimen ratio of 2:1. (a) 0.4 m, (b) 1.0 m, (c) 1.6 m, and (d) 6.04 m

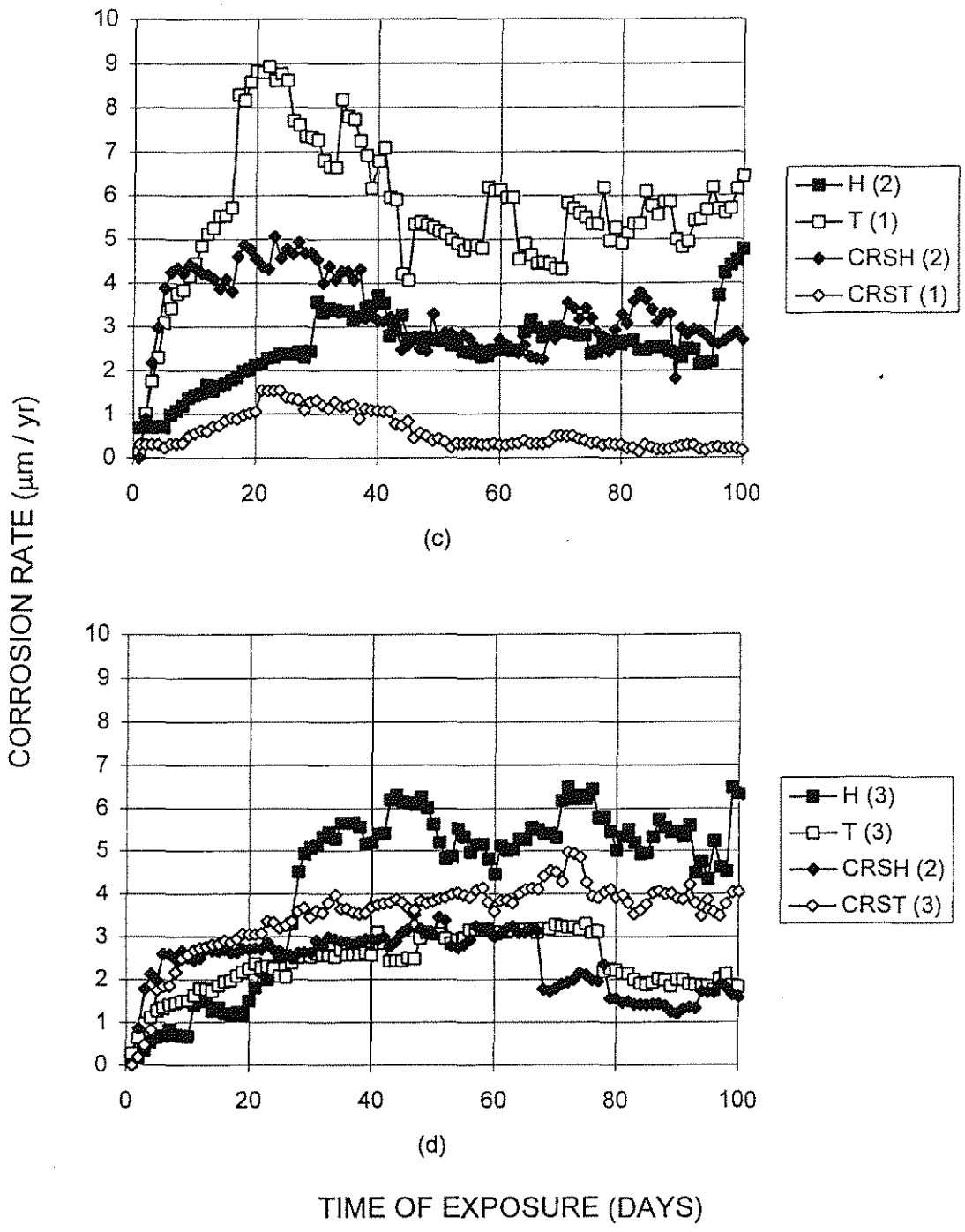

Fig. 3.14 (Continued) Macrocell Test: Average corrosion rates for different steels in different concentrations of NaCl and a cathode:anode specimen ratio of 2:1. (a) 0.4 m, (b) 1.0 m, (c) 1.6 m, and (d) 6.04 m

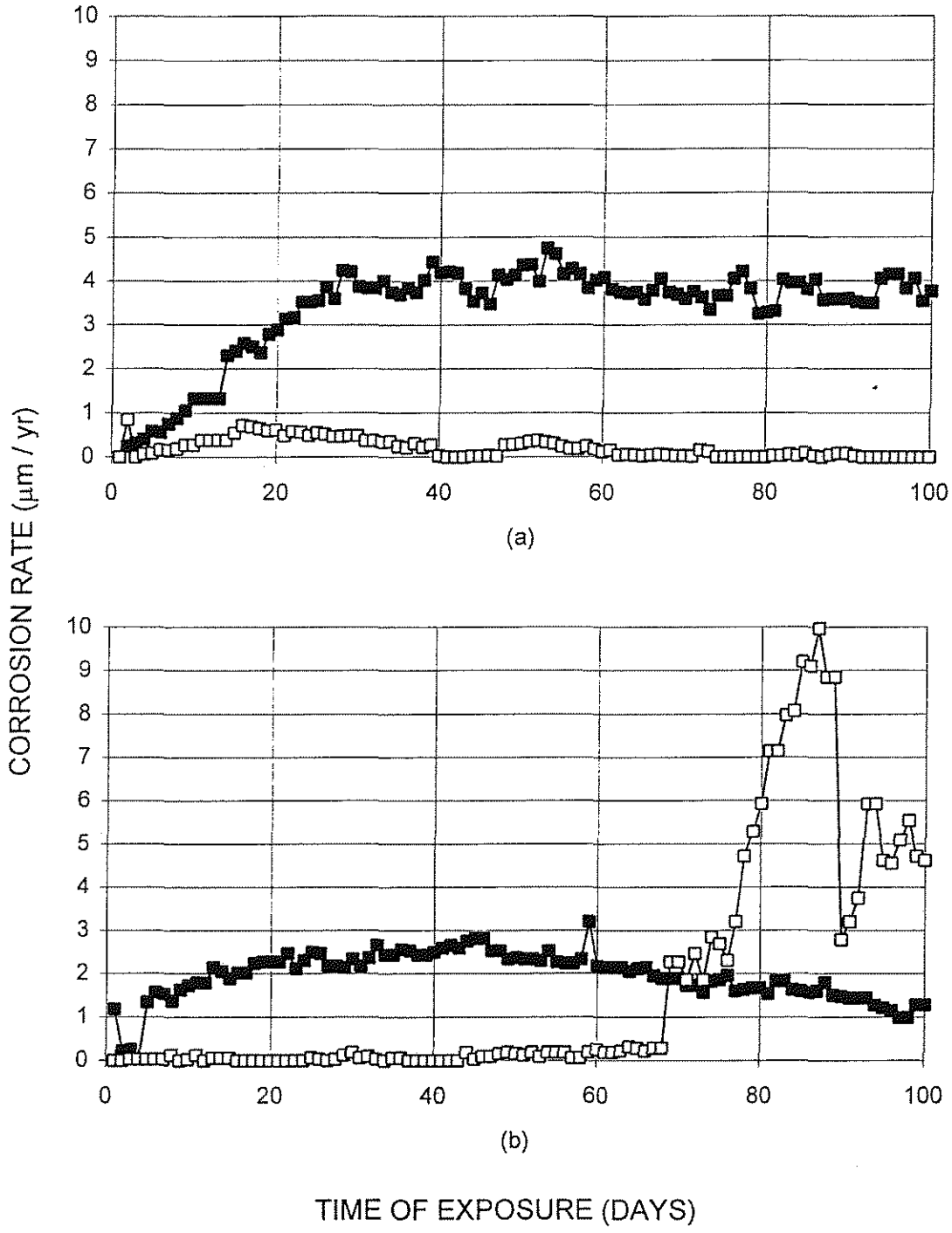

Fig. 3.15 Macrocell Test: Corrosion rate for H steel in different concentrations of NaCl and a cathode:anode specimen ratio of 2:1. (a) 0.4 m, (b) 1.0 m, (c) 1.6 m, and (d) 6.04 m

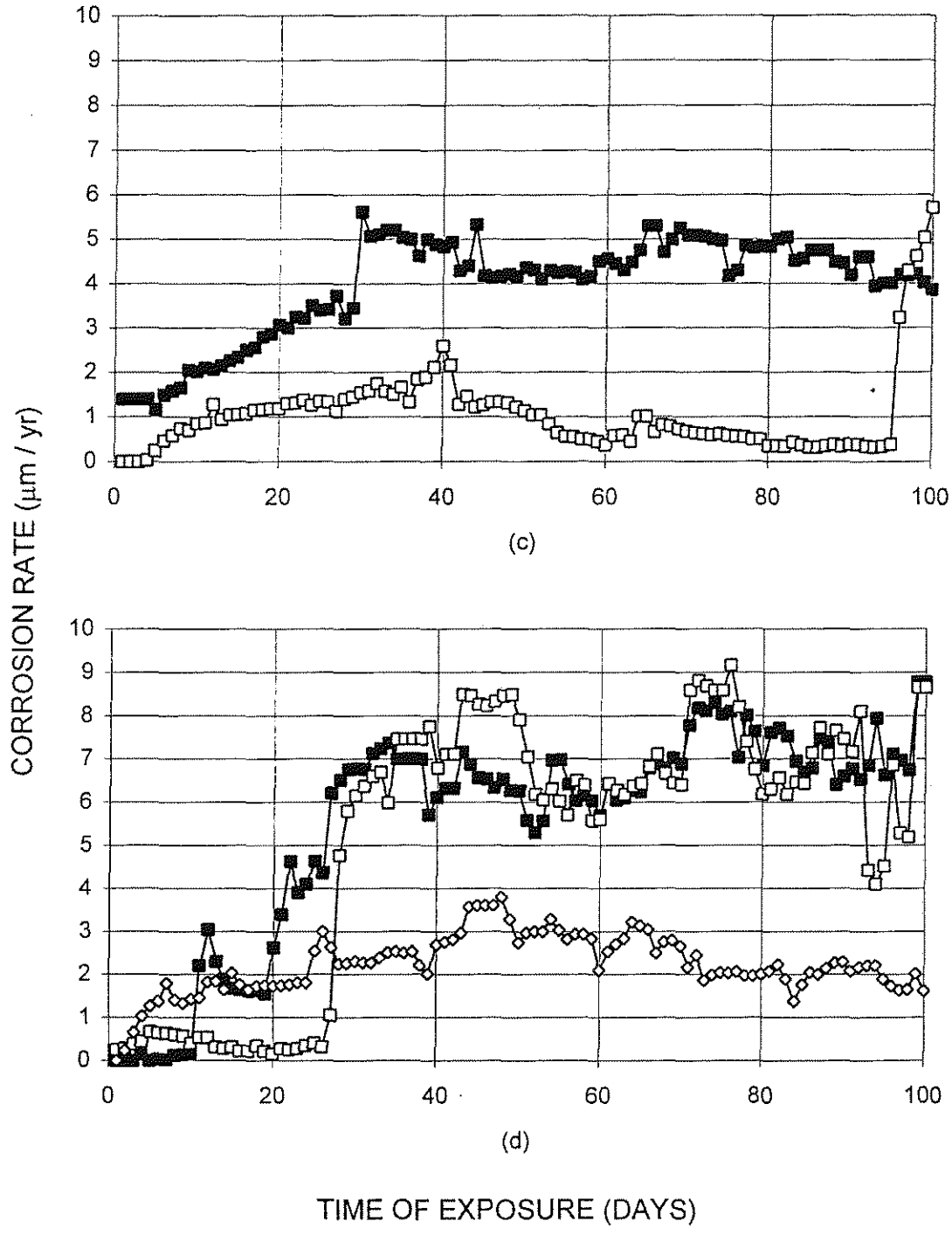

Fig. 3.15 (Continued) Macrocell Test: Corrosion rate for H steel in different concentrations of NaCl and a cathode:anode specimen ratio of 2:1. (a) 0.4 m, (b) 1.0 m, (c) 1.6 m, and (d) 6.04 m

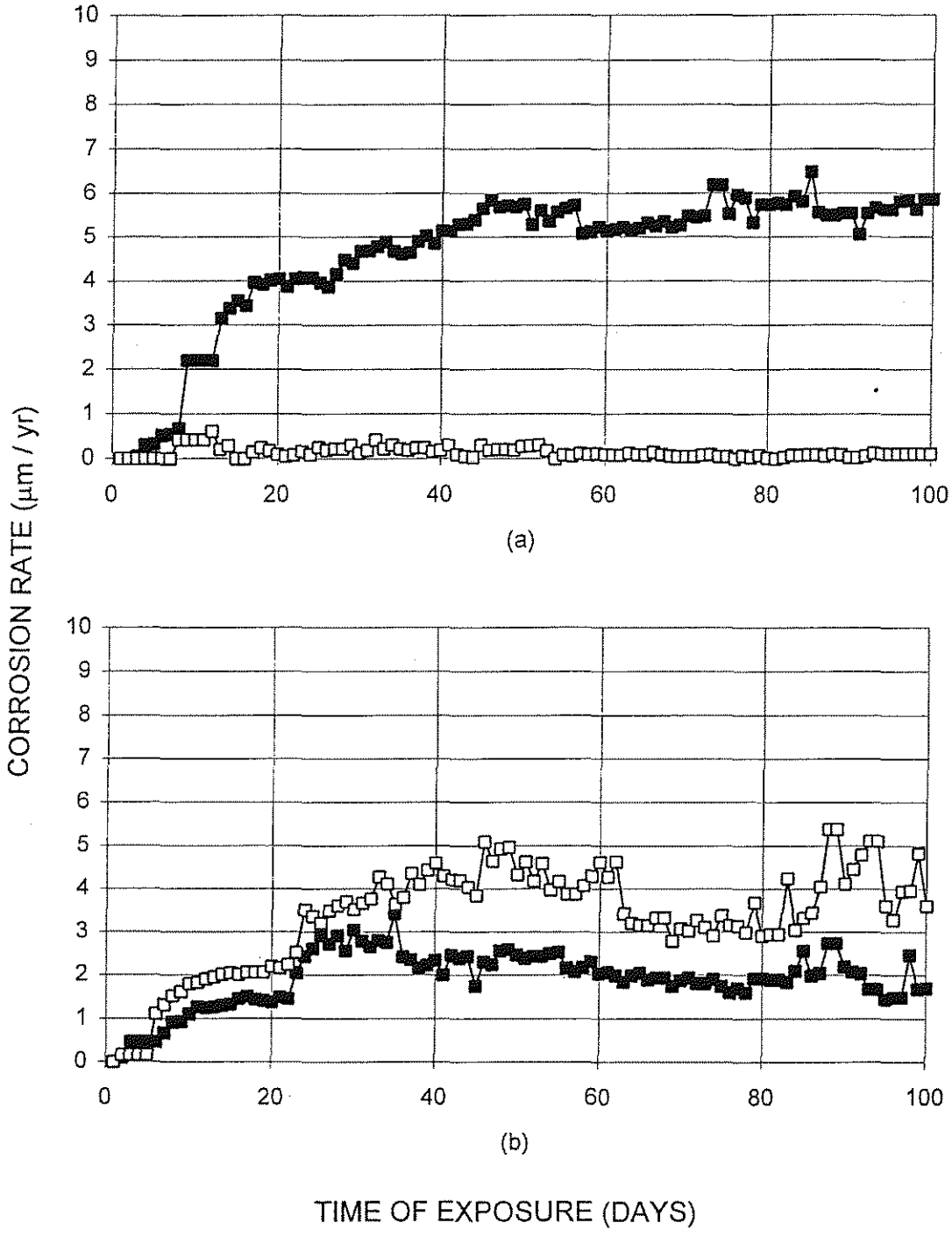

Fig. 3.16 Macrocell Test: Corrosion rate for T steel in different concentrations of NaCl and a cathode:anode specimen ratio of 2:1. (a) 0.4 m, (b) 1.0 m, (c) 1.6 m, and (d) 6.04 m

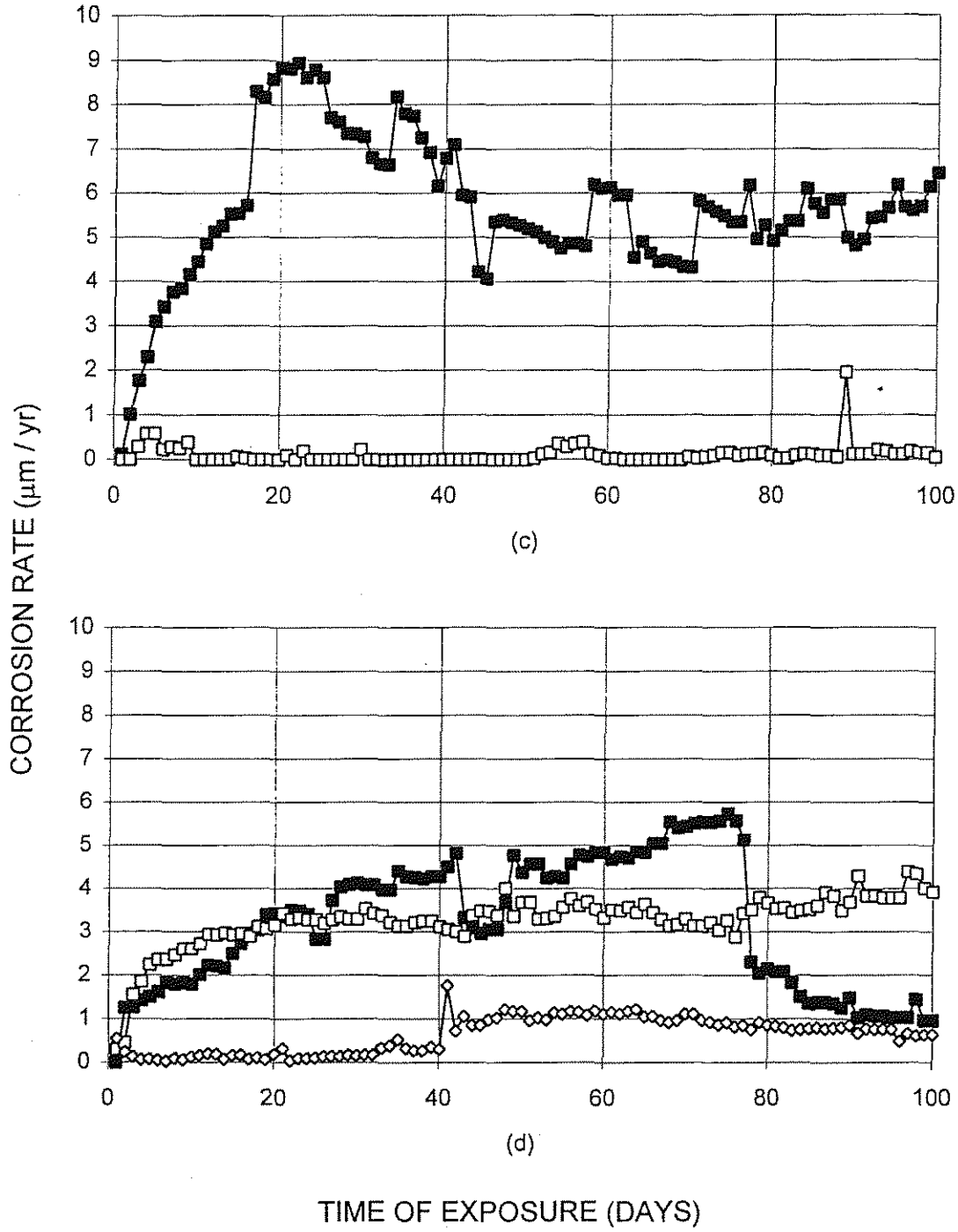

Fig. 3.16 (Continued) Macrocell Test: Corrosion rate for T steel in different concentrations of NaCl and a cathode:anode specimen ratio of 2:1. (a) 0.4 m, (b) 1.0 m, (c) 1.6 m, and (d) 6.04 m

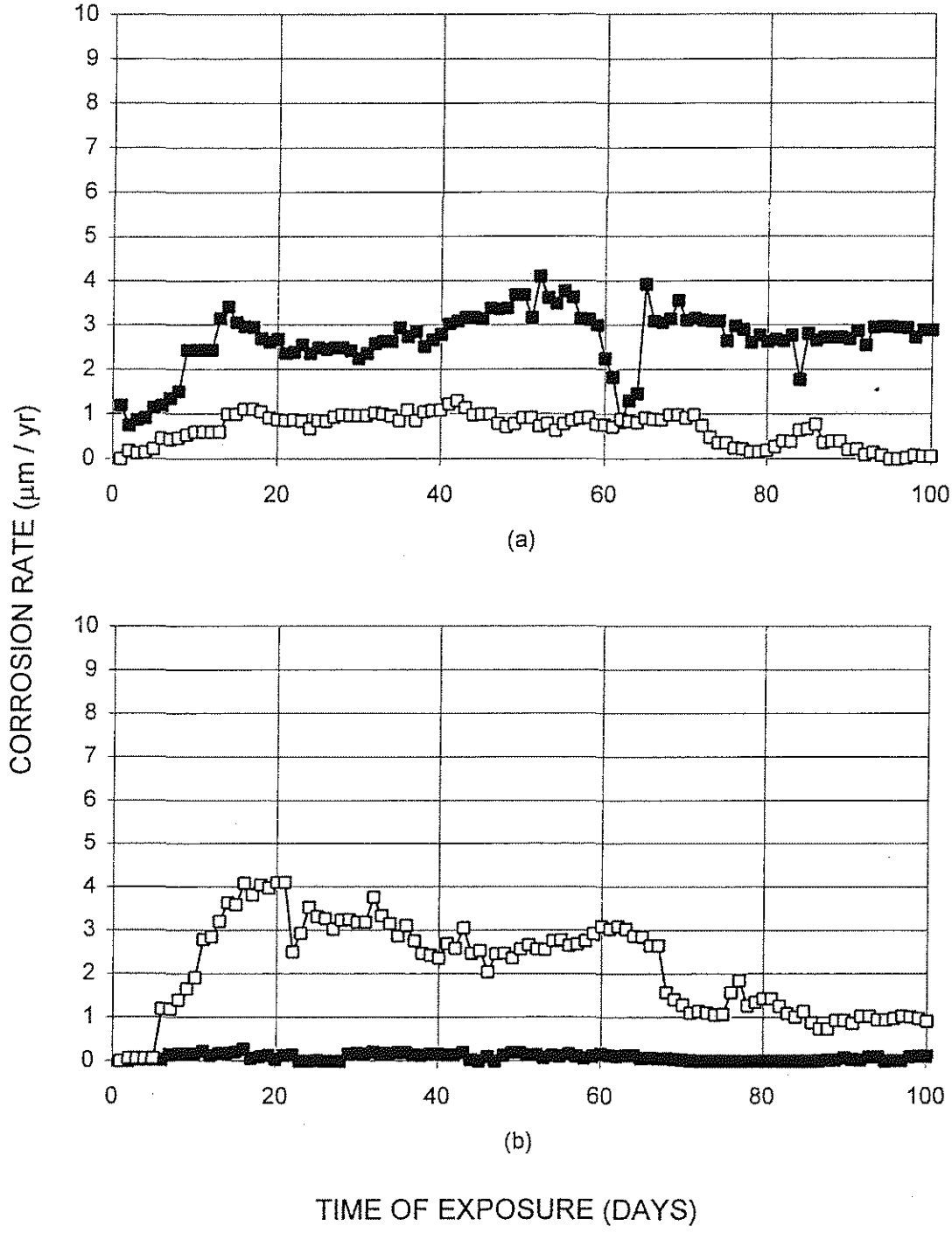

Fig. 3.17 Macrocell Test: Corrosion rate for CRSH steel in different concentrations of NaCl and a cathode:anode specimen ratio of 2:1. (a) 0.4 m, (b) 1.0 m, (c) 1.6 m, and (d) 6.04 m

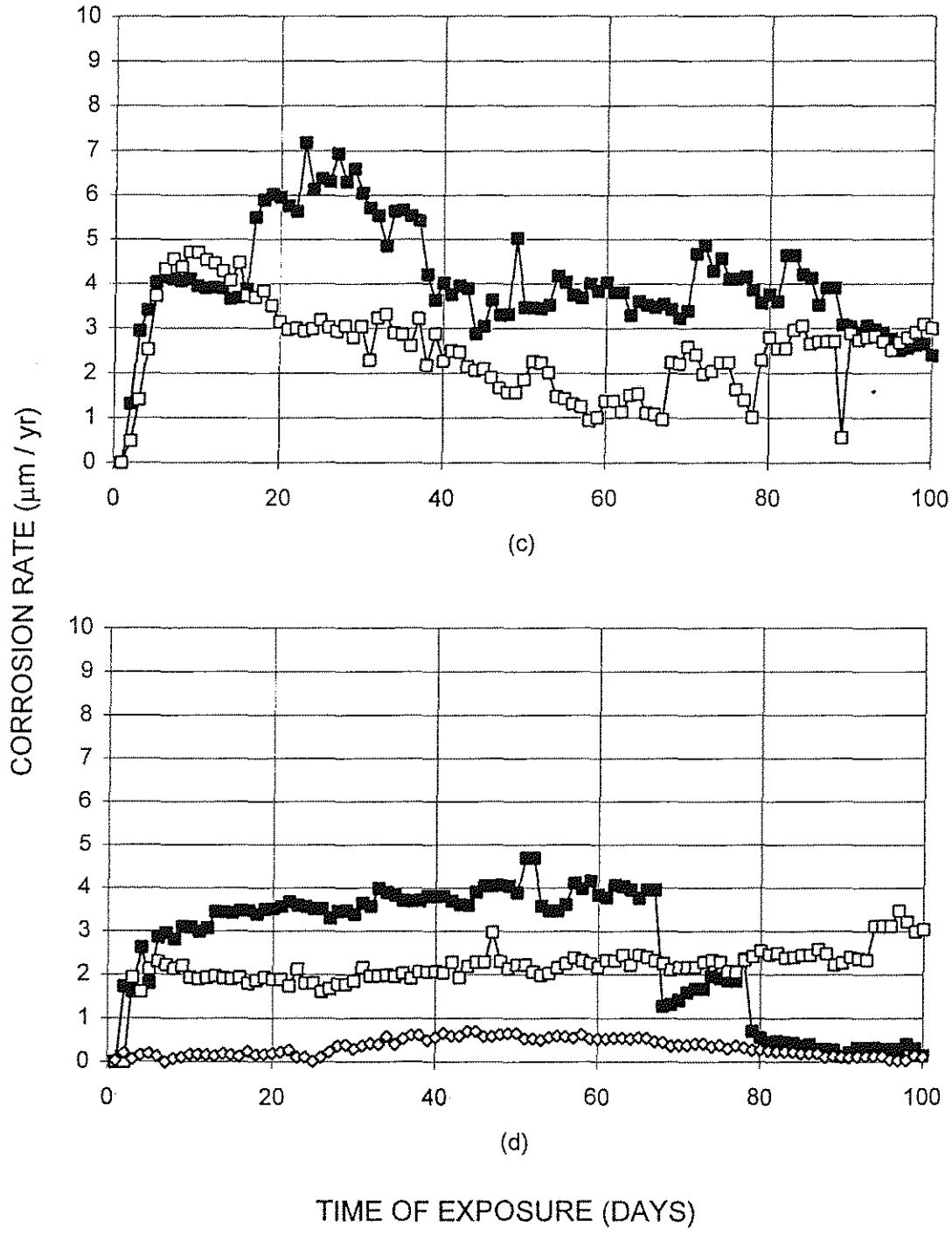

Fig. 3.17 (Continued) Macrocell Test: Corrosion rate for CRSH steel in different concentrations of NaCl and a cathode:anode specimen ratio of 2:1. (a) 0.4 m, (b) 1.0 m, (c) 1.6 m, and (d) 6.04 m

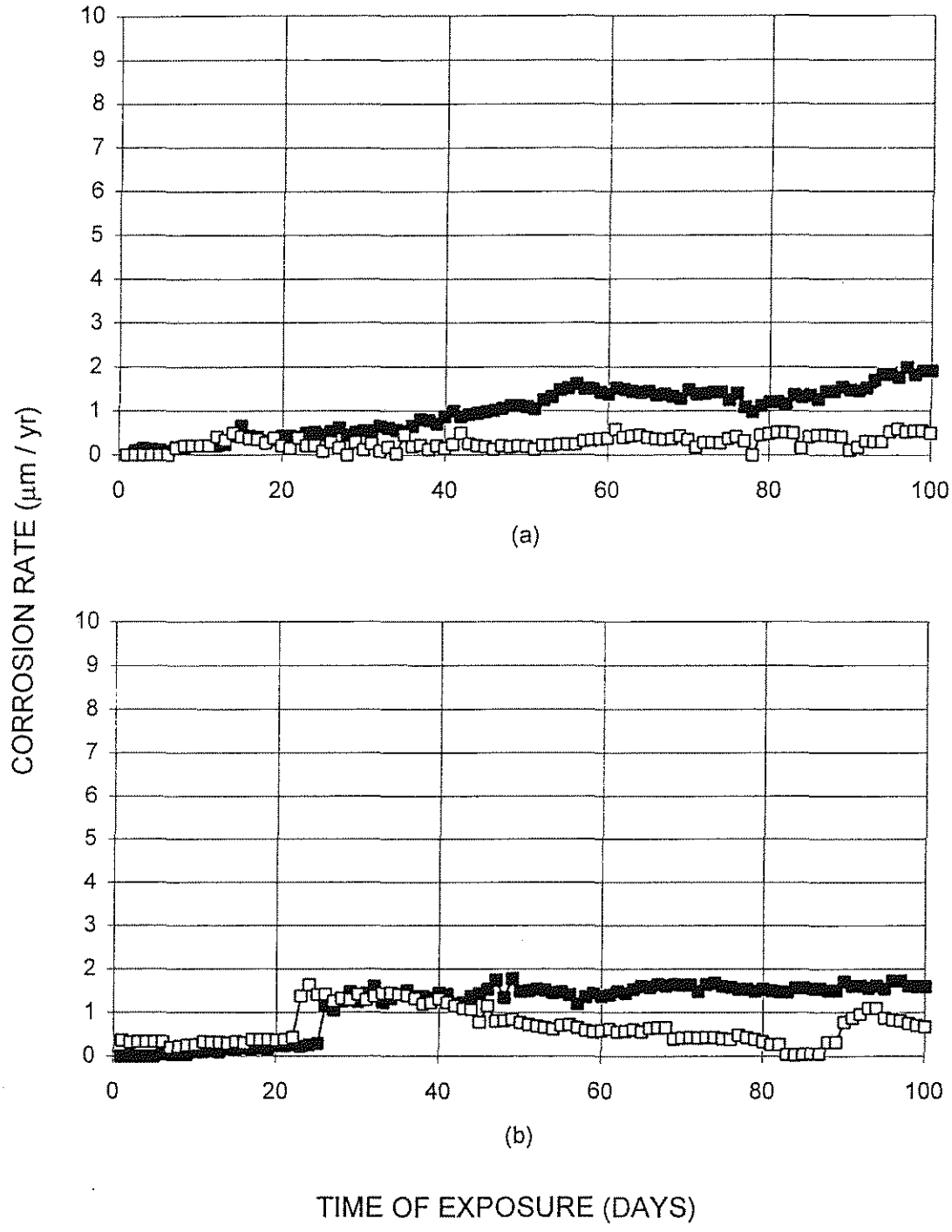

Fig. 3.18 Macrocell Test: Corrosion rate for CRST steel in different concentrations of NaCl and a cathode:anode specimen ratio of 2:1. (a) 0.4 m, (b) 1.0 m, (c) 1.6 m, and (d) 6.04 m

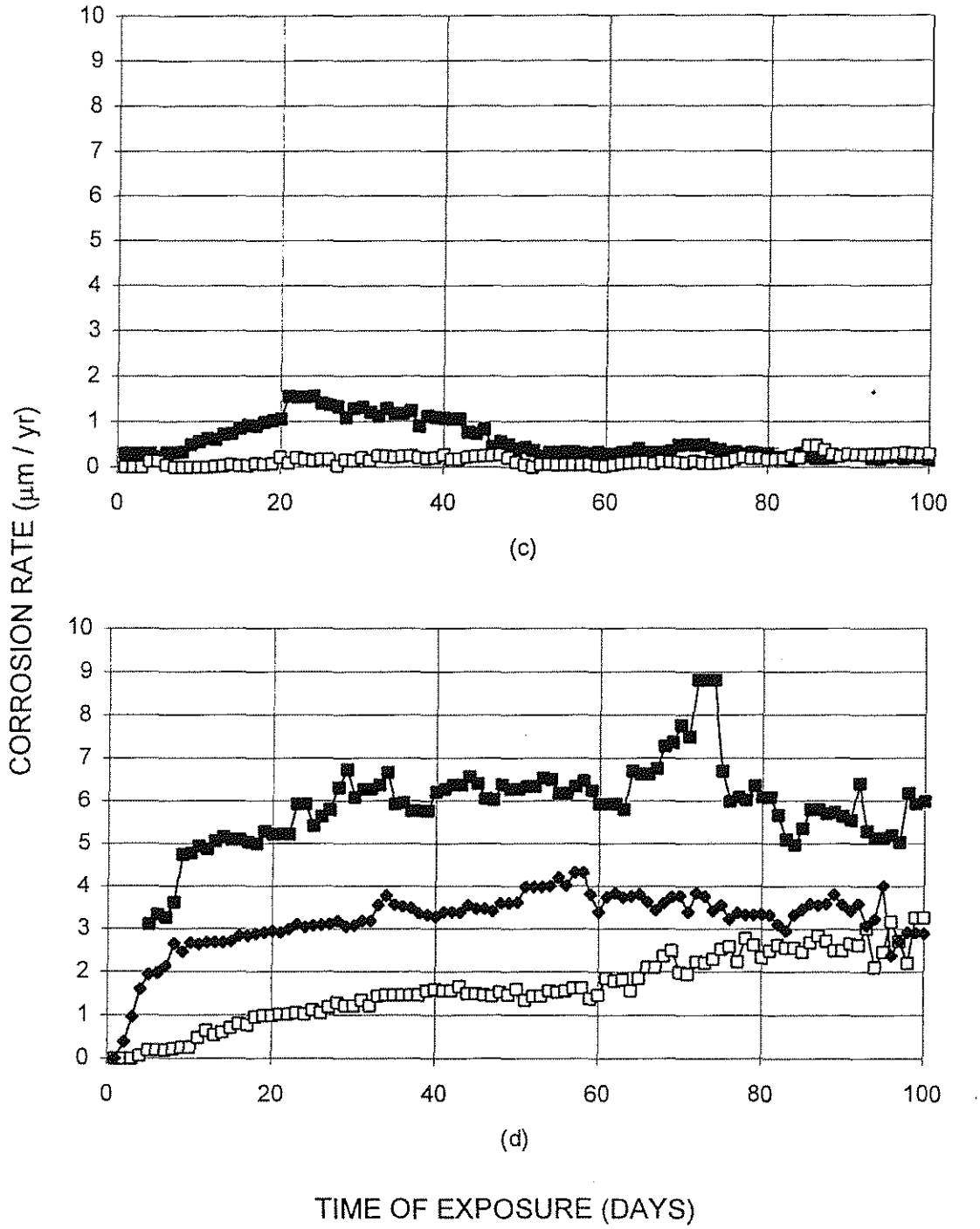

Fig. 3.18 (Continued) Macrocell Test: Corrosion rate for CRST steel in different concentrations of NaCl and a cathode:anode specimen ratio of 2:1. (a) 0.4 m, (b) 1.0 m, (c) 1.6 m, and (d) 6.04 m

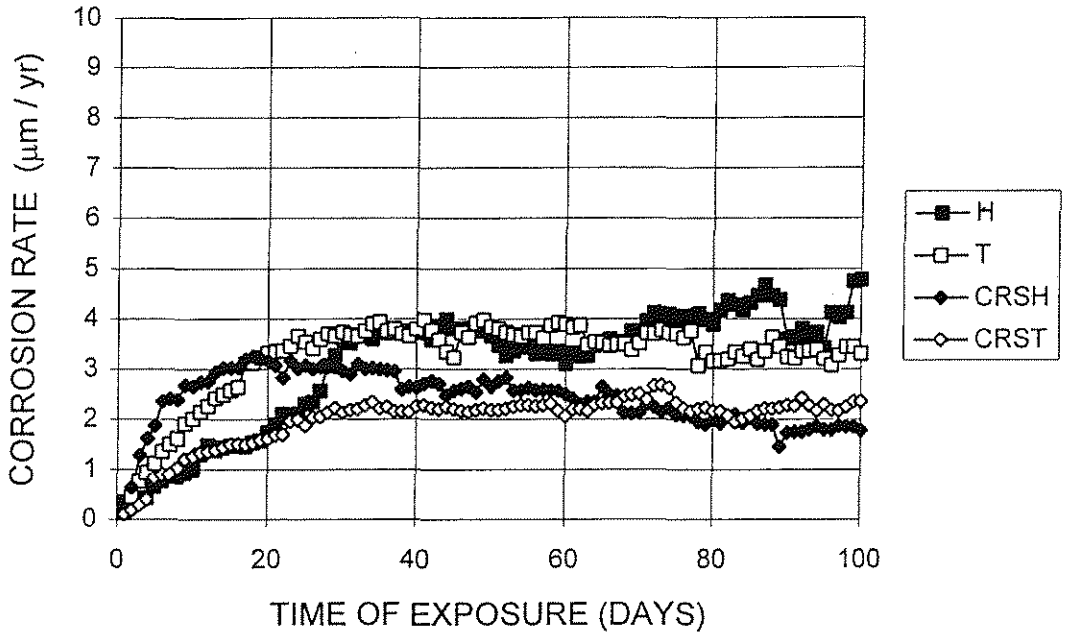

Fig. 3.19 Macrocell Test: Relative average corrosion rates for different steels at all NaCl concentrations.

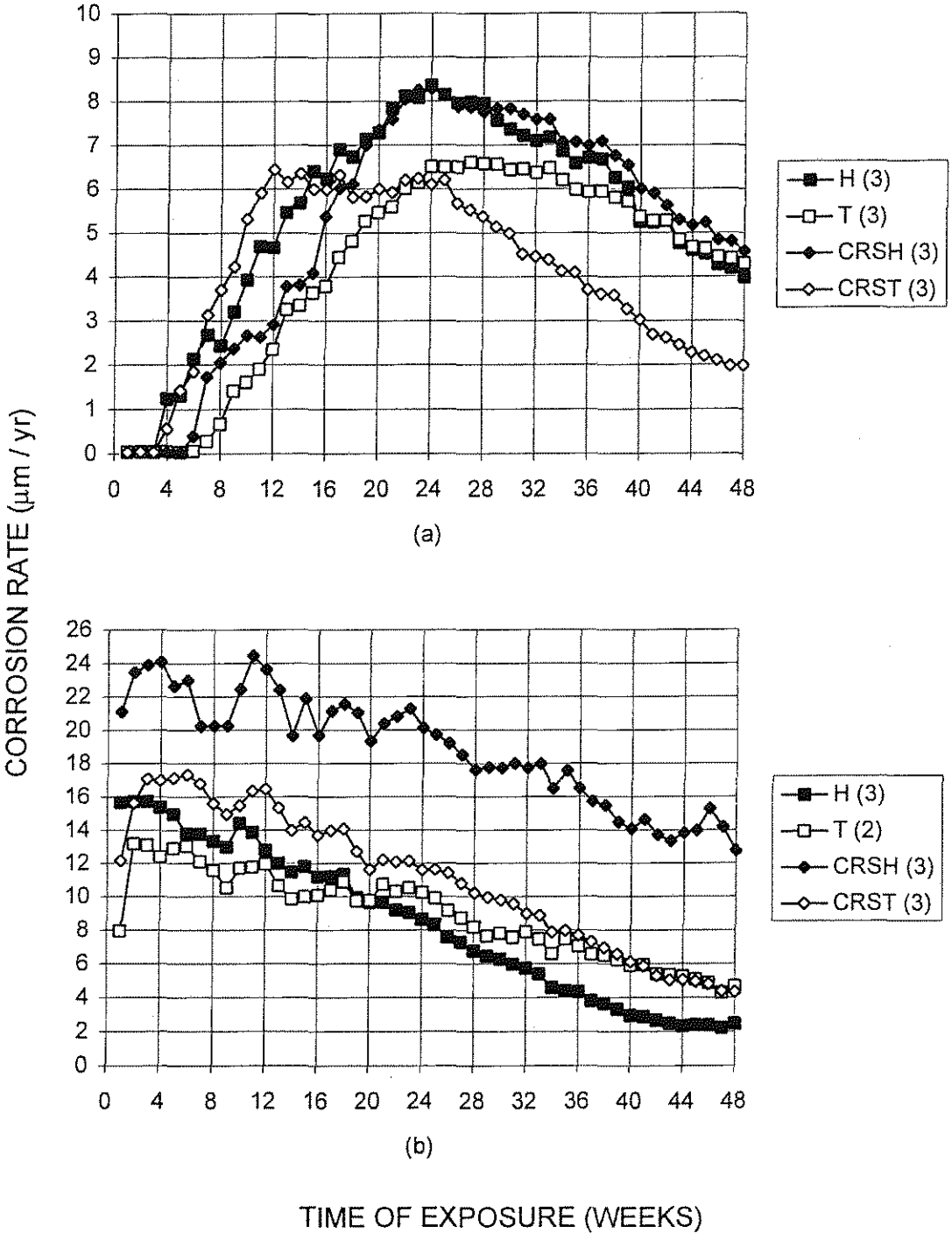

Fig. 3.20 Average macrocell corrosion rates for all four steels in regular concrete. a) Southern Exposure and b) Cracked Beam

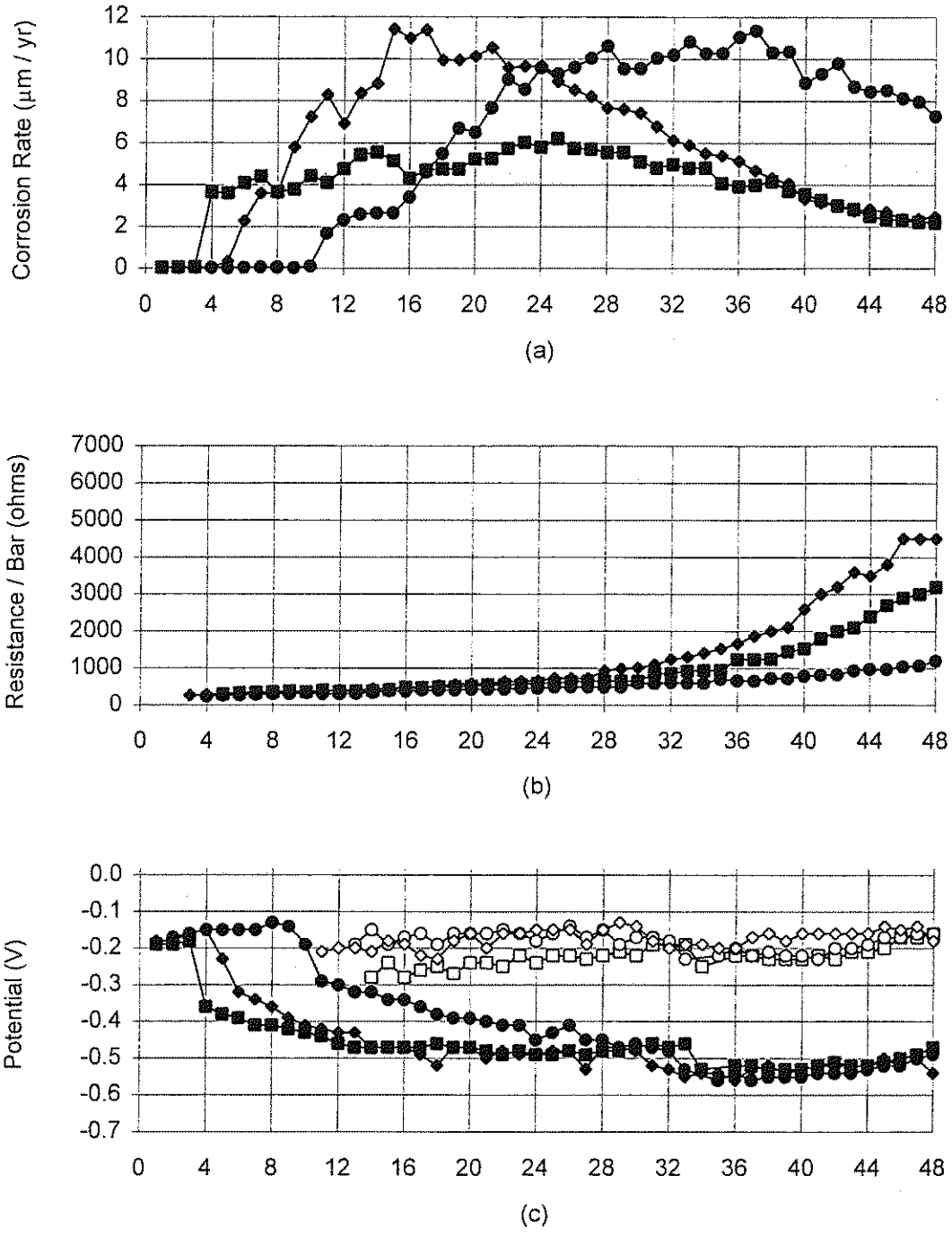

Fig. 3.21 Southern Exposure test results for H steel. a) Macrocell Corrosion Rate, b) Mat-To-Mat Resistance, and c) Potential of the Anode (solid) and Cathode (clear)

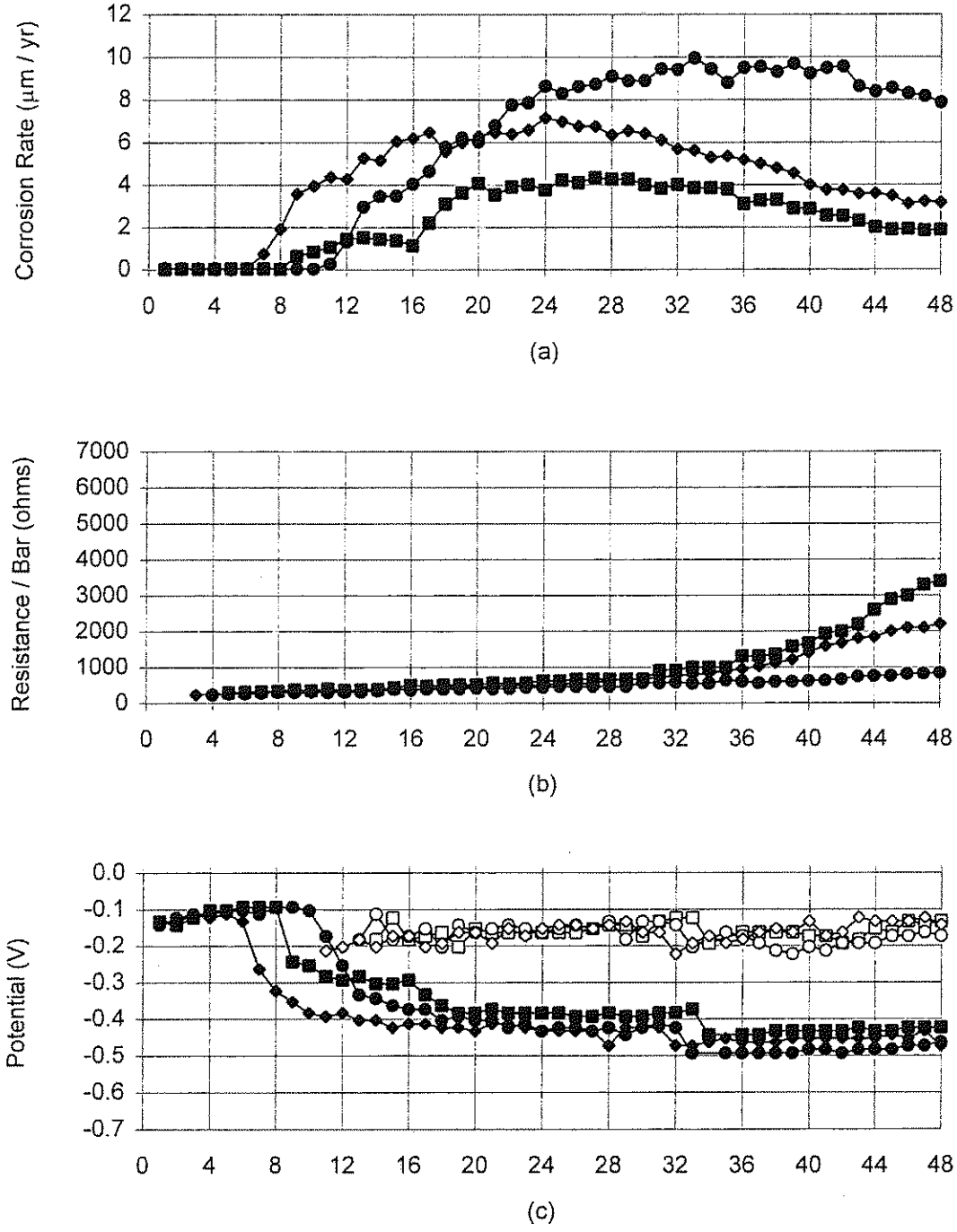

Fig. 3.22 Southern Exposure test results for T steel. a) Macrocell Corrosion Rate, b) Mat-To-Mat Resistance, and c) Potential of the Anode (solid) and Cathode (clear)

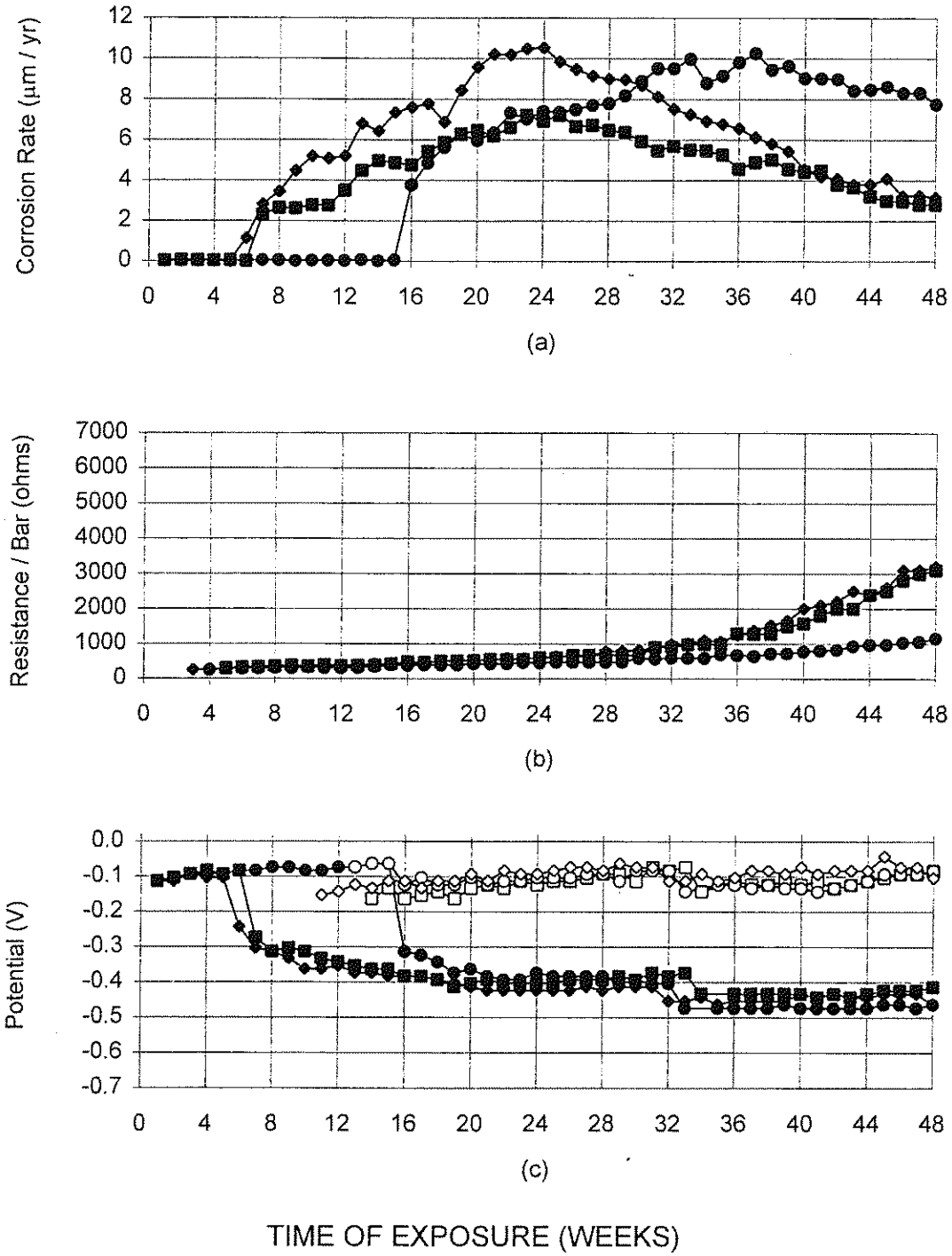

Fig. 3.23 Southern Exposure test results for CRSH steel. a) Macrocell Corrosion Rate, b) Mat-To-Mat Resistance, and c) Potential of the Anode (solid) and Cathode (clear)

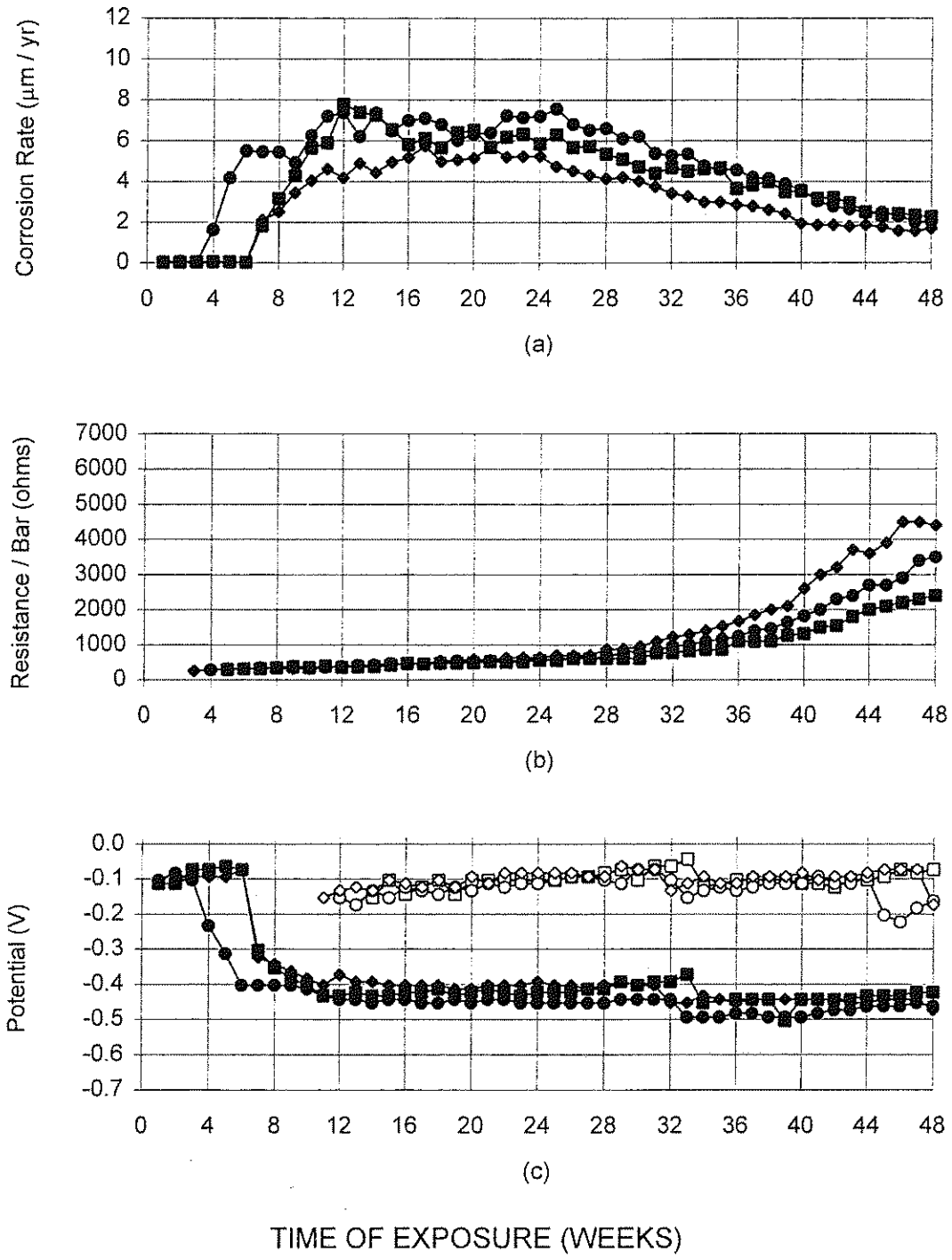

Fig. 3.24 Southern Exposure test results for CRST steel. a) Macrocell Corrosion Rate, b) Mat-To-Mat Resistance, and c) Potential of the Anode (solid) and Cathode (clear)

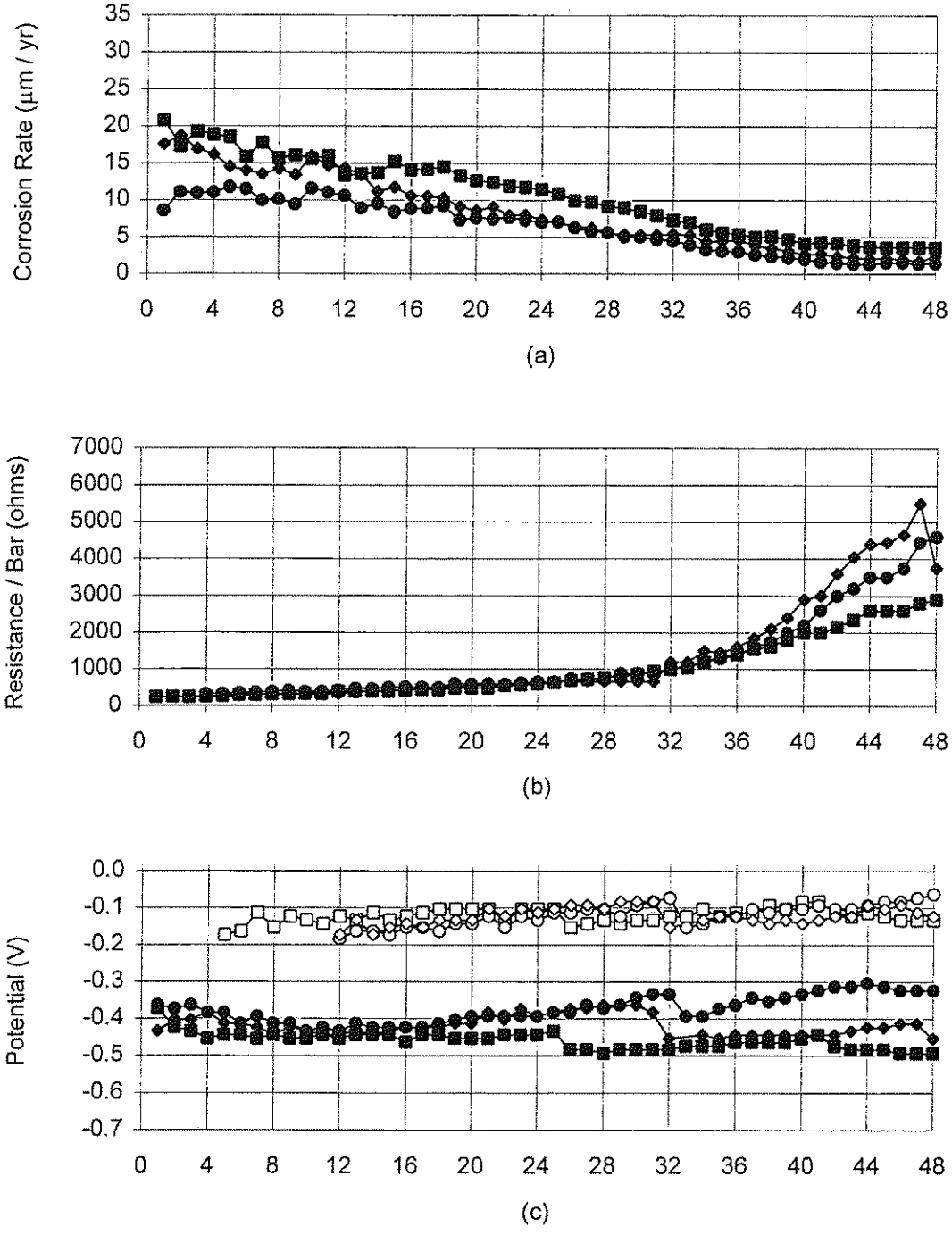

Fig. 3.25 Cracked Beam test results for H steel. a) Macrocell Corrosion Rate, b) Mat-To-Mat Resistance, and c) Potential of the Anode (solid) and Cathode (clear)

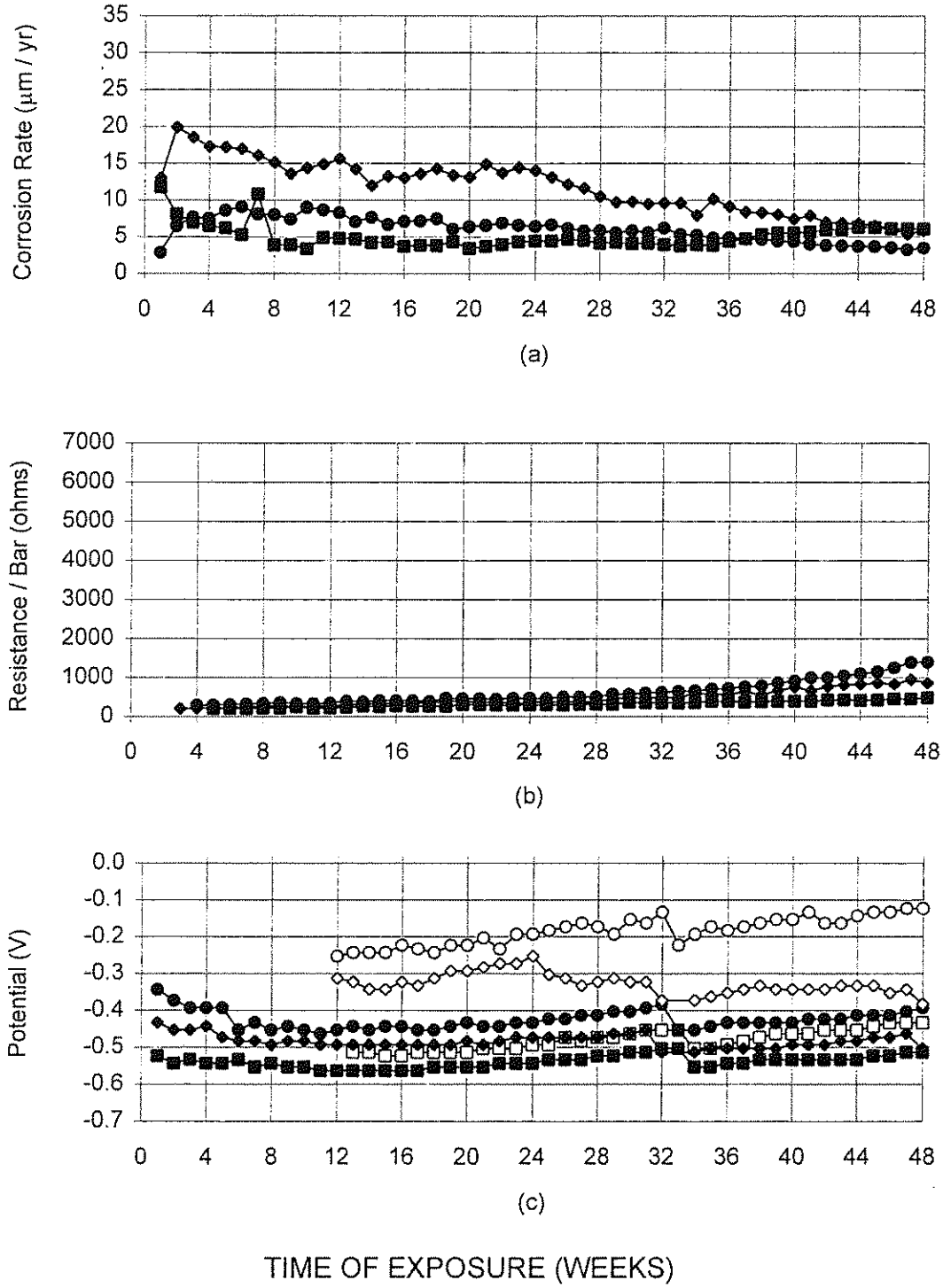

Fig. 3.26 Cracked Beam test results for T steel. a) Macrocell Corrosion Rate, b) Mat-To-Mat Resistance, and c) Potential of the Anode (solid) and Cathode (clear)

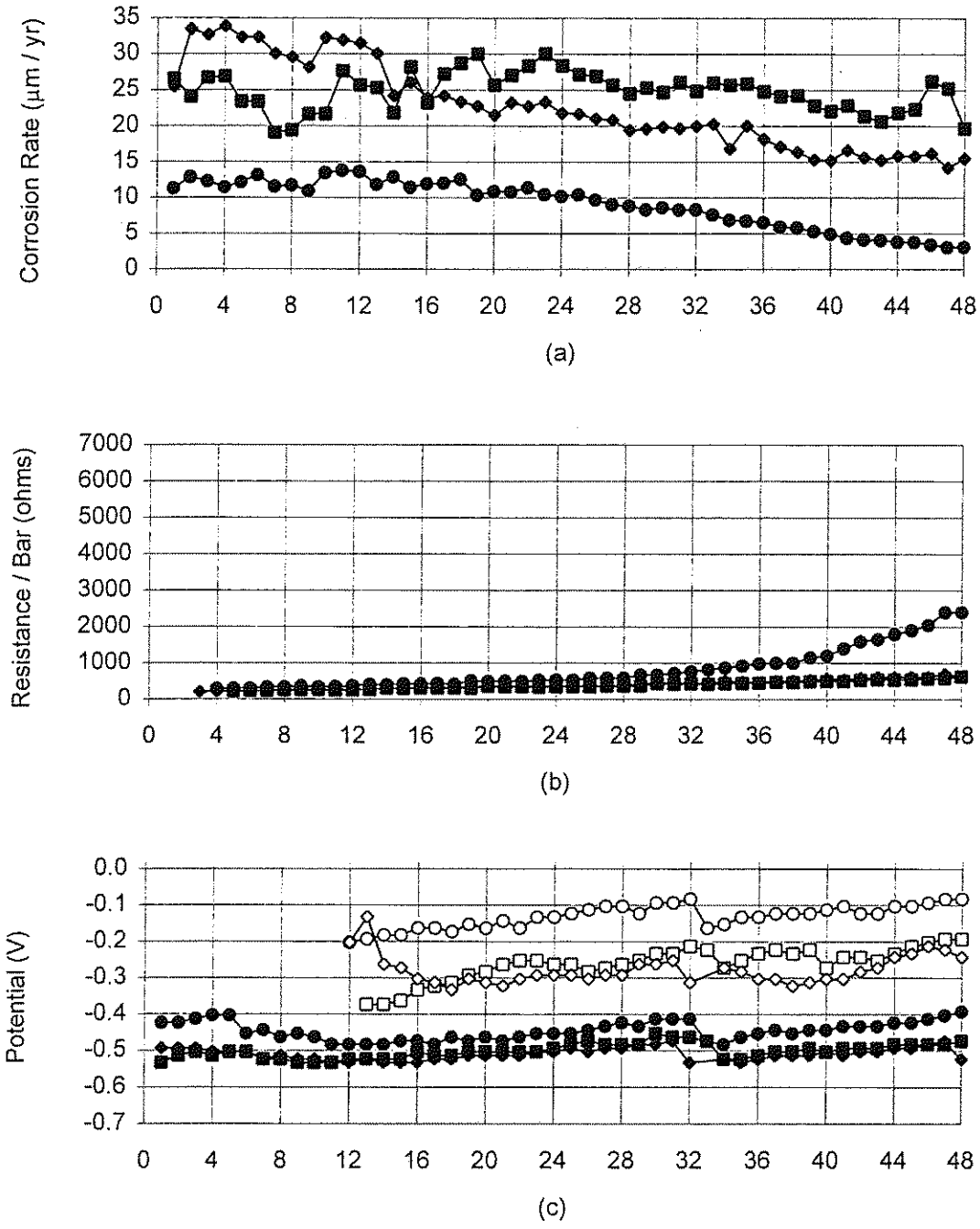

Fig. 3.27 Cracked Beam test results for CRSH steel. a) Macrocell Corrosion Rate, b) Mat-To-Mat Resistance, and c) Potential of the Anode (solid) and Cathode (clear)

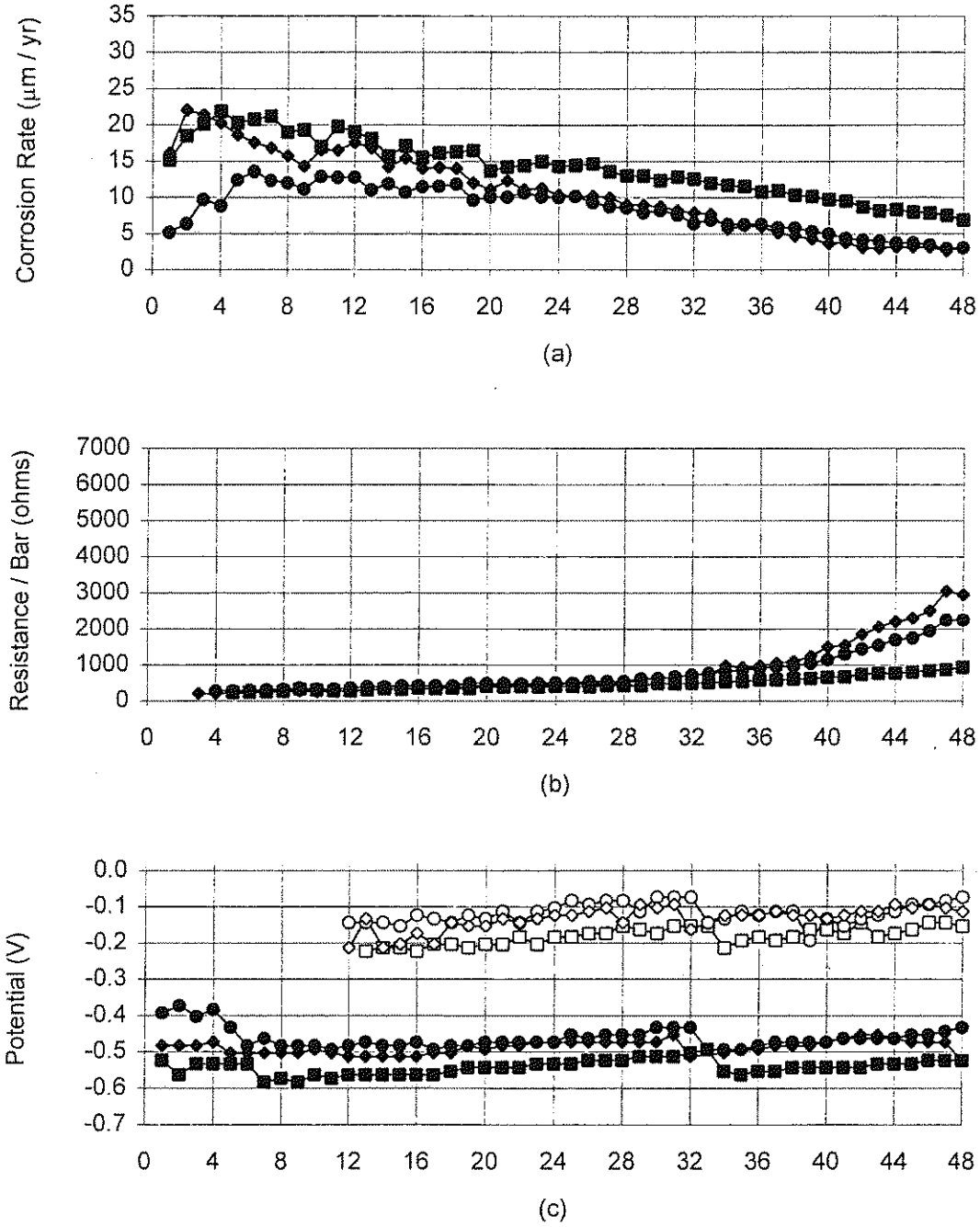

Fig. 3.28 Cracked Beam test results for CRST steel. a) Macrocell Corrosion Rate, b) Mat-To-Mat Resistance, and c) Potential of the Anode (solid) and Cathode (clear)

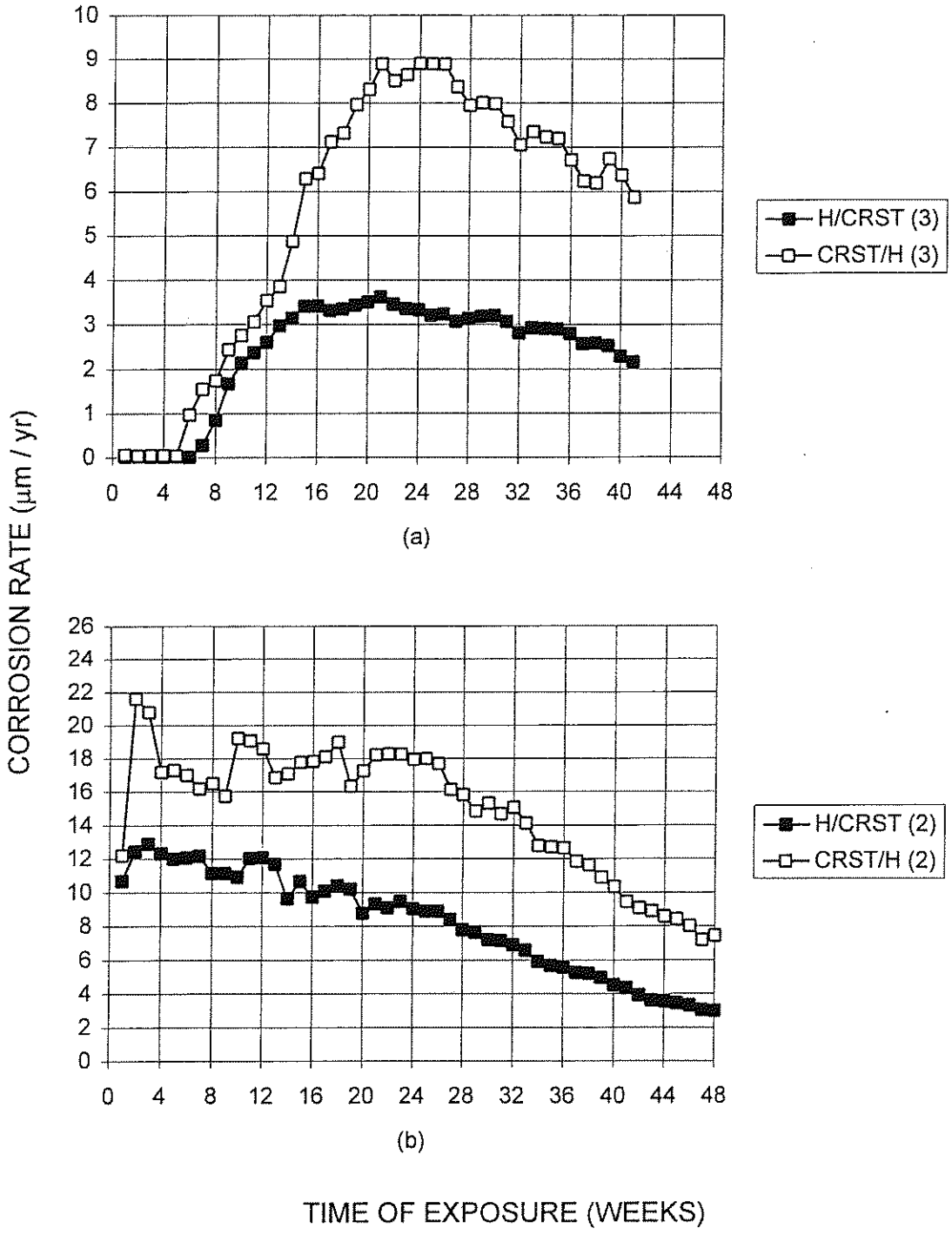

Fig. 3.29 Average macrocell corrosion rates for steel combinations H/CRST and CRST/H. a) Southern Exposure and b) Cracked Beam

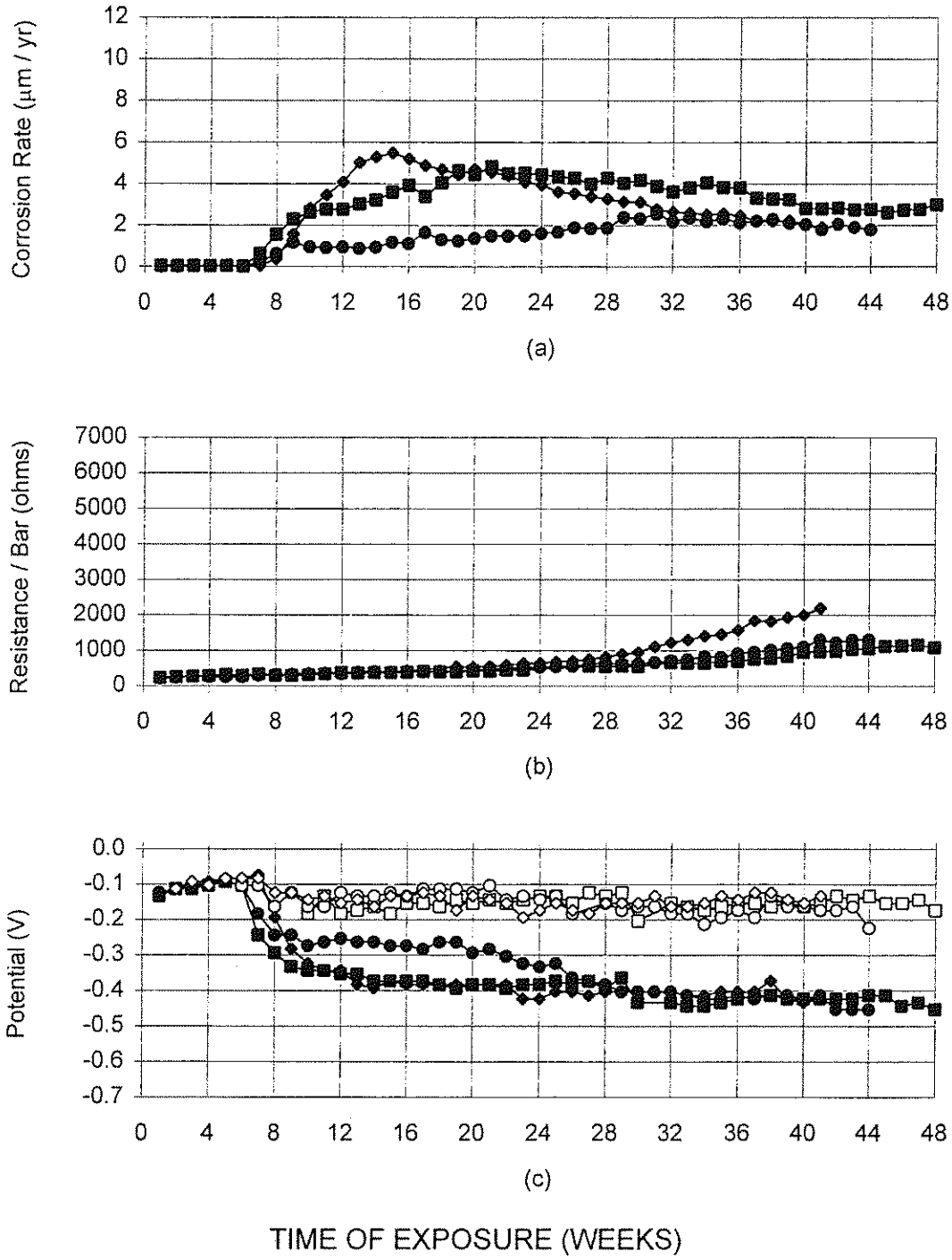

Fig. 3.30 Southern Exposure test results for steel combination H/CRST.
a) Macrocell Corrosion Rate, b) Mat-To-Mat Resistance, and
c) Potential of the Anode (solid) and Cathode (clear)

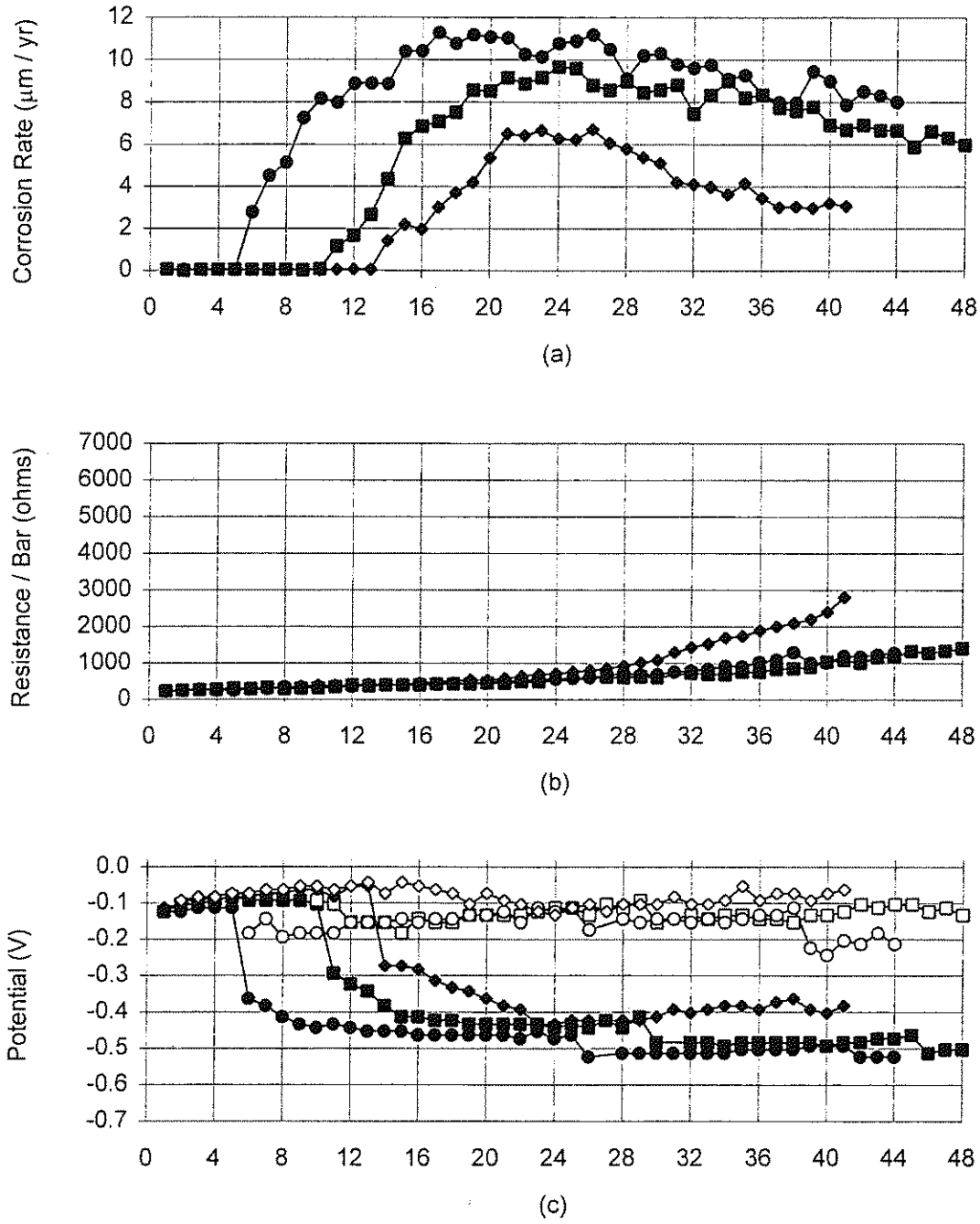

Fig. 3.31 Southern Exposure test results for steel combination CRST/H.
a) Macrocell Corrosion Rate, b) Mat-To-Mat Resistance, and
c) Potential of the Anode (solid) and Cathode (clear)

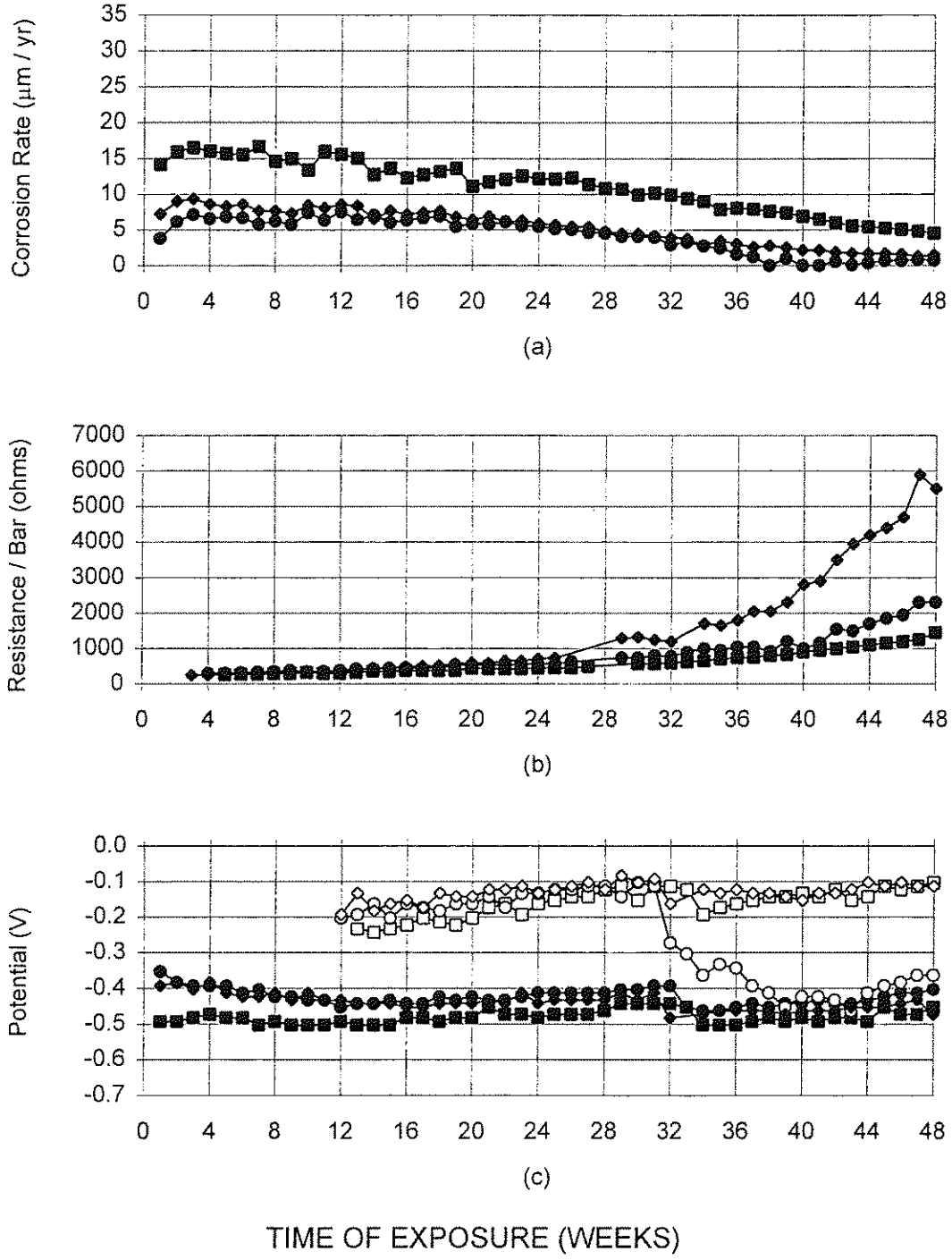

Fig. 3.32 Cracked Beam test results for steel combination H/CRST.
a) Macrocell Corrosion Rate, b) Mat-To-Mat Resistance, and
c) Potential of the Anode (solid) and Cathode (clear)

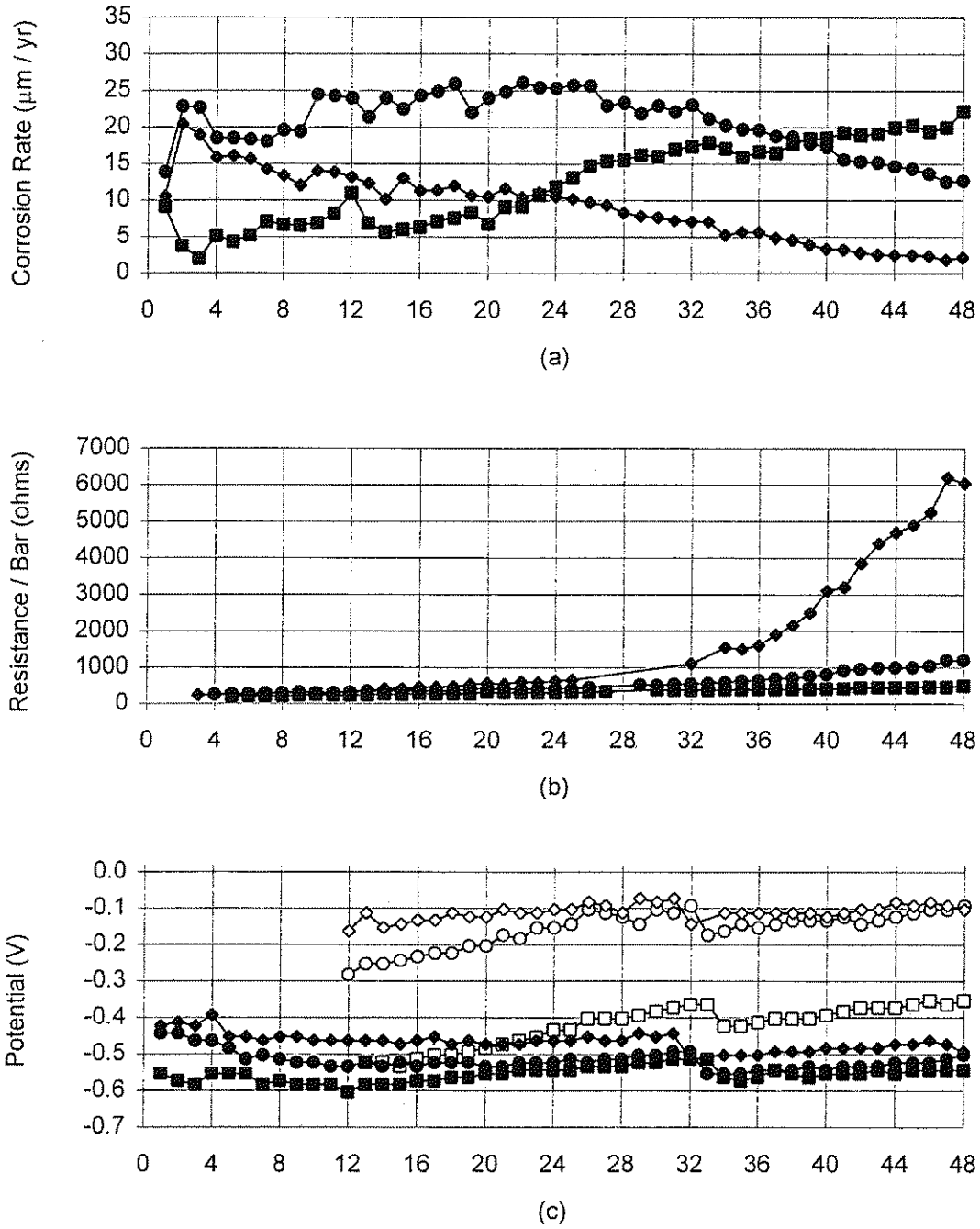

Fig. 3.33 Cracked Beam test results for steel combination CRST/H.
a) Macrocell Corrosion Rate, b) Mat-To-Mat Resistance, and
c) Potential of the Anode (solid) and Cathode (clear)

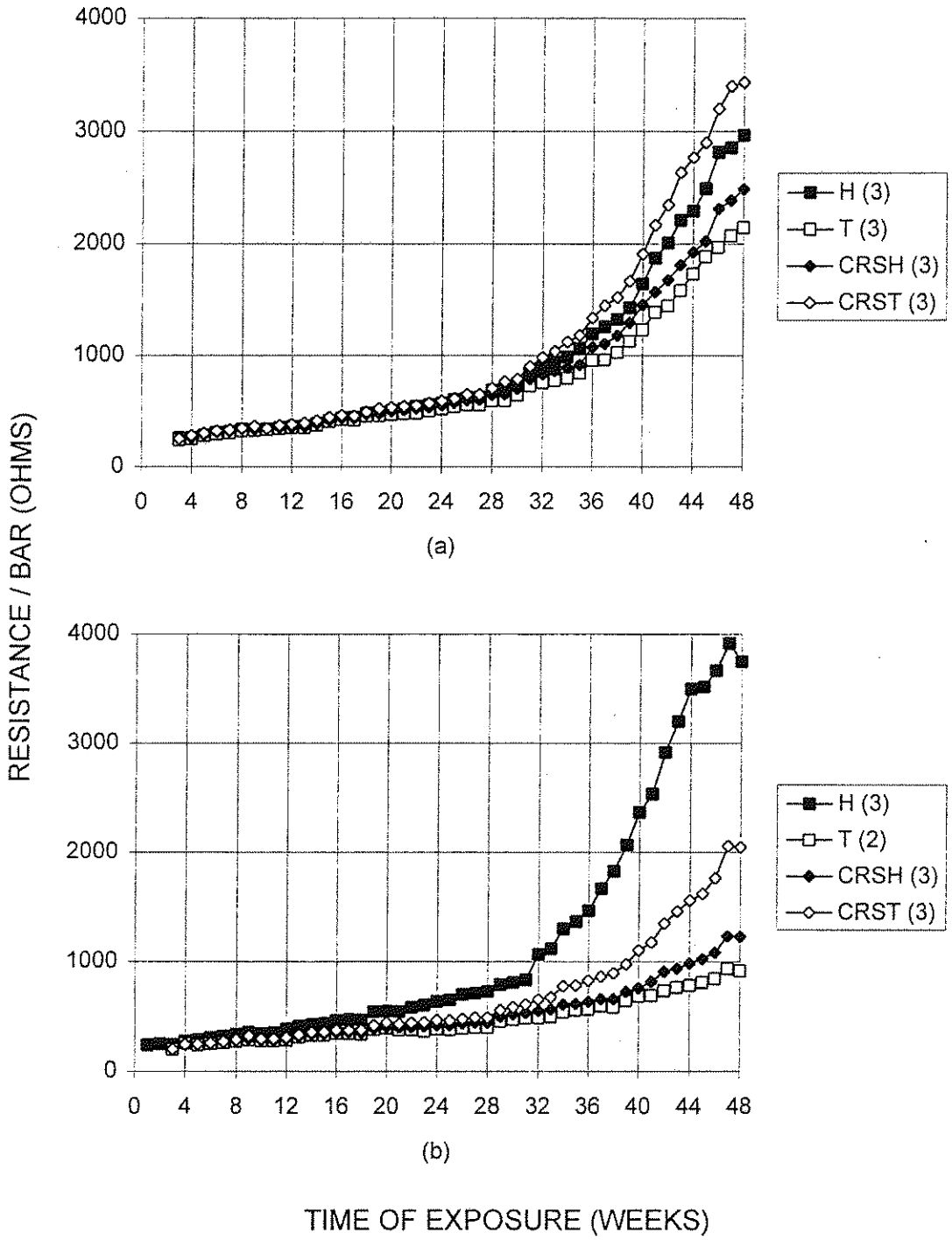

Fig. 3.34 Average mat-to-mat resistance for all four stees cast in regular concrete. a) Southern Exposure and b) Cracked Beam

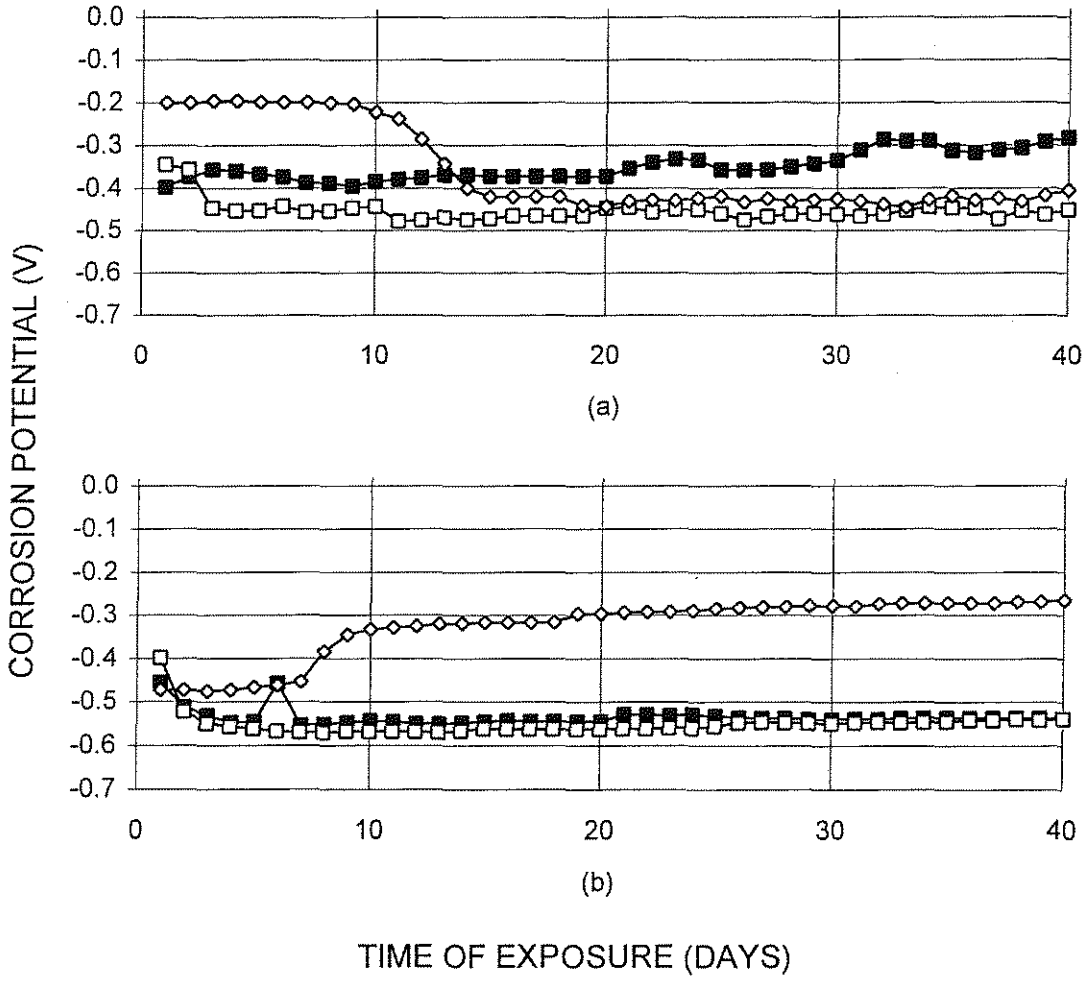

Fig. 3.35 Corrosion Potential Test: Corrosion resistant steels cast in mortar with the inorganic inhibitor and exposed to a 1.0 m NaCl concentration.
(a) CRSH and (b) CRST

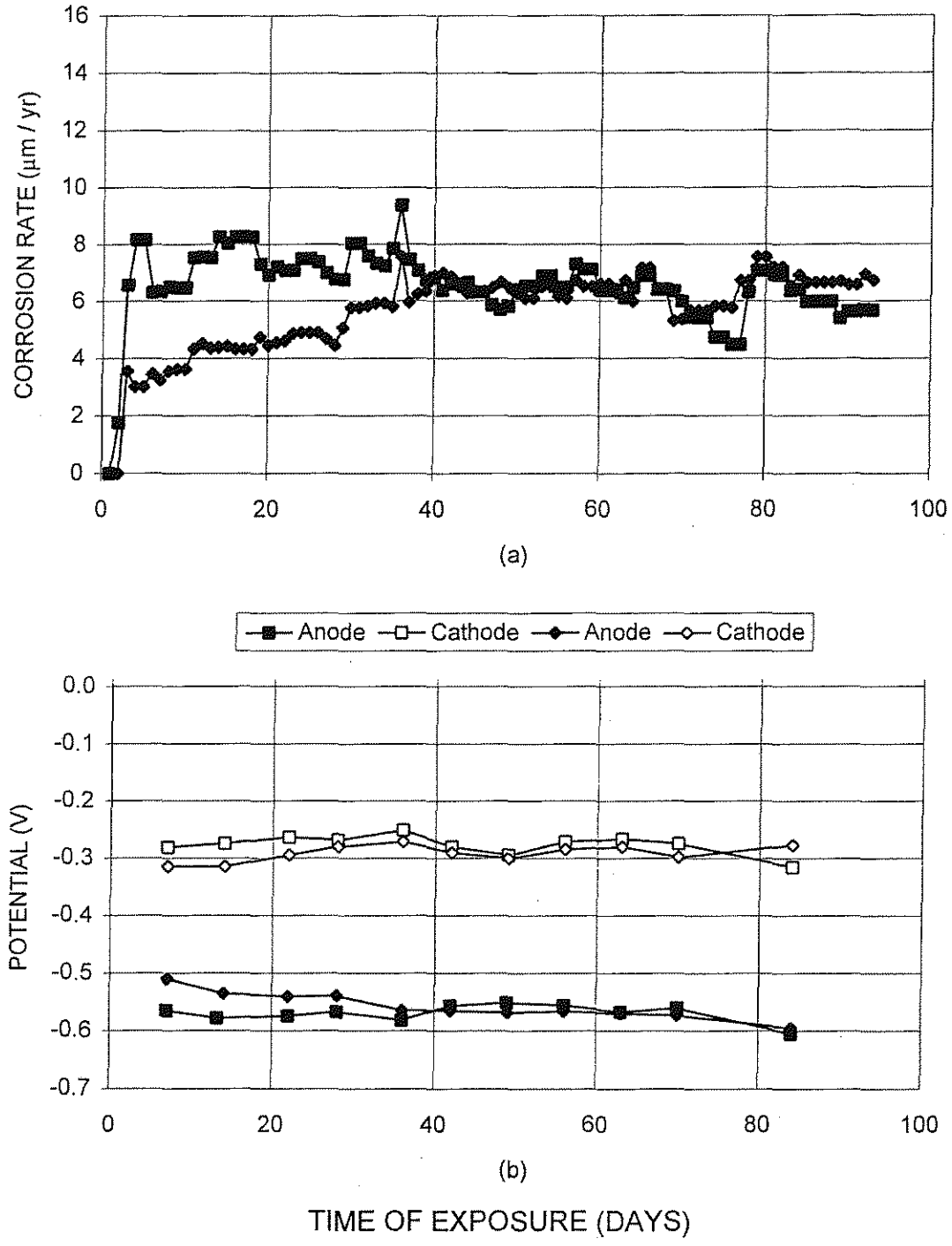

Fig. 3.36 Corrosion Potential and Macrocell Tests: H steel cast in mortar with the inorganic inhibitor and exposed to a 1.6 m NaCl concentration.
(a) Macrocell Corrosion Rate and (b) Corrosion Potential

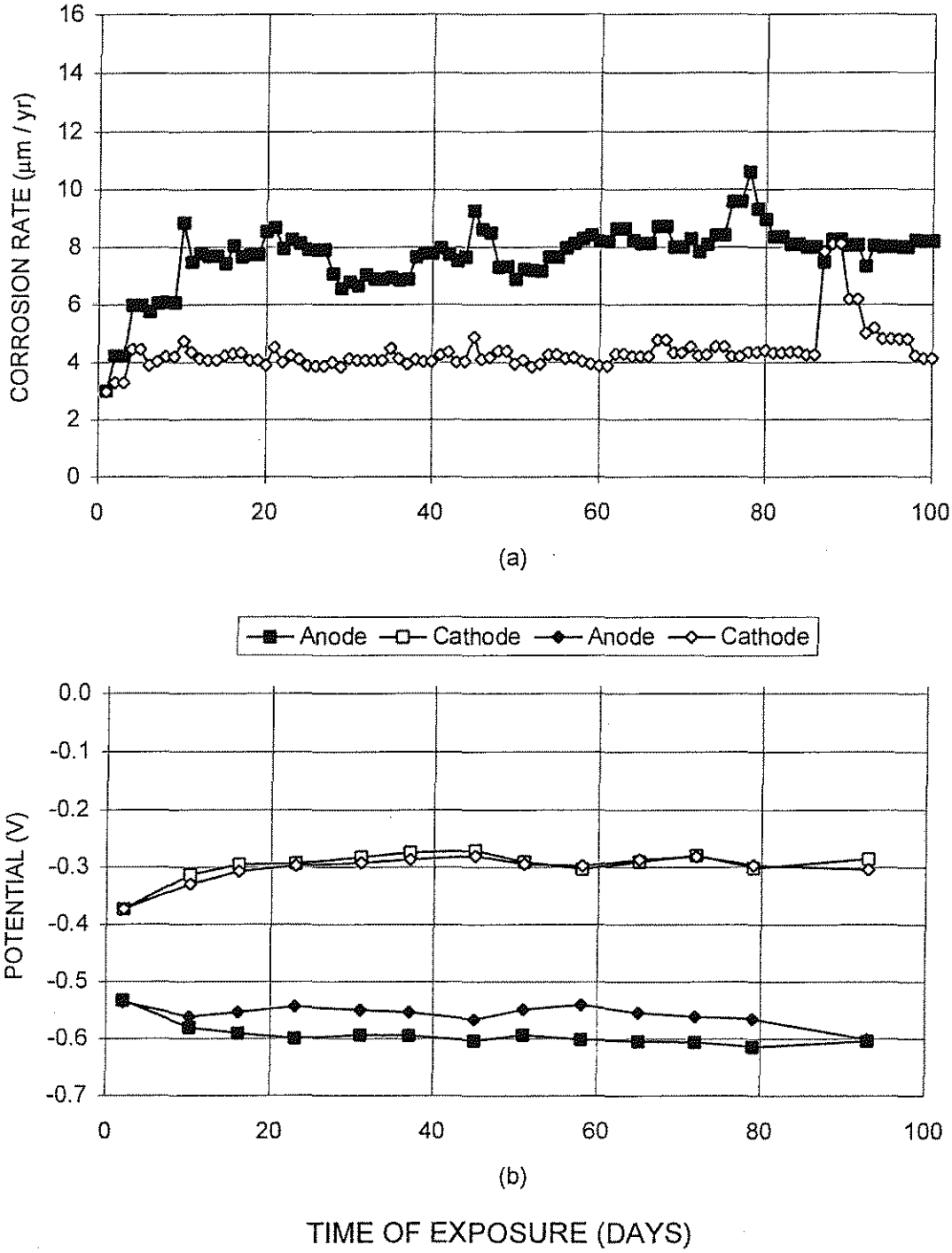

Fig. 3.37 Corrosion Potential and Macrocell Tests: T steel cast in mortar with the inorganic inhibitor and exposed to a 1.6 m NaCl concentration.
(a) Macrocell Corrosion Rate and (b) Corrosion Potential

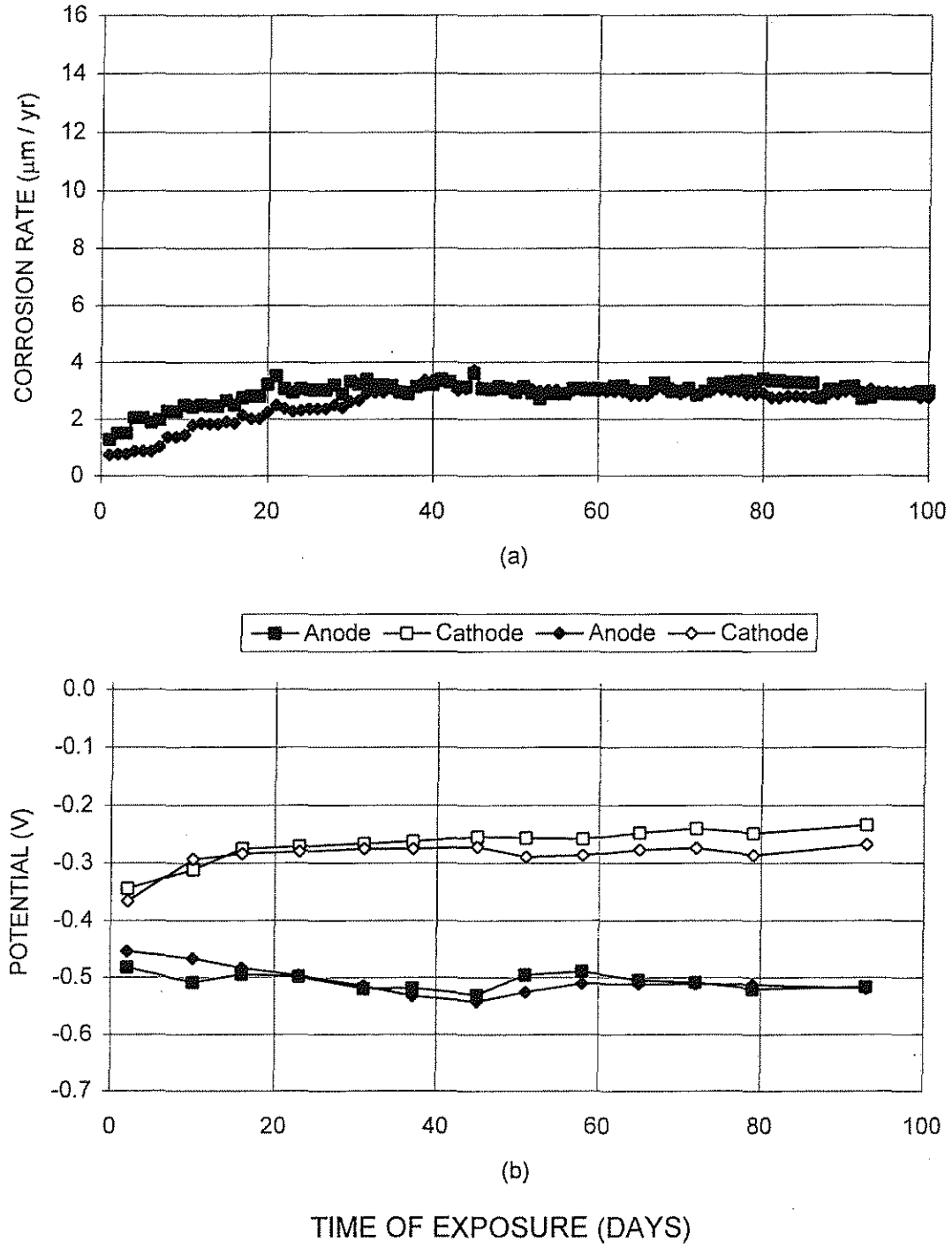

Fig. 3.38 Corrosion Potential and Macrocell Tests: CRSH steel cast in mortar with the inorganic inhibitor and exposed to a 1.6 m NaCl concentration. (a) Macrocell Corrosion Rate and (b) Corrosion Potential

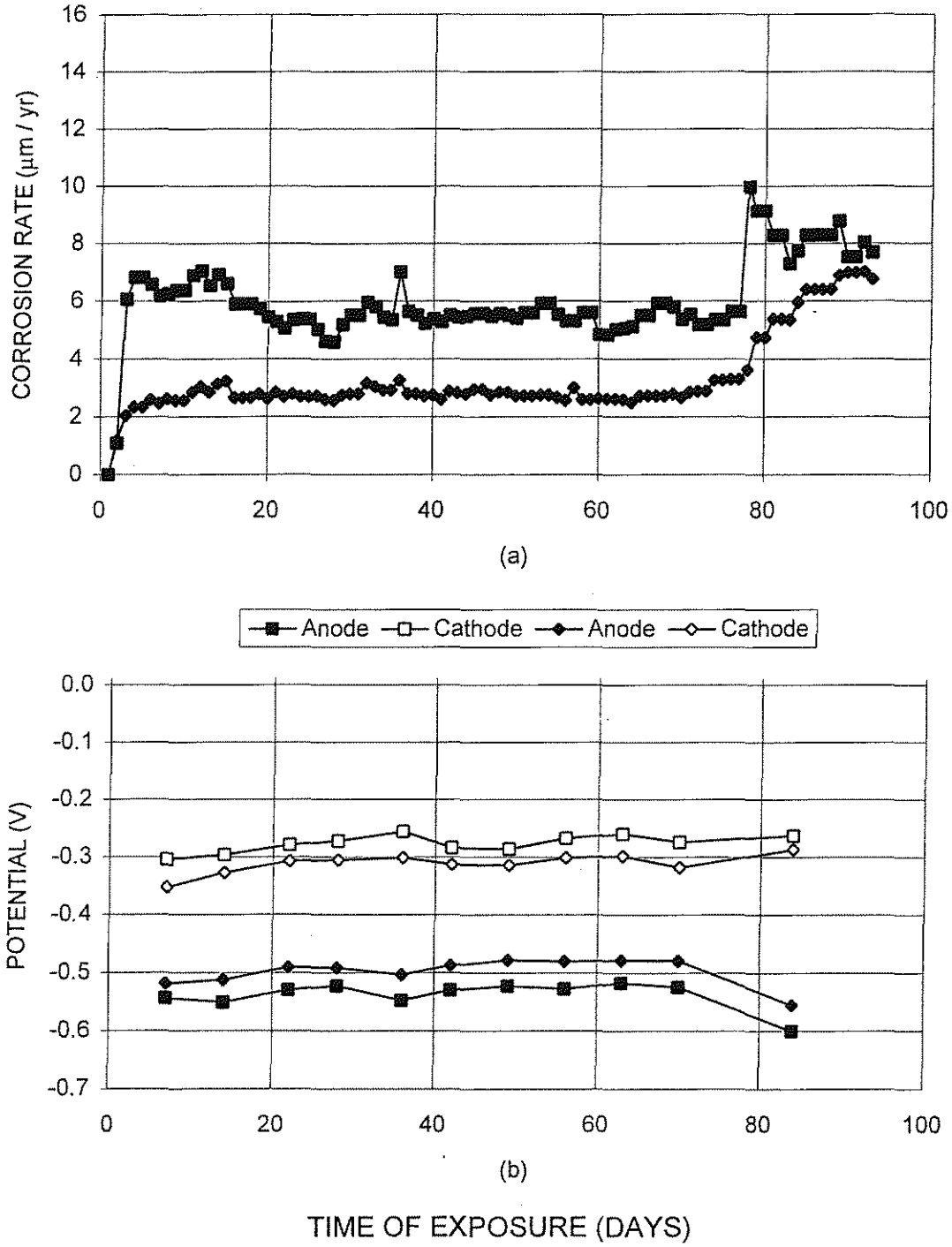

Fig. 3.39 Corrosion Potential and Macrocell Tests: CRST steel cast in mortar with the inorganic inhibitor and exposed to a 1.6 m NaCl concentration. (a) Macrocell Corrosion Rate and (b) Corrosion Potential

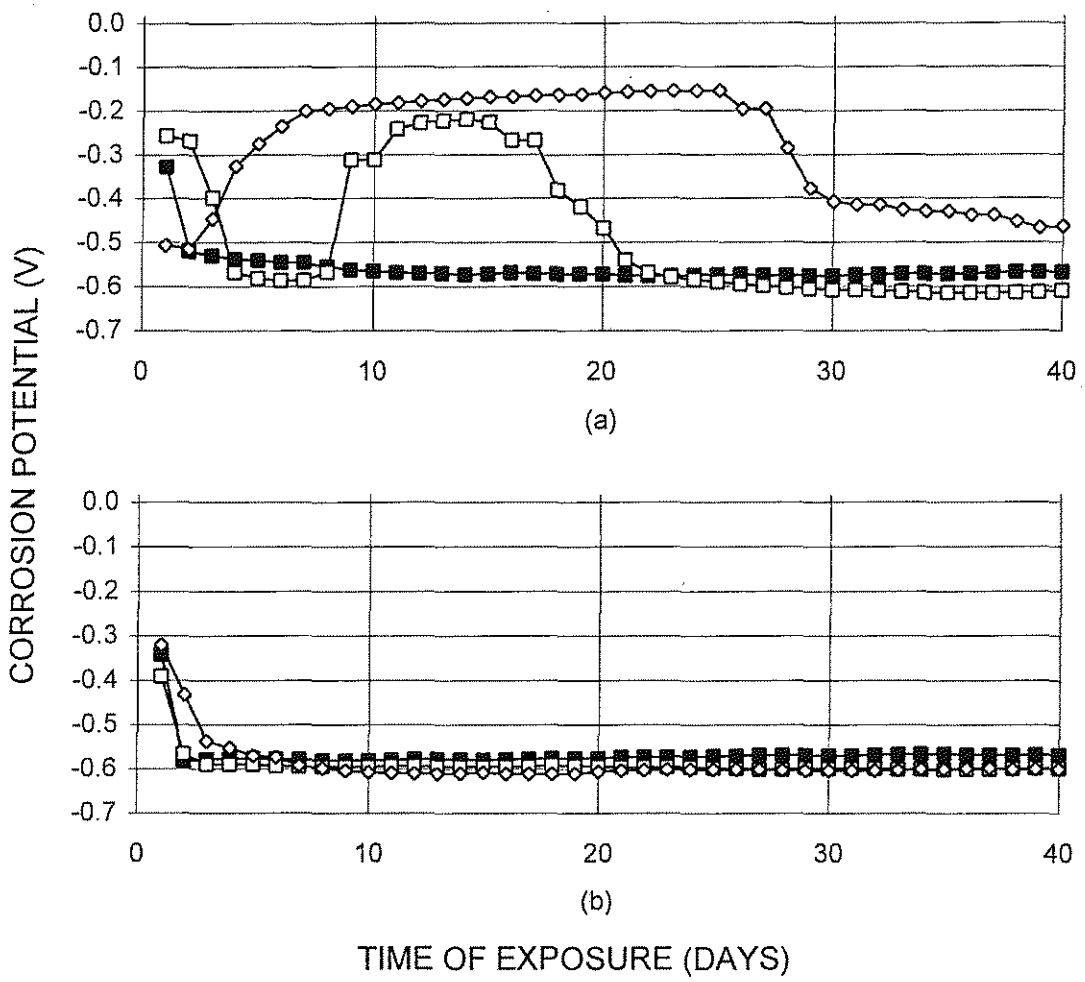

Fig. 3.40 Corrosion Potential Test: Corrosion resistant steels cast in mortar with the organic inhibitor and exposed to a 6.04 m NaCl concentration.
(a) CRSH and (b) CRST

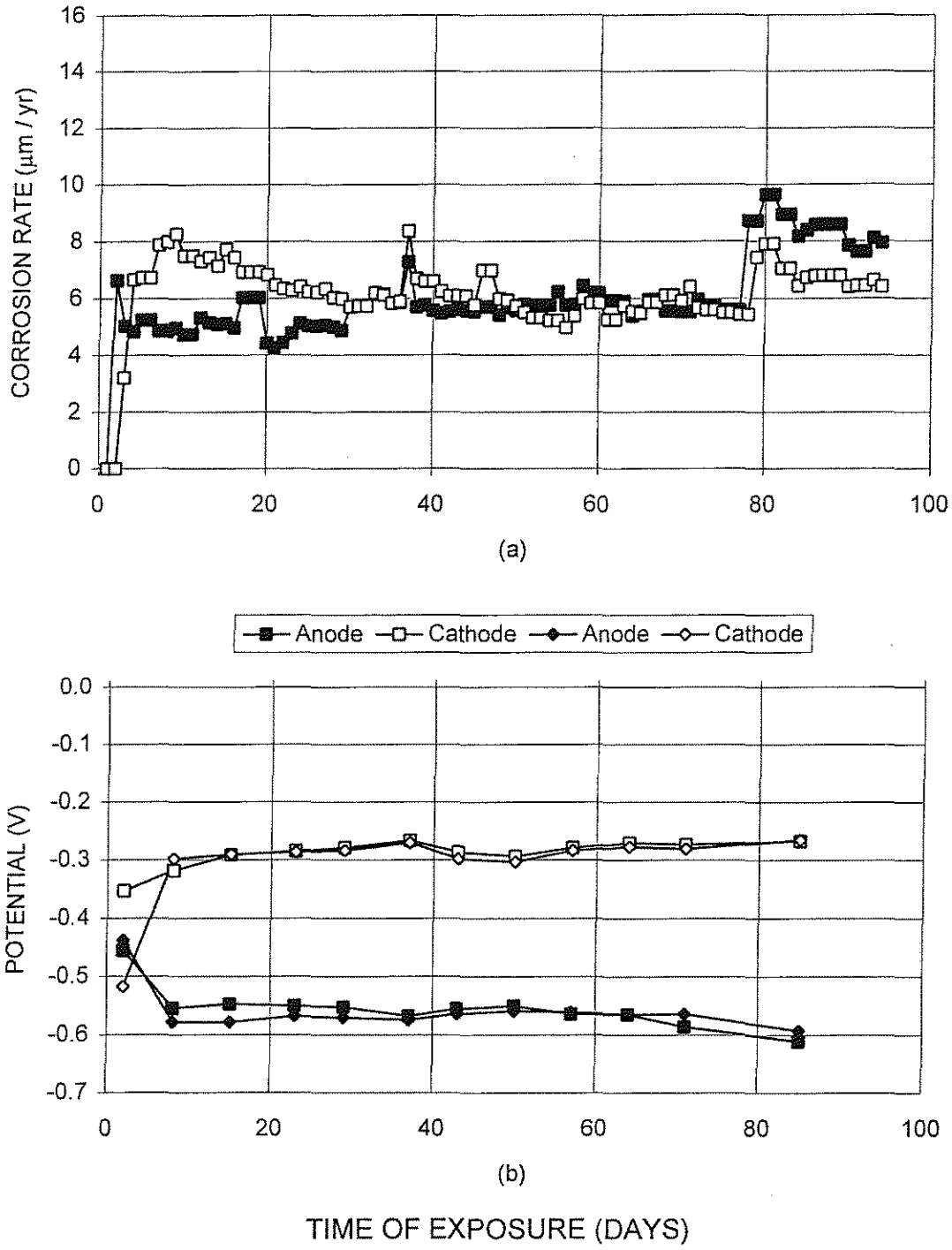

Fig. 3.41 Corrosion Potential and Macrocell Tests: H steel cast in mortar with the organic inhibitor and exposed to a 1.6 m NaCl concentration.
(a) Macrocell Corrosion Rate and (b) Corrosion Potential

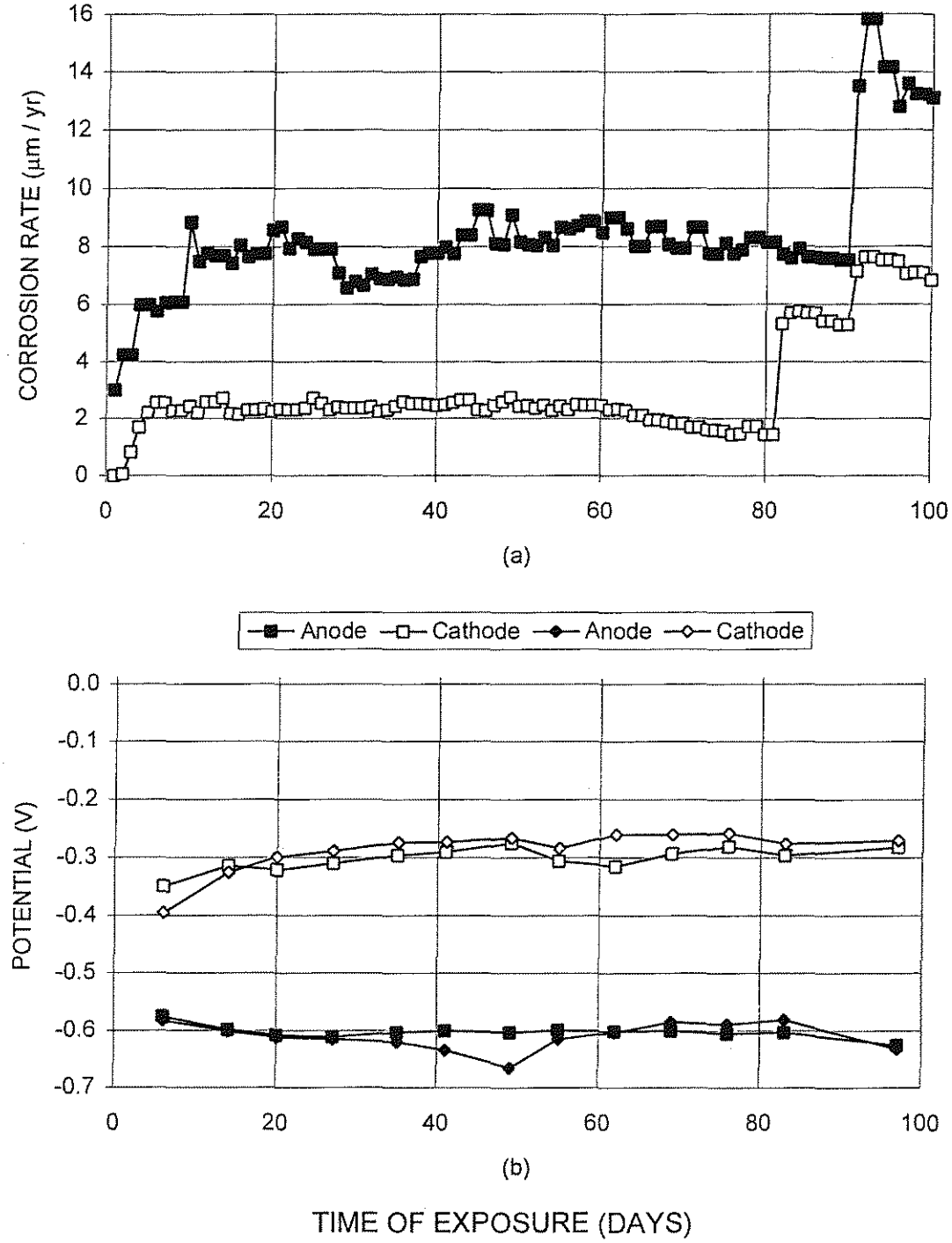

Fig. 3.42 Corrosion Potential and Macrocell Tests: T steel cast in mortar with the organic inhibitor and exposed to a 1.6 m NaCl concentration.
(a) Macrocell Corrosion Rate and (b) Corrosion Potential

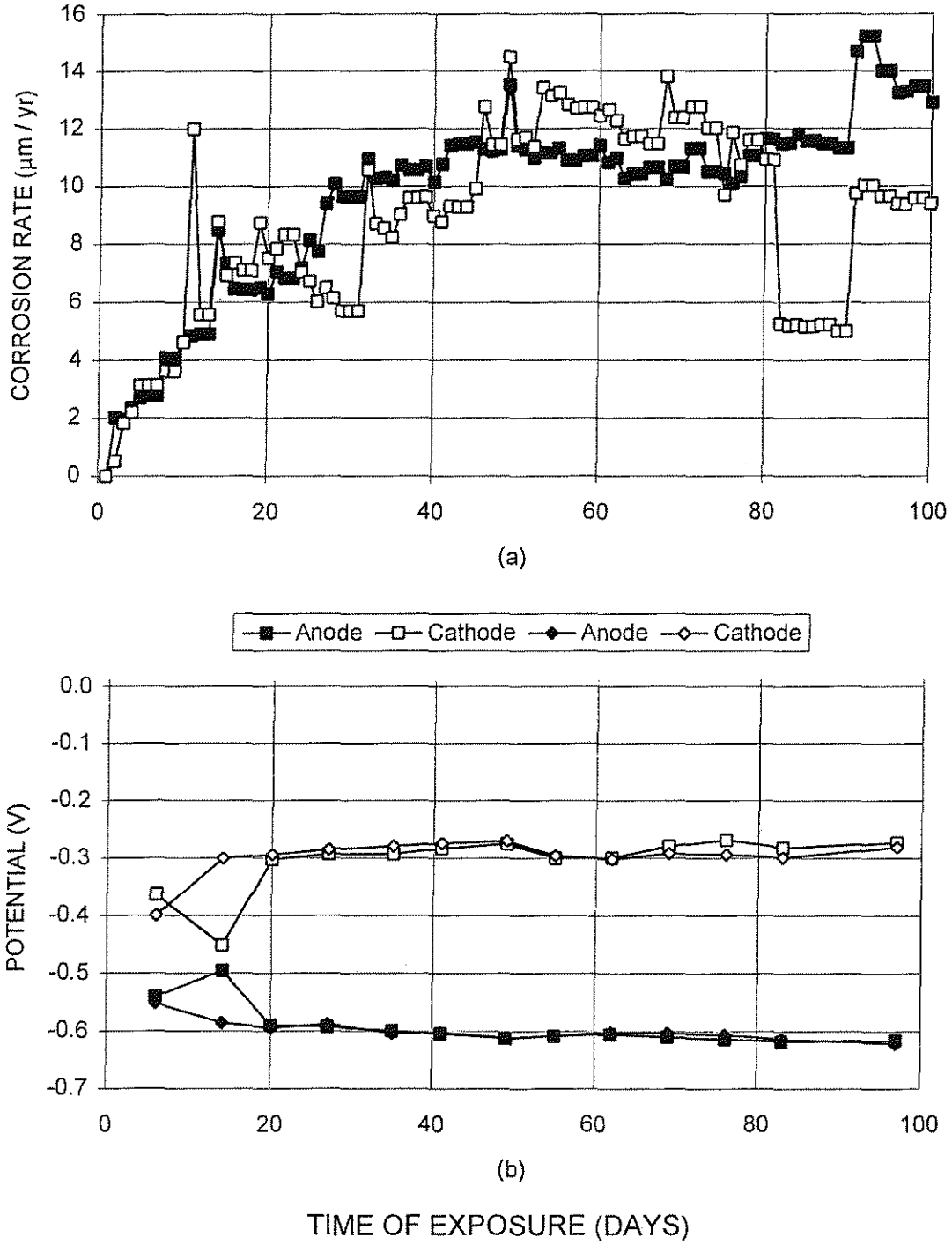

Fig. 3.43 Corrosion Potential and Macrocell Tests: CRSH steel cast in mortar with the organic inhibitor and exposed to a 1.6 m NaCl concentration. (a) Macrocell Corrosion Rate and (b) Corrosion Potential

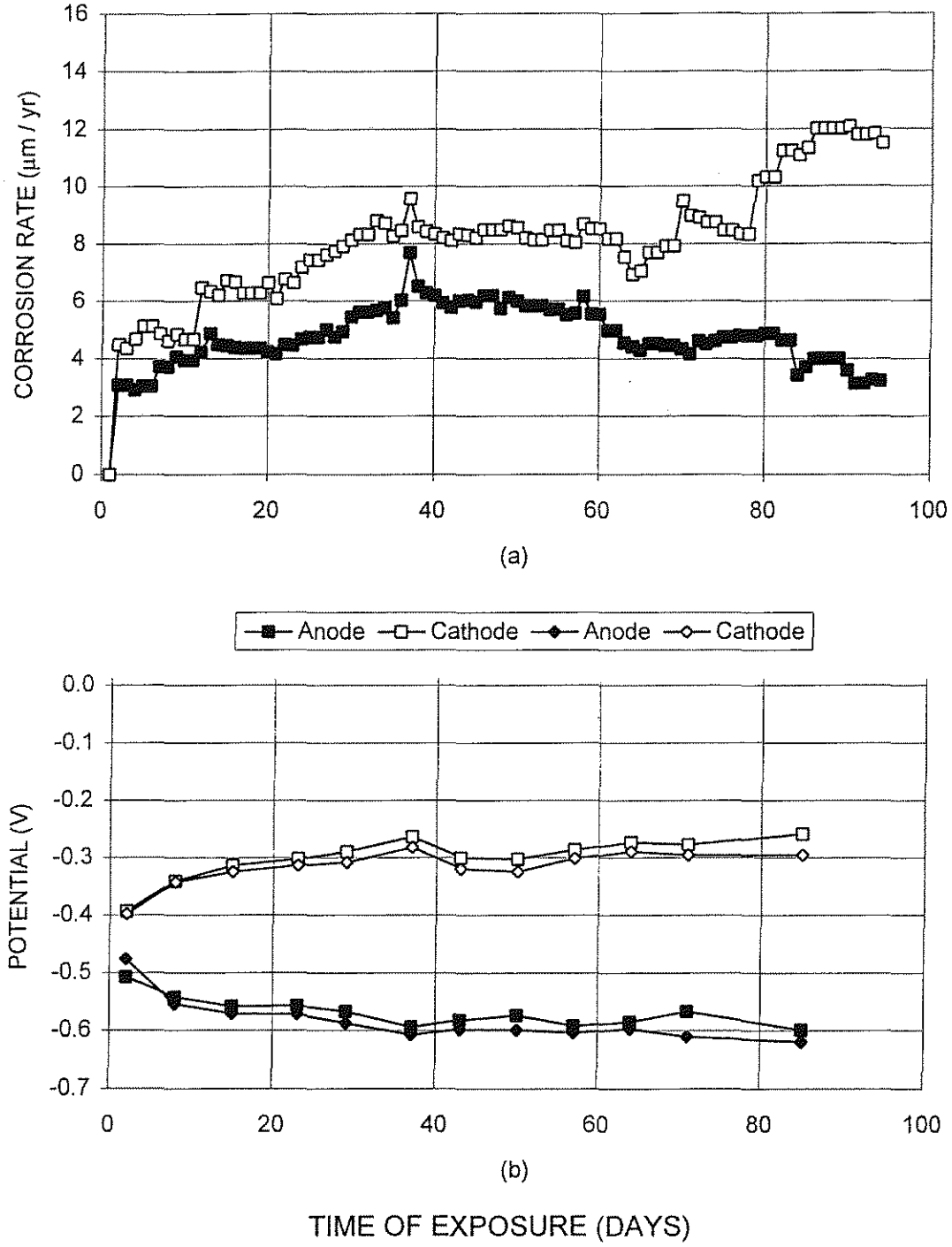

Fig. 3.44 Corrosion Potential and Macrocell Tests: CRST steel cast in mortar with the organic inhibitor and exposed to a 1.6 m NaCl concentration. (a) Macrocell Corrosion Rate and (b) Corrosion Potential

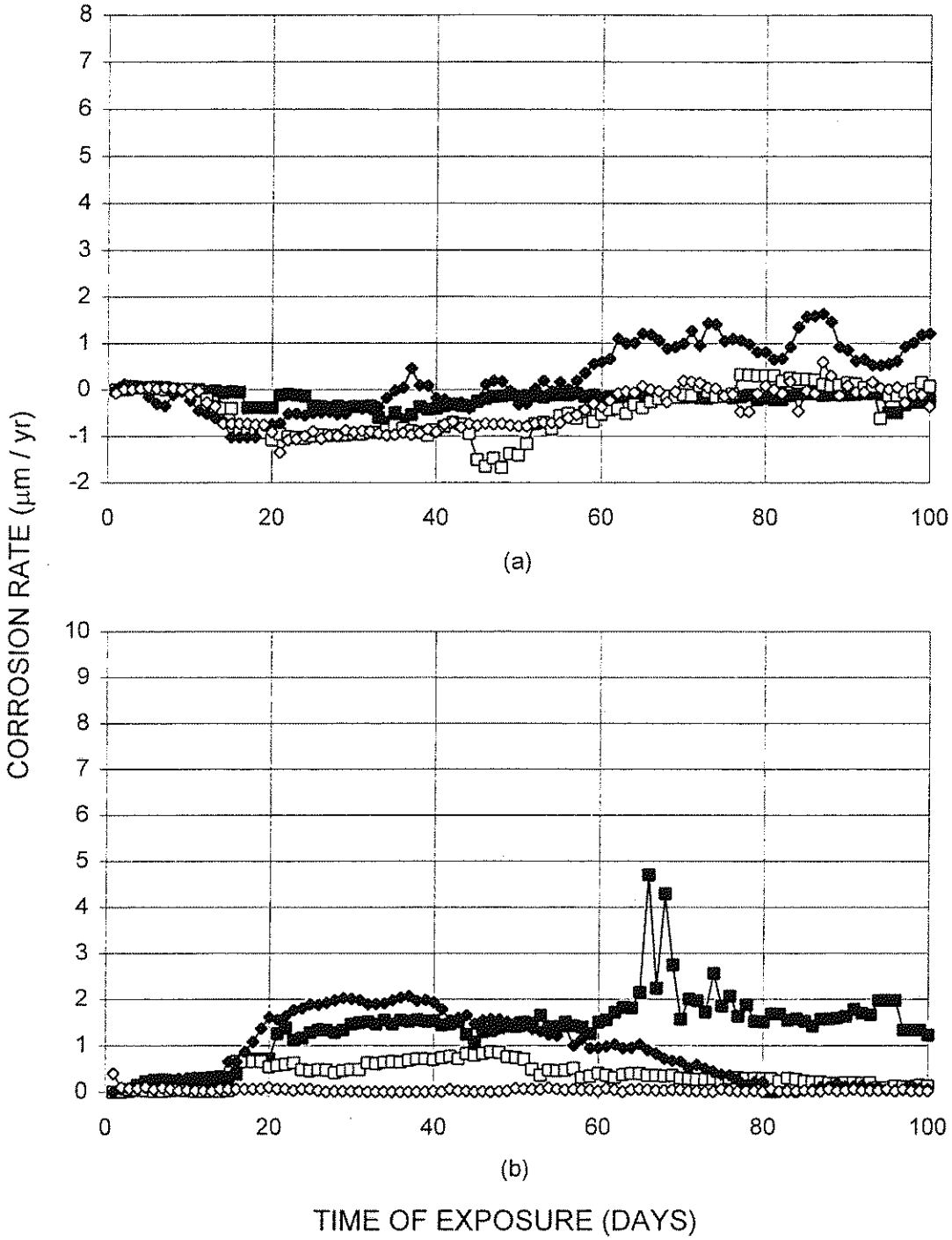

Fig. 3.45 Macrocell Test: Corrosion resistant steels cast in mortar with the inorganic inhibitor and exposed to a 1.0 m NaCl concentration.
(a) CRSH and (b) CRST

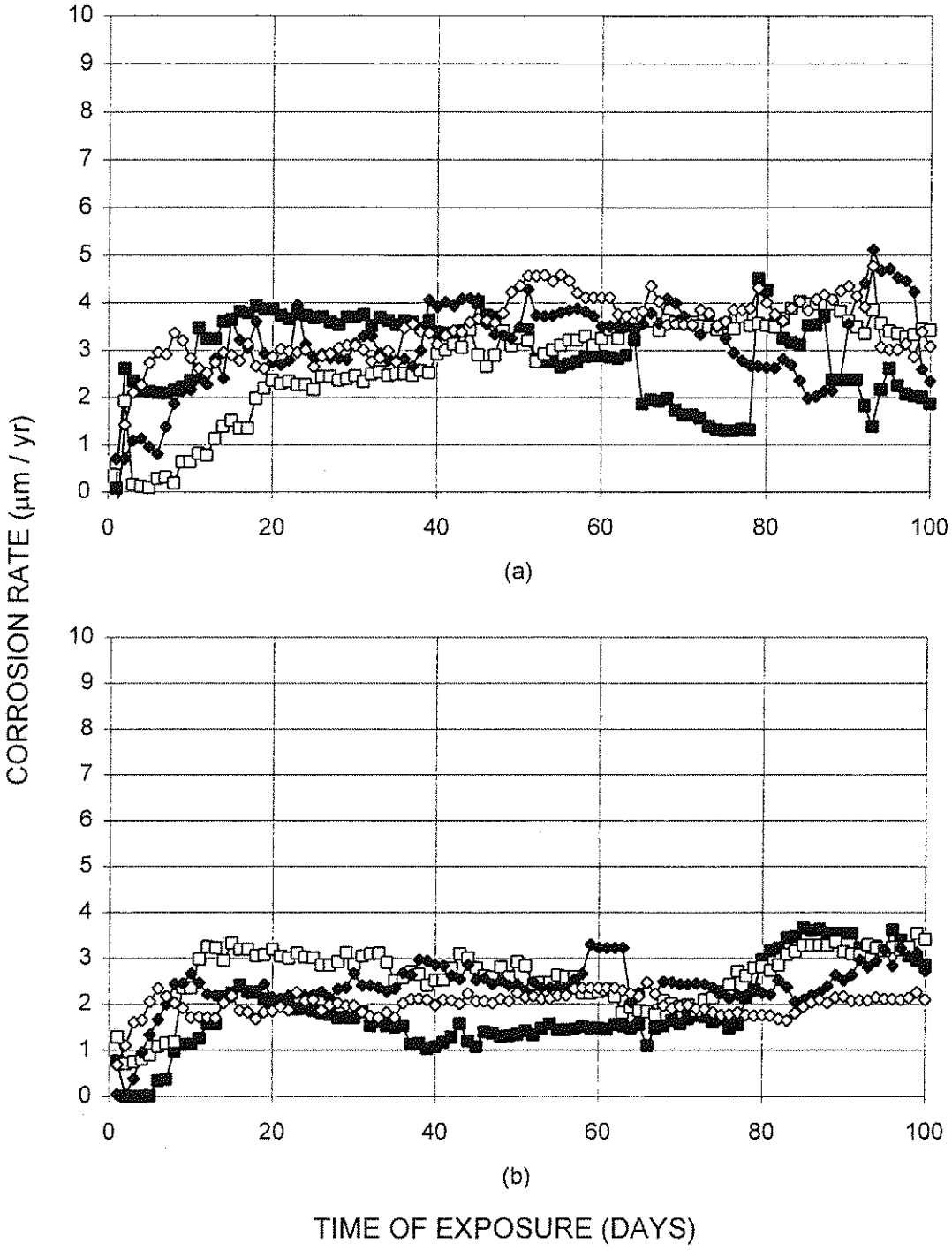

Fig. 3.46 Macrocell Test: Corrosion resistant steels cast in mortar with the organic inhibitor and exposed to a 6.04 m NaCl concentration.
(a) CRSH and (b) CRST

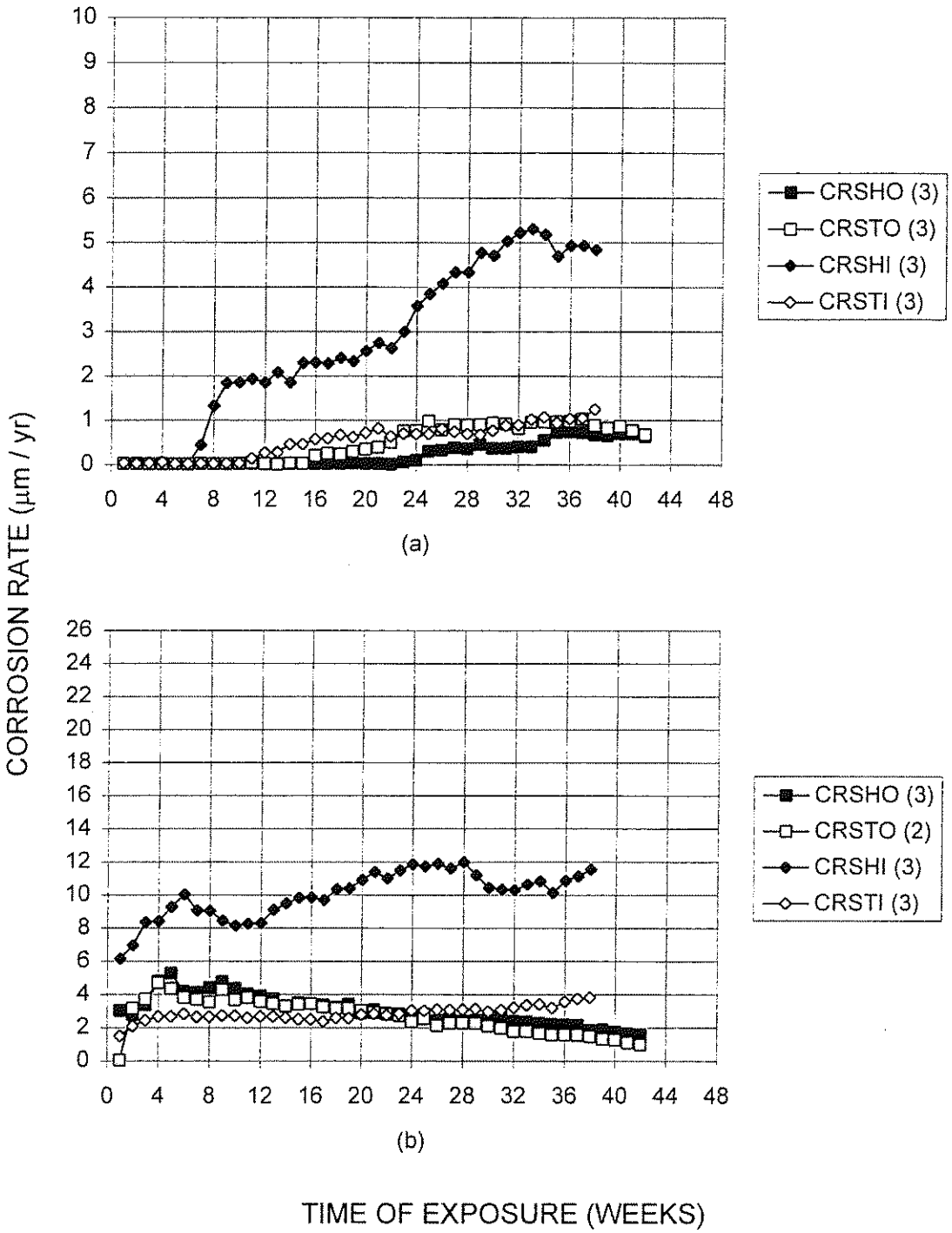

Fig. 3.47 Average macrocell corrosion rates for the corrosion resistant steels cast with the organic and inorganic inhibitors. (a) Southern Exposure and (b) Cracked Beam

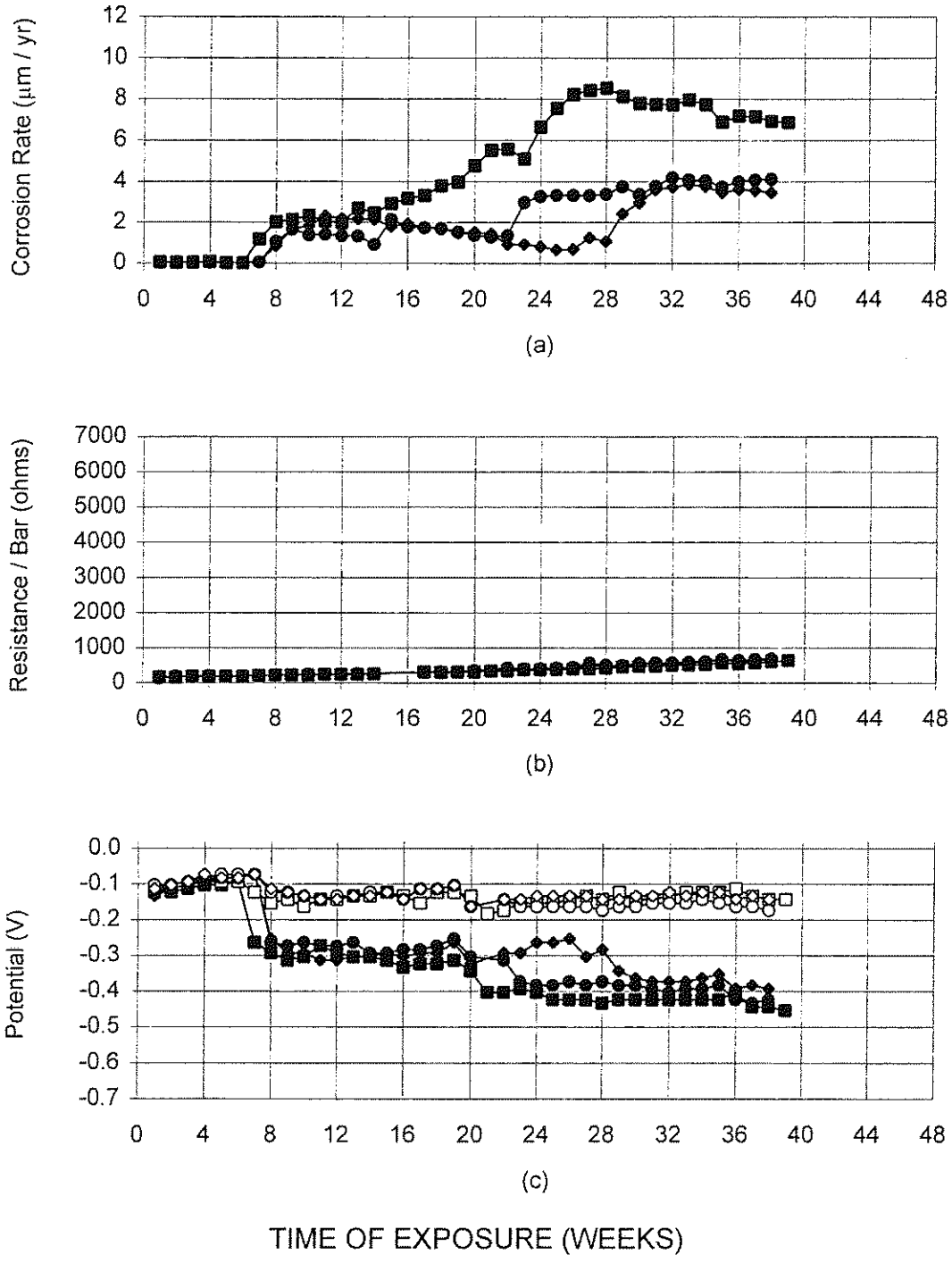

Fig. 3.48 Southern Exposure test results for CRSH steel cast with the inorganic inhibitor. (a) Macrocell Corrosion Rate, (b) Mat-To-Mat Resistance, and (c) Potential of the Anode (solid) and Cathode (clear)

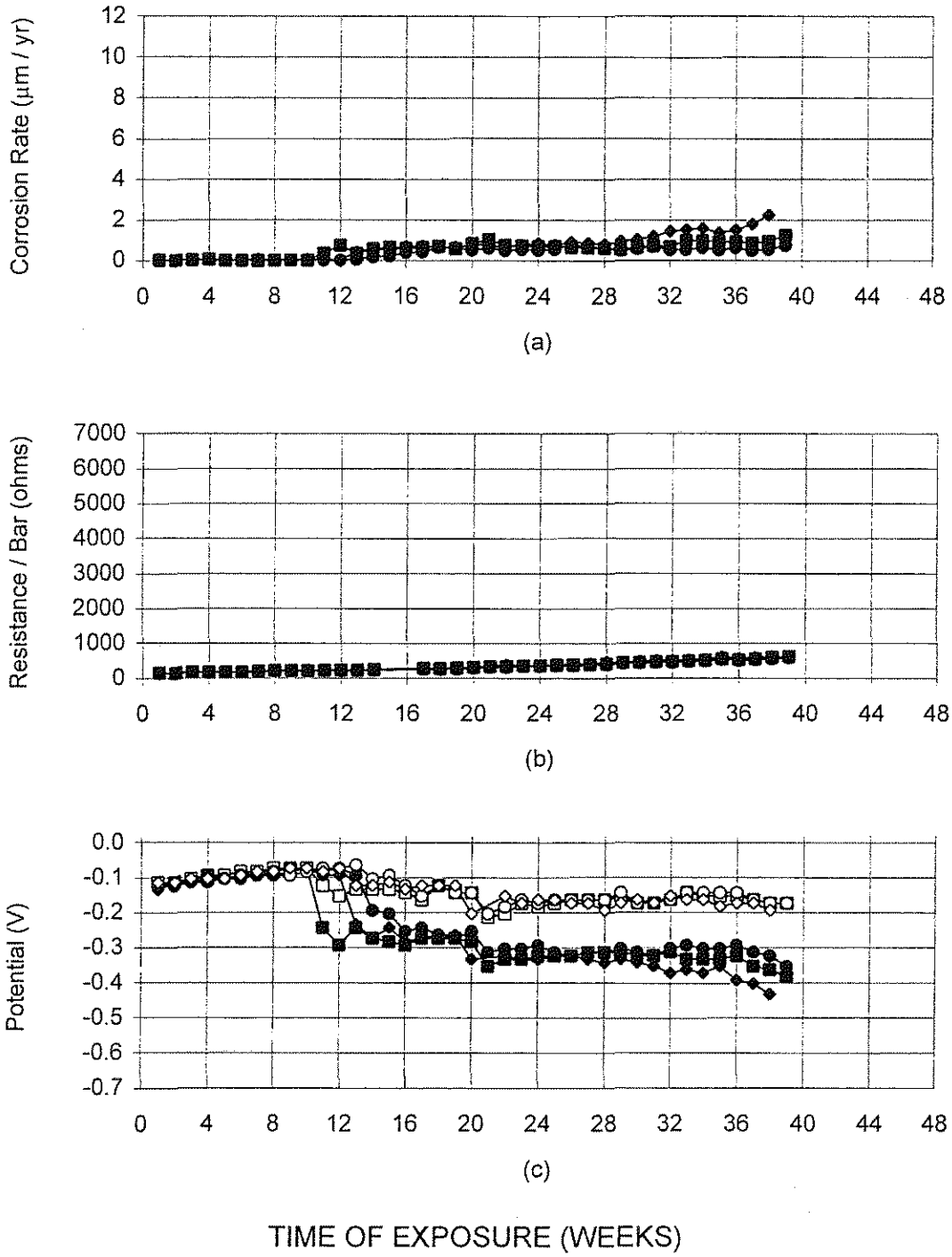

Fig. 3.49 Southern Exposure test results for CRST steel cast with the inorganic inhibitor. (a) Macrocell Corrosion Rate, (b) Mat-To-Mat Resistance, and (c) Potential of the Anode (solid) and Cathode (clear)

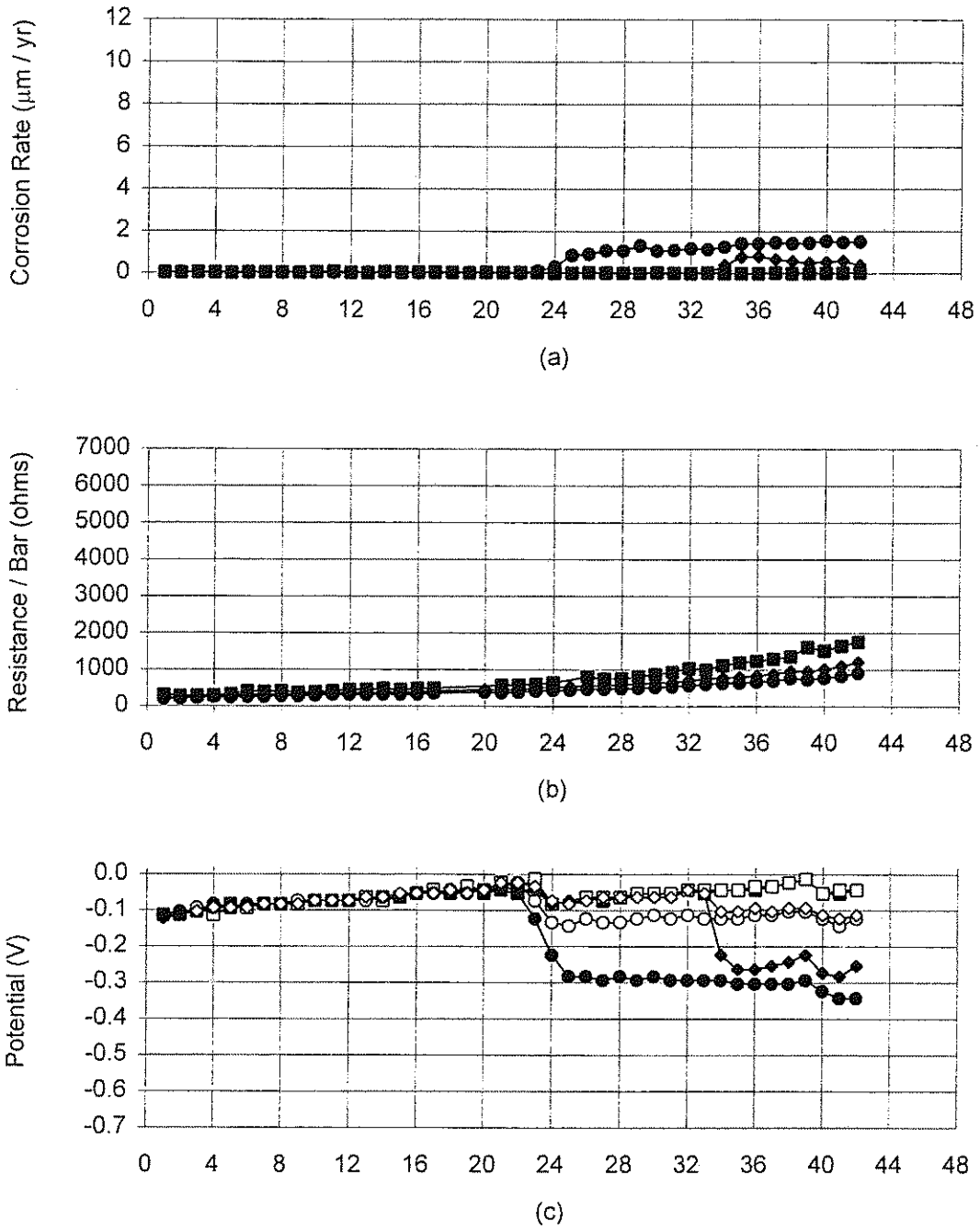

Fig. 3.50 Southern Exposure test results for CRSH steel cast with the organic inhibitor. (a) Macrocell Corrosion Rate, (b) Mat-To-Mat Resistance, and (c) Potential of the Anode (solid) and Cathode (clear)

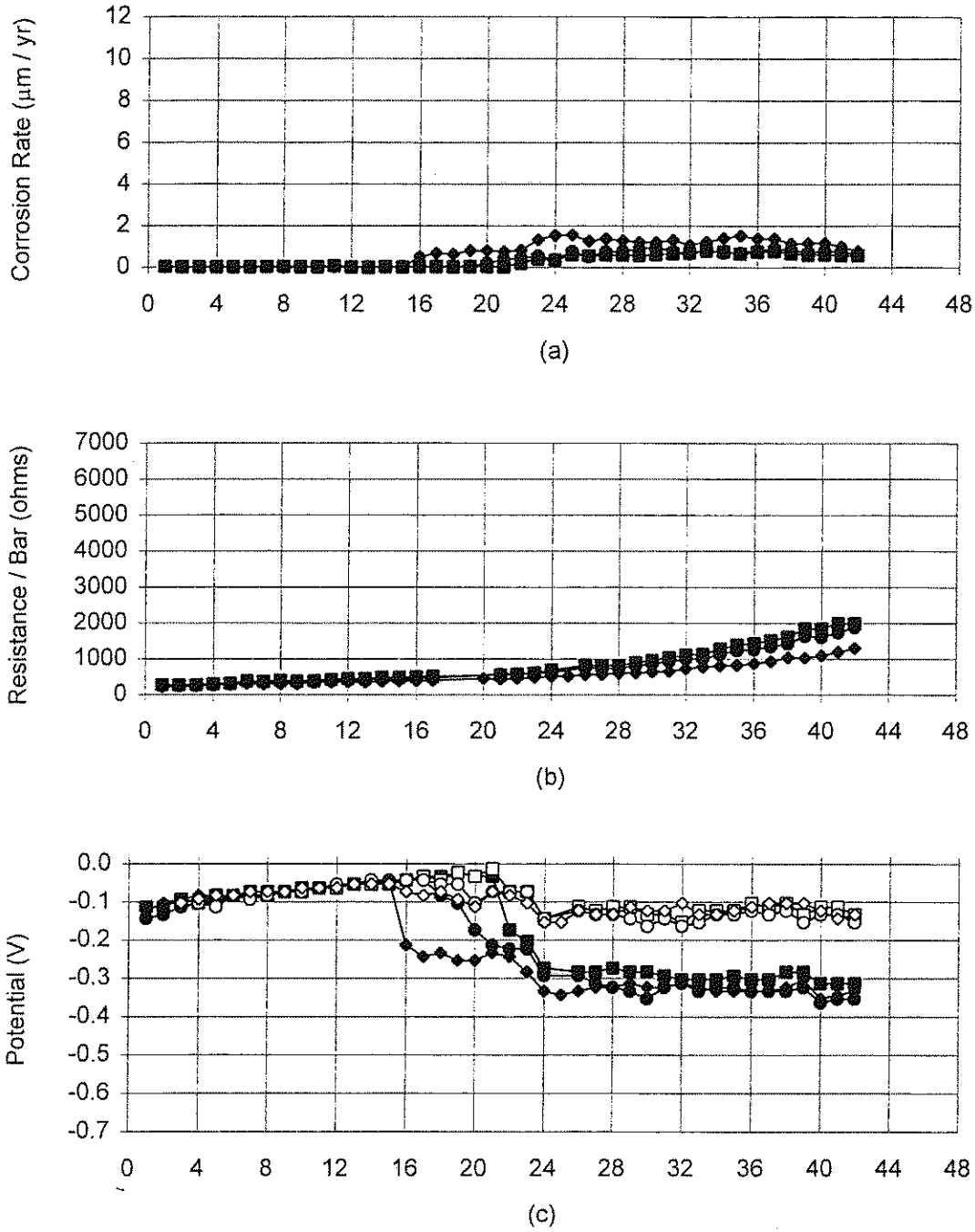

Fig. 3.51 Southern Exposure test results for CRST steel cast with the organic inhibitor. (a) Macrocell Corrosion Rate, (b) Mat-To-Mat Resistance, and (c) Potential of the Anode (solid) and Cathode (clear)

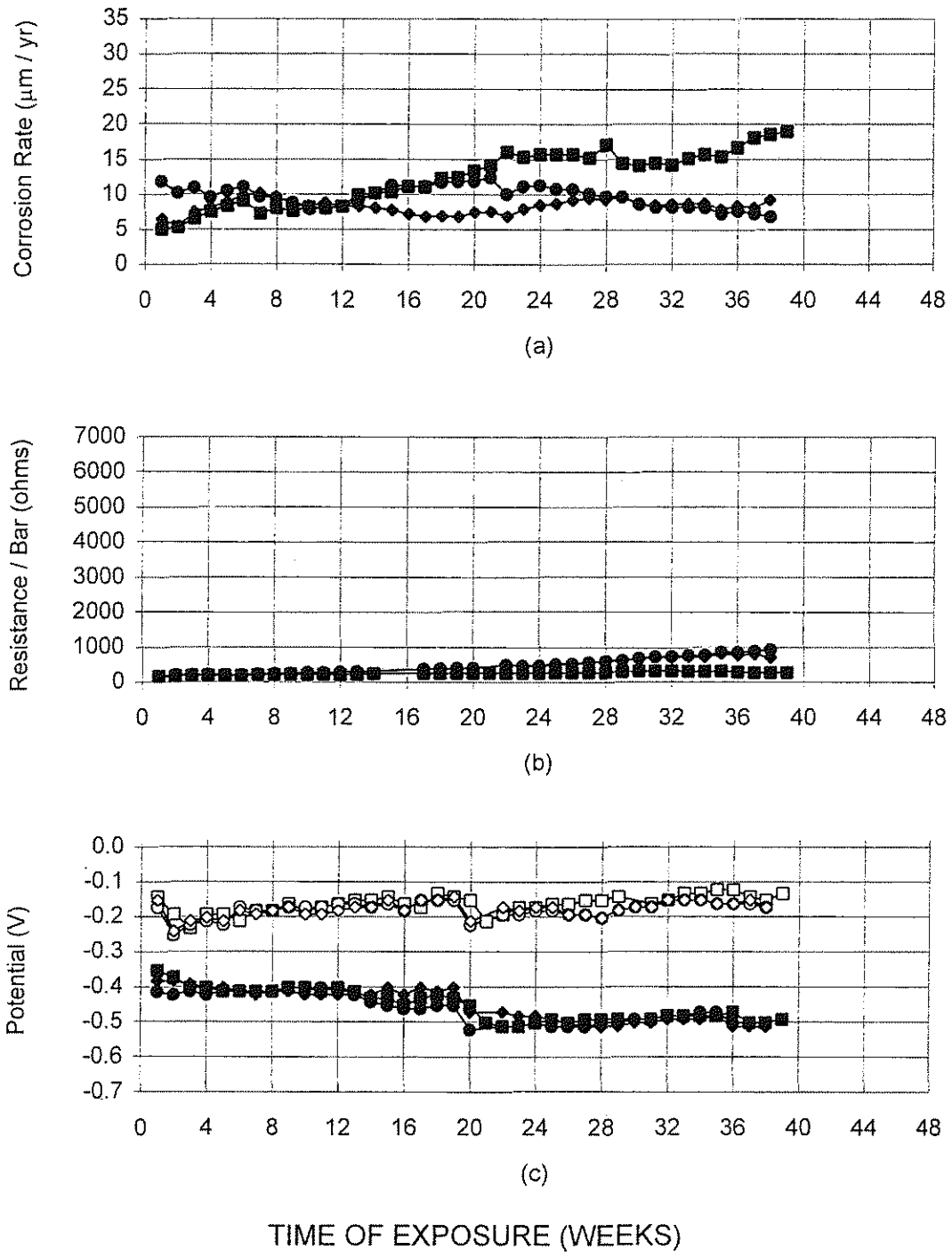

Fig. 3.52 Cracked Beam test results for CRSH steel cast with the inorganic inhibitor. (a) Macrocell Corrosion Rate, (b) Mat-To-Mat Resistance, and (c) Potential of the Anode (solid) and Cathode (clear)

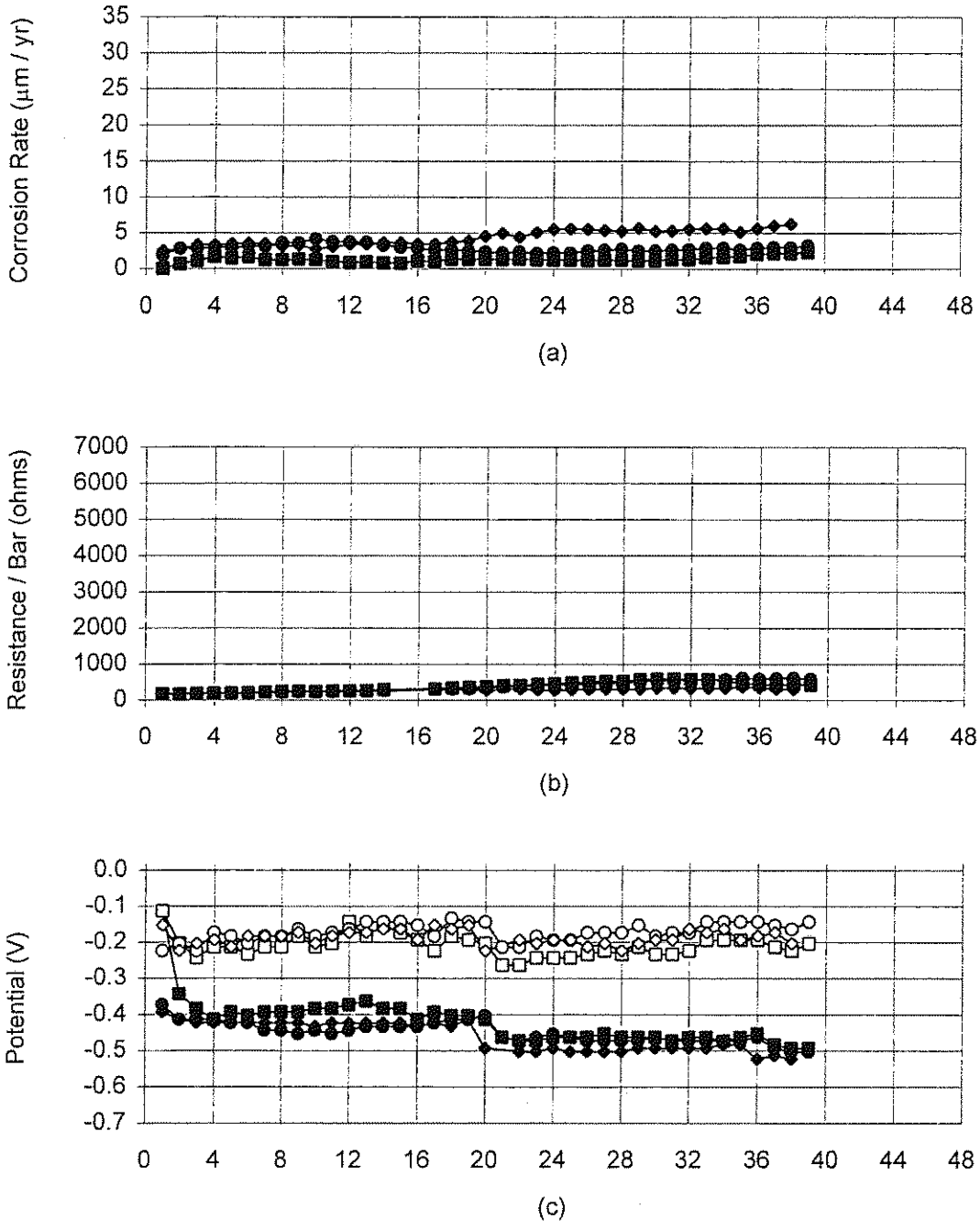

Fig. 3.53 Cracked Beam test results for CRST steel cast with the inorganic inhibitor. (a) Macrocell Corrosion Rate, (b) Mat-To-Mat Resistance, and (c) Potential of the Anode (solid) and Cathode (clear)

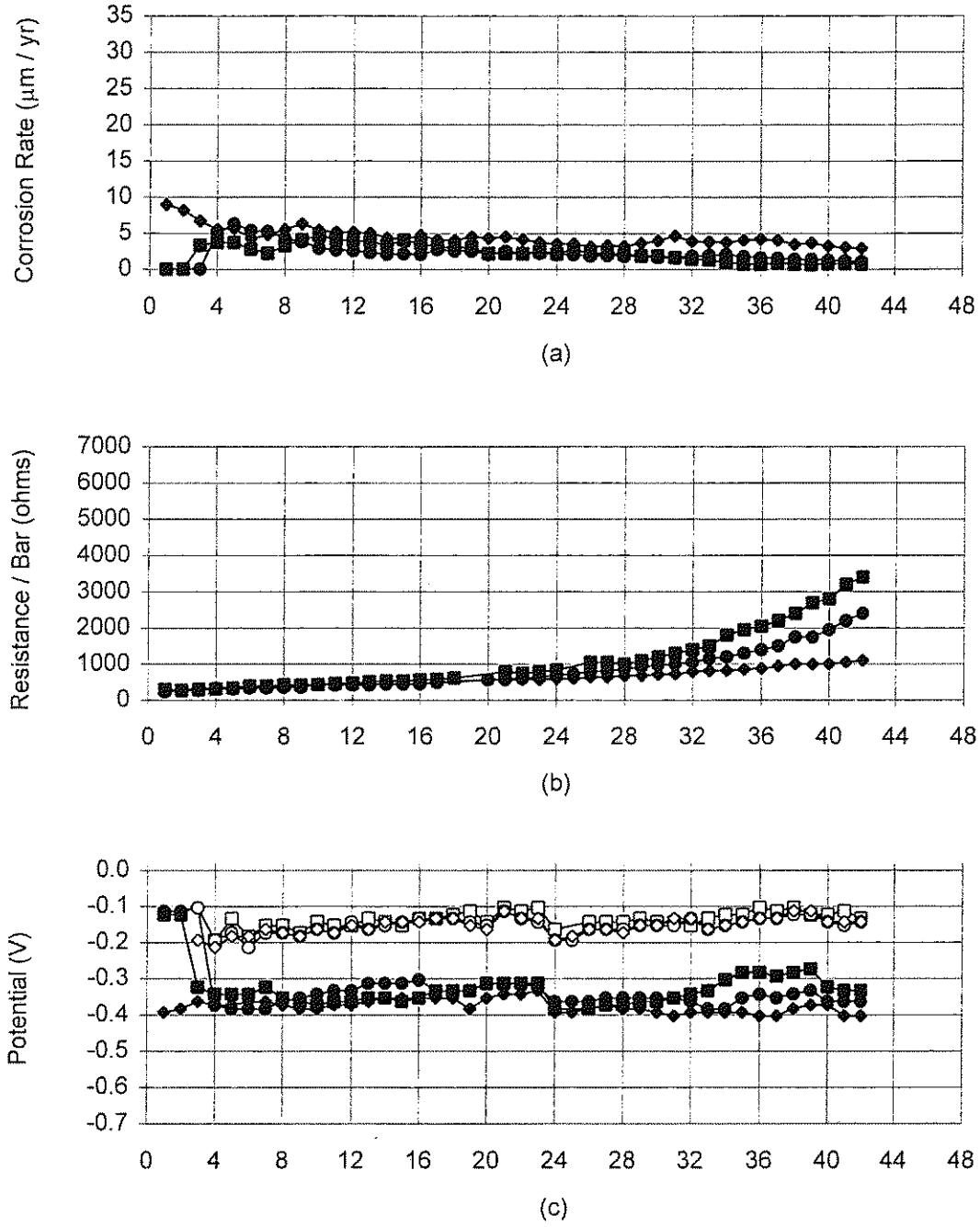

Fig. 3.54 Cracked Beam test results for CRSH steel cast with the organic inhibitor. (a) Macrocell Corrosion Rate, (b) Mat-To-Mat Resistance, and (c) Potential of the Anode (solid) and Cathode (clear)

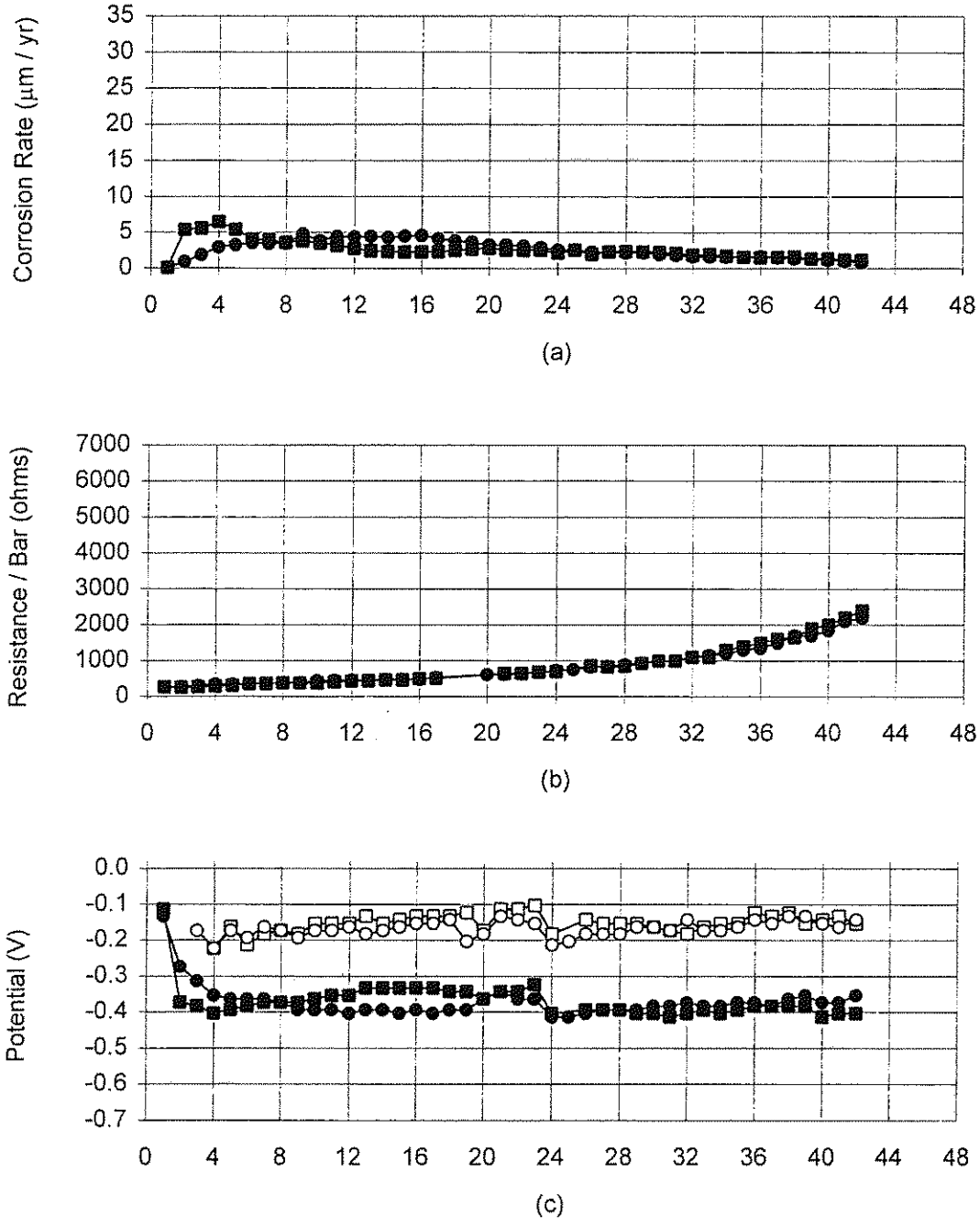

Fig. 3.55 Cracked Beam test results for CRST steel cast with the organic inhibitor. (a) Macrocell Corrosion Rate, (b) Mat-To-Mat Resistance, and (c) Potential of the Anode (solid) and Cathode (clear)

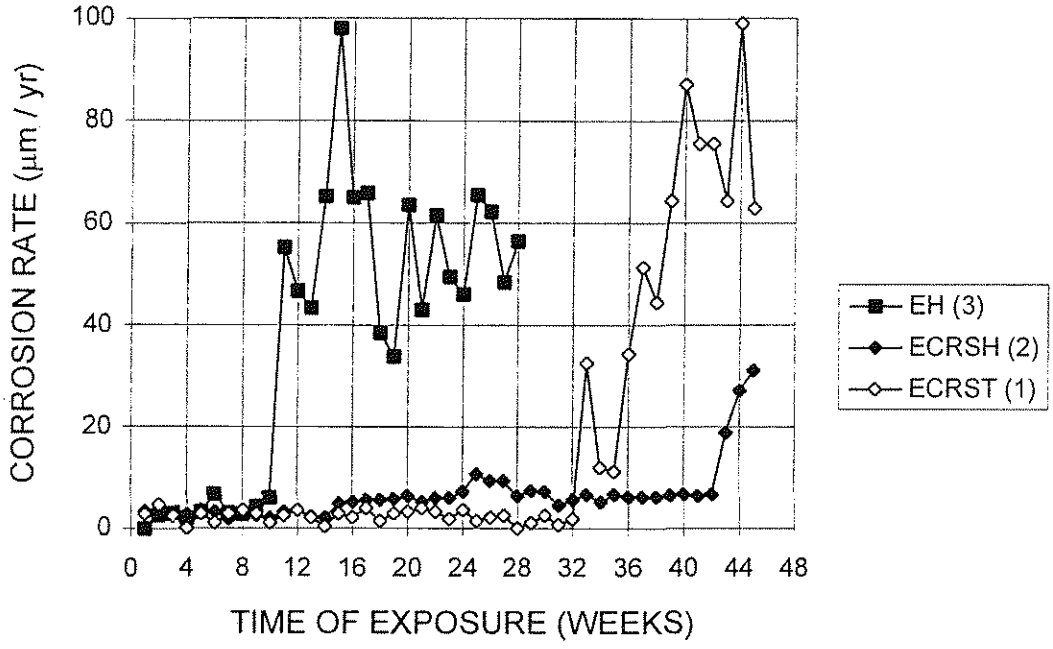

Fig. 3.56 Average macrocell corrosion rates for Southern Exposure tests with damaged epoxy-coated reinforcing bars.

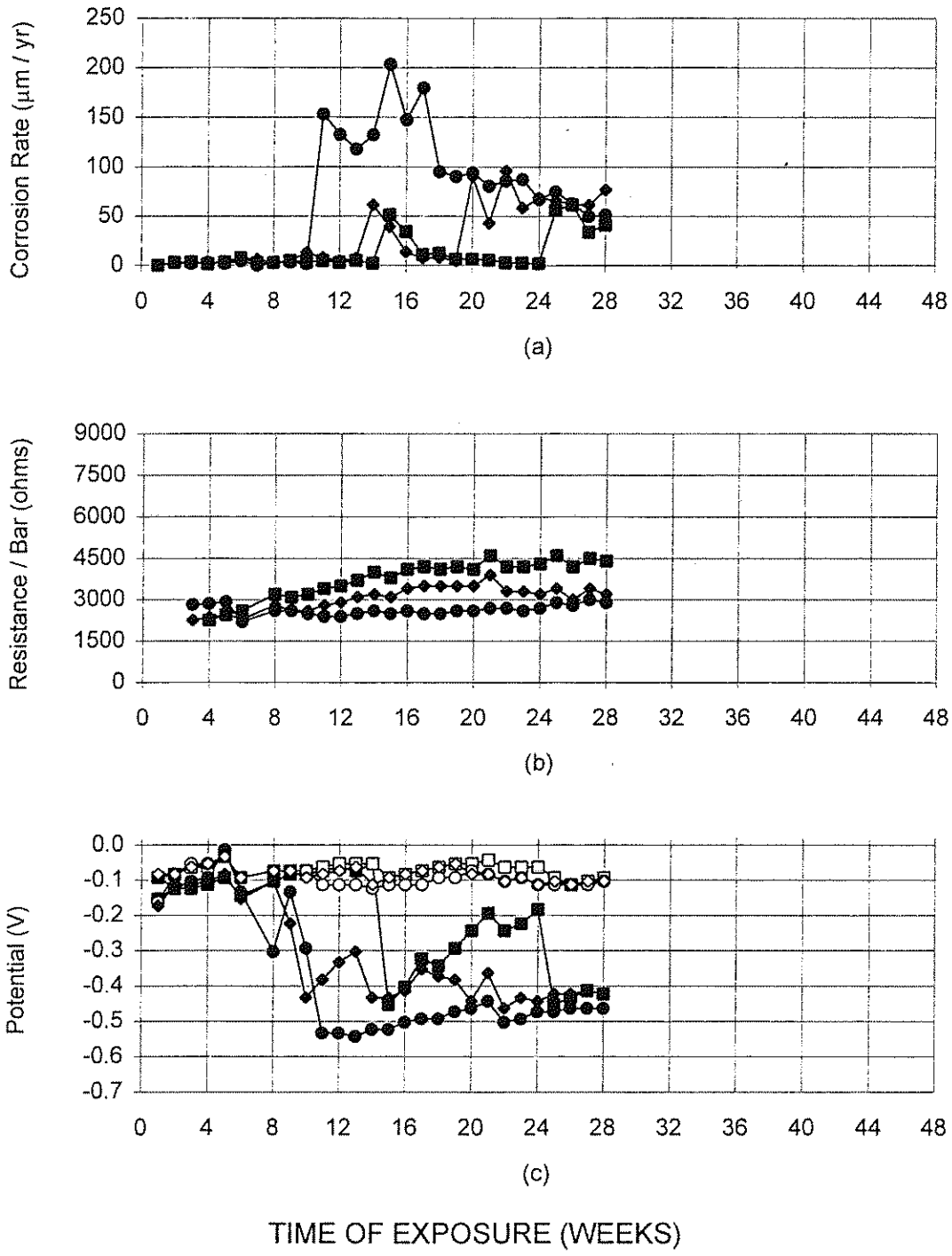

Fig. 3.57 Southern Exposure test results for steel combination EH (epoxy-coated H steel at the anode and uncoated H steel at the cathode). (a) Macrocell Corrosion Rate, (b) Mat-To-Mat Resistance, and (c) Potential of the Anode (solid) and Cathode (clear)

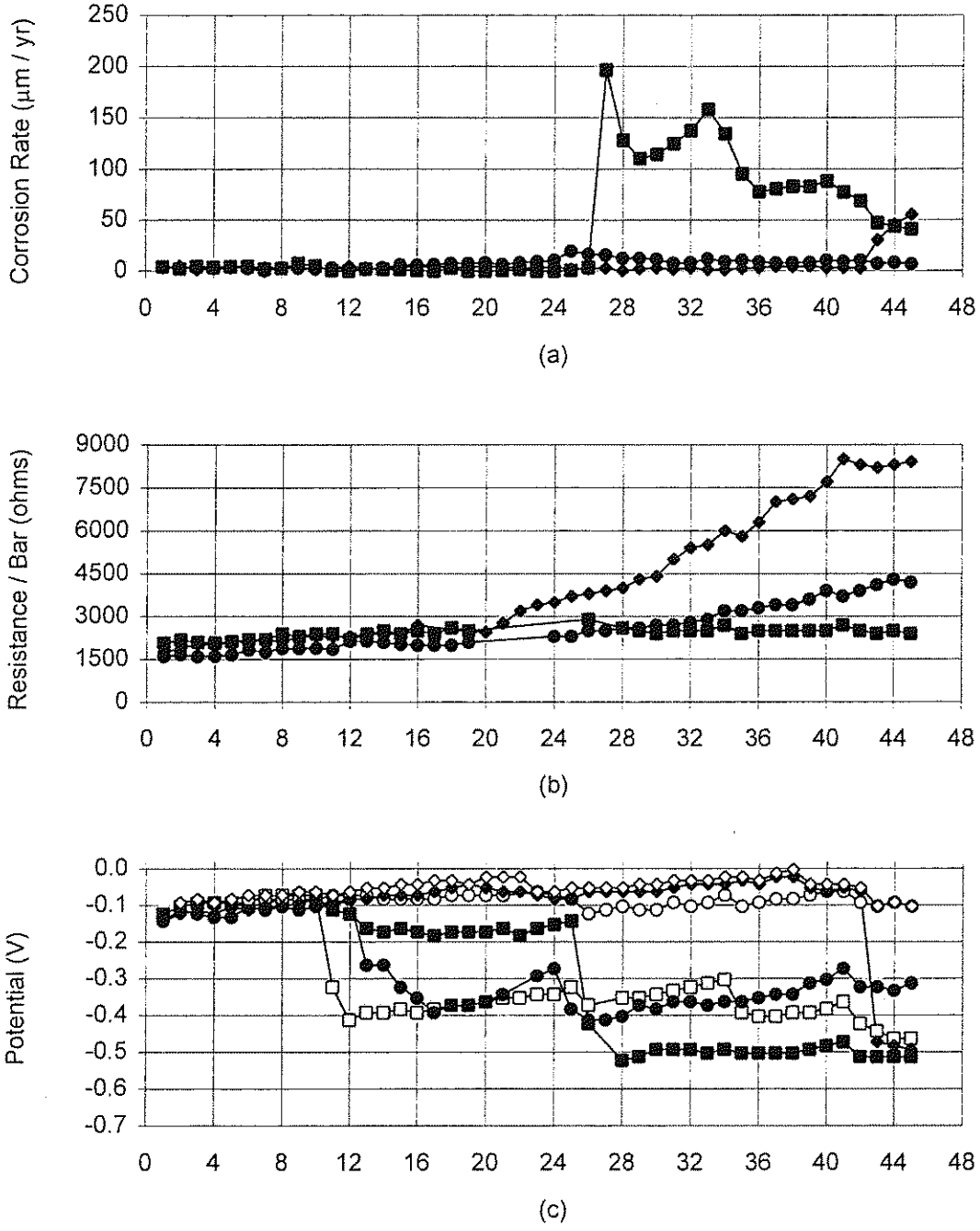

Fig. 3.58 Southern Exposure test results for steel combination ECRSH (epoxy-coated CRSH steel at the anode and uncoated CRSH steel at the cathode). (a) Macrocell Corrosion Rate, (b) Mat-To-Mat Resistance, and (c) Potential of the Anode (solid) and Cathode (clear)

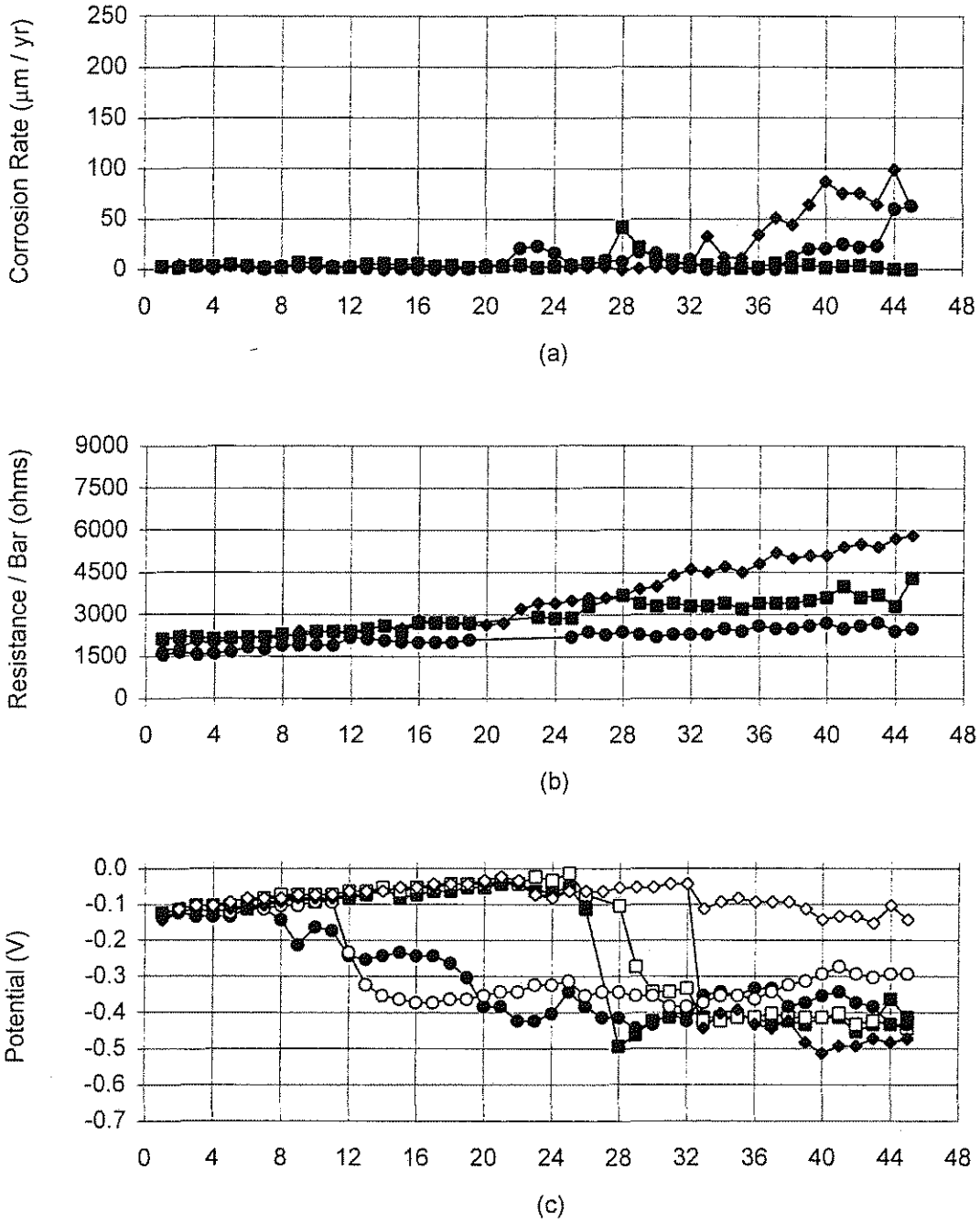

Fig. 3.59 Southern Exposure test results for steel combination ECRST (epoxy-coated CRST steel at the anode and uncoated CRST steel at the cathode).
(a) Macrocell Corrosion Rate, (b) Mat-To-Mat Resistance, and (c) Potential of the Anode (solid) and Cathode (clear)

APPENDIX-A
SAMPLE CALCULATIONS

Macrocell Corrosion Rate Calculation:

Faraday's Law: $Rate = (i \cdot a) / (n \cdot F \cdot D)$

Rate = depth of metal loss per year, μm/yr

i = current density of the macrocell, mA/cm^2

a = atomic weight of the metal

= 55.8 grams/gram-atom for iron

n = number of ion equivalents exchanged

= 2 equivalents/gram-atom for iron

F = Faraday's constant

= 96,500 coulombs/equivalent

D = density of the metal, g/cm^3

= 7.87 g/cm^3 for iron

Current Density: $i = V / (\Omega \cdot A)$

V = voltage drop across the resistor, mV

= reading

Ω = resistance of the resistor

= 10 ohms

A = area of exposed metal in concrete at the anode bar(s), cm^2

$$Rate = \frac{(reading) \cdot (V / 1000\ mV) \cdot 55.8\ g \cdot 31.5xE6\ s/yr \cdot (10{,}000\ \mu m / cm)}{10\ \Omega \cdot 2\ equivalents \cdot 96{,}500\ coulombs/equivalent \cdot 7.87\ g/cm^3 \cdot A}$$

$$= reading \cdot 1160 / A$$

Note: $V / \Omega = amp = coulombs / s$

Corrosion Rate for (Rapid) Macrocell Corrosion Test:

The exposed surface area of steel in concrete in one test specimen is 36.2 cm^2.
If one specimen is used for the anode, A = 36.2 cm^2.

Rate = reading · 1160 / 36.2
= reading · 32

Corrosion Rate for Southern Exposure and Cracked Beam Tests:

The exposed surface area of steel in concrete for one bar is 139 cm^2.

The Southern Exposure test specimen has two bars at the anode, therefore A = 278 cm^2.
Rate = reading · 1160 / 278
= reading · 4.16

The Cracked Beam test specimen has one bar at the anode, therefore A = 139 cm^2.
Rate = reading · 1160 / 139
= reading · 8.32